

Impaired behavioral and neuropathological outcomes following blast neurotrauma

Venkata Siva Sai Sujith Sajja

Dissertation submitted to the faculty of the Virginia Polytechnic Institute and State University in partial fulfillment of the requirements for the degree of

Doctor of Philosophy
In
Biomedical Engineering

Pamela J. VandeVord, Chair
Matthew P. Galloway
Warren N. Hardy
YongWoo Lee
Stephen M. LaConte

July 26th, 2013
Blacksburg, Virginia

Keywords: Blast, neurotrauma, memory, anxiety, glial scarring

Impaired behavioral and neuropathological outcomes following blast neurotrauma

Venkata Siva Sai Sujith Sajja

Abstract

Blast-induced neurotrauma (BINT) is a major societal concern due to the complex expression of neuropathological disorders after exposure to blast. Disruptions in neuronal function, proximal in time to the blast exposure, may eventually contribute to the late emergence of the clinical deficits. Besides complications with differential clinical diagnosis, the biomolecular mechanism underlying BINT that gives rise to cognitive deficits is poorly understood. Some pre-clinical studies have demonstrated cognitive deficits at an acute stage following blast overpressure (BOP) exposure. However, the behavioral deficit type (e.g., working memory) and the mechanism underlying injury prognosis that onsets the cognitive deficits remains to be further investigated. An established rodent model of blast neurotrauma was used in order to study impaired behavioral and neuropathological outcomes following blast. Anesthetized rats were exposed to a calibrated BOP using a blast simulator while control animals were not exposed to BOP. Behavioral changes in working memory and anxiety were assessed with standard behavioral techniques (novel object recognition paradigm and light and dark box test) at acute and chronic stages (range: 3 hours – 3 months). In addition, brains were assayed for neurochemical changes using proton magnetic resonance spectroscopy (MRS) and neuropathology with immunohistochemistry in cognitive regions of brain (hippocampus, amygdala, frontal cortex and nucleus accumbens)

Early metabolic changes and oxidative stress were observed along with a compromise in energy metabolism associated with sub-acute (7 days following BOP exposure) active neurodegeneration and glial scarring. Data suggested GABA shunting pathway was activated and phospholipase A2 regulated arachadonic acid pathway may be involved in cellular death cascades. In addition, increased *myo*-inositol levels in medial pre-frontal cortex (PFC) further supported the glial scarring and were associated with impaired working memory at a sub-acute stage (7 days) following BOP exposure. Chronic working memory issues and anxiety associated behavior could be related to chronic activation of microglia in hippocampus and astrocytes in amygdala respectively. Furthermore, these results from MRS could be directly translated into clinical studies to provide a valuable insight into diagnosis of BINT, and it is speculated that gliosis associated markers (*myo*-inositol) may be a potential biomarker for blast-induced memory impairment.

Author's Acknowledgements

This work could not have been completed without the support and help from many fantastic colleagues. I would like to thank my advisor, Dr. Pamela Vandevord, for the never ending support, guidance and mentoring which motivated me throughout my Ph.D. I would also like to thank my committee members who provided lab equipment and support for the research conducted. A special thanks goes to Drs. Galloway and Perrine for providing magnetic resonance and behavior paradigm facilities respectively. I would also like to thank my fellow lab members and journal manuscript co-authors for great ideas and assistance with this research. Most of all, I would also like to thank my parents and friends for their support throughout the program without which I would not have been able to complete my Ph.D.

Table of Contents

Chapter 1.....	1
Introduction	1
Statement of problem.....	1
Literature Review.....	1
Mechanisms of primary blast injury.....	1
Background.....	2
Effects of Primary Blast Injury.....	3
Propagation of Blast Wave.....	4
Biomechanical mechanisms underlying BINT.....	5
Bio-molecular mechanisms underlying blast injury.....	6
Ongoing research review.....	7
Oxidative stress and cytokine release.....	8
Pro-inflammatory changes in BINT.....	8
Anatomy of major cognitive regions in brain of humans and rats.....	9
Hippocampus.....	10
Anatomy.....	10
Function and pathology.....	11
Role of hippocampus in BINT.....	12
Prefrontal cortex.....	13
Anatomy.....	13
Function and pathology.....	13
Role of prefrontal cortex in BINT.....	14
Amygdala.....	14
Anatomy.....	14
Function and pathology.....	15
Role of amygdala in BINT.....	16
Nucleus accumbens.....	17
Anatomy.....	17
Function and pathology.....	17
Role of nucleus accumbens in BINT.....	19
Chapter 2.....	20
Specific Aims and Hypothesis.....	20

Hypothesis.....	20
Specific Aims.....	20
Specific Aim 1.....	20
Specific Aim 2.....	20
Specific Aim 3.....	20
Specific Aim 4.....	20
Materials and methods.....	21
Blast exposure.....	21
Specific Aim 1.....	22
Materials and methods.....	22
Proton magnetic resonance spectroscopy (1H-MRS) analysis.....	22
Specific Aim 2.....	24
Materials and methods.....	24
Tissue sectioning.....	24
Fluoro-Jade B (FJB) analysis.....	24
GFAP, Iba1, SOD1, NeuN and caspase-3.....	25
Specific Aim 3.....	26
Materials and methods.....	26
Novel object recognition test.....	26
Data collection and exclusion criteria.....	26
Light/dark box.....	27
Specific Aim 4.....	27
Materials and methods.....	28
Statistics.....	28
Chapter 3.....	29
Blast-induced neurotrauma leads to neurochemical changes and neuronal degeneration in the rat hippocampus.....	29
Abstract.....	30
Introduction.....	31
Materials and methods.....	32
Animals and testing parameters.....	32
1H-MRS analysis.....	34
Immunohistochemistry.....	36
Fluoro-Jade B (FJB) analysis.....	36

β-Amyloid precursor protein (β-app), and caspase-3.....	36
Western blotting.....	37
Statistics.....	37
Results.....	37
Neurochemical assessment by 1H-MRS.....	37
Immunohistochemistry.....	39
β-amyloid precursor protein.....	39
FluoroJade B (FJB).....	39
Caspase-3.....	41
Western blotting.....	42
Discussion.....	43
Metabolic response to BINT.....	44
Cellular response to BINT.....	45
Conclusions.....	46
Acknowledgements.....	46
Disclosures.....	47
References.....	48
Chapter 4.....	54
Effects of Blast-Induced Neurotrauma on the Nucleus Accumbens.....	54
Introduction.....	55
Methods.....	56
Animal handling and care.....	56
Testing parameters.....	56
1H-MRS analysis.....	57
High performance liquid chromatography (HPLC).....	59
Western blotting.....	59
Statistics.....	60
Results.....	60
Neurochemical profiling using 1H-MRS.....	60
Neurochemical profiling using HPLC.....	60
Western blotting.....	63
Discussion.....	65
Neurochemical changes.....	66

Cellular injury response.....	67
Acknowledgements.....	69
References.....	69
Chapter 5.....	74
Blast neurotrauma impairs short-term memory and disrupts prefrontal myo-inositol levels in rats.....	75
Abstract.....	76
Introduction.....	77
Materials and methods.....	78
Animals and blast overpressure exposure.....	78
Novel object recognition test (NOR).....	78
High resolution magic angle spinning proton-magnetic resonance spectroscopy (HRMAS 1H-MRS) analysis:.....	79
Immunohistochemistry.....	80
FluoroJade B (FJB) analysis.....	81
GFAP analysis.....	81
Statistics.....	82
Results.....	82
Object recognition behavior and working memory.....	82
Neurochemical Assessment by 1H-MRS.....	83
NOR versus Ins Correlation.....	84
FJB and GFAP.....	85
Discussion.....	86
Behavioral outcome.....	86
Neurochemical assessment using 1H-MRS.....	87
Astrogliosis and neurodegeneration.....	89
Correlation between behavior and myo-inositol.....	89
Conclusion.....	89
Acknowledgements.....	90
References.....	90
Chapter 6.....	101
Summary.....	101
Neurochemical and histopathological outcome following BOP exposure.....	101
Behavioral outcomes (working memory and anxiety) following BOP exposure.....	112

Conclusion.....	115
Limitations.....	117
Future Directions.....	118
References.....	121

List of Figures

Figure 1.1: Classification of the blast overpressure induced neurotrauma.....	2
Figure 1.2: Chronological development of blast.....	3
Figure 1.3: A schematic depicting the characteristic of Friedlander’s wave that results from detonations.....	4
Figure 1.4: Effects and propagation of blast shock wave.....	6
Figure 1.5: Signaling of subfields of hippocampus with entorhinal cortex and subiculum.....	11
Figure 1.6: Main afferent and efferent connection of hippocampal signaling.....	12
Figure 1.7: Different nuclei of amygdala.....	15
Figure 1.8: Amygdalar efferent and afferent signals.....	16
Figure 1.9: Anatomy of nucleus accumbens in coronal view.....	17
Figure 1.10: Nucleus accumbens afferent and efferent connections to other regions of brain. γ -amino butyric acid, GABA; Glutamate, Glu; Dopamine, DA; Serotonin, 5-HT.....	19
Figure 2.1: Schematic of shock tube with a pressure center calibration set up at the animal location.....	21
Figure 2.2: Virginia Tech shock tube with an arrow pointing at animal location.....	22
Figure 2.3: Representative HR-MAS 1H-MRS chemical shift spectrum from ~ 2 mg rat brain hippocampus (256 averages) demonstrates resolution of constituents and sensitivity at 500 MHz.....	24
Figure 2.4: Schematic of NOR task for working memory.....	27
Figure 2.5: Schematic representing an aerial view of light and dark box.....	27
Figure 3.1: (A) The Wayne State University Bioengineering shock tube generates a consistent shock wave profile. (B) The placement of the animals is 1.09 m into the shock tube.....	34
Figure 3.2: Chemical shift spectrum from ~2 mg of rat brain hippocampus (256 averages) demonstrates the resolution of constituents and sensitivity at 500 MHz. Peak	

assignments are based on identical chemical shifts of standards dissolved in the same buffer (identical pH, temperature) as used for tissue analysis (see Materials and methods). The basis set for the customized LCModel used for rat brain also compensates for nonspecific lipid resonances at 1.2, 1.4, 1.6 and 1.7 ppm.....38

Figure 3.3: Summary of statistically significant changes in MR-visible neurochemical profiles 24 h after blast-induced neurotrauma (BINT). Each bar is the mean and standard error of the mean (SEM) from separate experiments at 24 and 48 h; absolute concentrations are presented in the table. CRE, creatine; GABA, g-aminobutyric acid; GLU, glutamate; GSH, glutathione; LAC, lactate; NAA, N-acetylaspartate; PEA, phosphorylethanolamine; SUC, succinate. *p < 0.05; #p = 0.08.....40

Figure 3.4: Active neurodegeneration in the hippocampus, indicated by positive FluoroJade B (FJB) staining, increased substantially after blast-induced neurotrauma (BINT). Forty-eight hours after BINT, FJB-positive neurons indicate active degeneration in CA1 (A) and CA3 (C) subfields of the hippocampus, whereas sham-treated animals showed minimal FJB-positive staining in CA1 (B) or CA3 (D). Graph depicts the quantification of FJB-positive neurons, revealing a significant increase at both 24 and 48 h after blast overpressure (mean ± standard error of the mean; *p < 0.05; **p < 0.001).....41

Figure 3.5: Cleaved caspase-3-positive neurons in the CA1 subfield of the hippocampus were increased significantly 48 h after blast-induced neurotrauma (BINT). Representative sections from the sham group at 24 h (A) and 48 h (C). Although levels of cleaved caspase-3 were increased after 24 h (B), the effect only achieved statistical significance 48 h after BINT (D). Widespread caspase-3-positive cells are observed in the hippocampus (D). The graph depicts the quantification of caspase-3 across experimental groups, revealing a significant increase 48 h after BINT (mean ± standard error of the mean; *p < 0.001).....42

Figure 3.6: Early increase in glial fibrillary acidic protein (GFAP) is followed by a delayed increase in hippocampal Bax. Compared with the respective controls, GFAP, a measure of astrogliosis, increased significantly 24 h (representative blots show blast groups B1–B3 and sham groups S1–S3), but not 48 h, after blast-induced neurotrauma (BINT).

Bars represent mean standard error of the mean (*p < 0.02).....43

Figure 3.7: Levels of Bax, unchanged at 24 hours, were significantly increased 48 hours after BINT (mean + SEM, *p<0.01). Representative blots (A1-A5 are from blast exposed subjects) show increased levels of the apoptotic marker Bax in the blast group as compared to the shams (S1-S5).....43

Figure 4.1: Representative pressure profile of the shock wave that is generated from the shock tube.....57

Figure 4.2: Graphs depict the temporal neurochemical response following blast exposure. Elevated levels of Glu/Cre were observed, suggesting a potential excitotoxic effect at 72 hr postblast (*p < 0.05). Elevated levels of NAAG and Cre were observed at 48 hr following blast, demonstrating an ongoing neuroprotective effect. GPC, an inflammatory marker, was significantly increased at 48 and 72 hr postblast compared with sham.....62

Figure 4.3: Selective loss of 5-HT levels. *p < 0.01.....63

Figure 4.4: Increased levels of HVA and HVA/DA at 24 following blast, with no change in levels of DA suggest increased CA turnover. *p < 0.05.....63

Figure 4.5: At 24 h following blast, increased levels of the antiapoptotic marker Bcl-2 were found, indicating an ongoing neuroprotective effect in the NAC. Representative blot. B1–B4, blast group; S1–S4, sham group. *p < 0.01.....64

Figure 4.6: GFAP, a marker of astrogliosis, was increased at 24 hr following blast, showing ongoing astrocyte reactivity in the NAC. Representative blot. B1–B4, blast group; S1–S4, sham group. *p < 0.05.....64

Figure 4.7: Increased levels of the proapoptotic marker Bax at 48 hr post-blast, indicating triggering of the apoptotic pathway. Representative blot. B1–B4, blast group; S1–S4, sham group. *p < 0.01.....65

Figure 4.8: β -Actin, a major protein in the cytoskeleton and microtubules of the cell, was significantly decreased at 72 hr postblast. Representative blot. B1–B4, blast group; S1–S4, sham group. *p< 0.05.....65

Figure 5.1: Representative pressure profile of calibrated shock wave to which animals are exposed with a resultant peak positive overpressure at 117 KPa.....78

Figure 5.2: Sham rats learn the behavior and show good working memory (T1-T2 sham), while blast exposed rats do not show learning and are significantly different from sham rats in T2 from learning. T1 – Trial with familiar objects; T2 – Trial 2 with a novel object; *p<0.05, **p<0.002.....83

Figure 5.3: Temporal evaluation of the 1H-MRS neurochemical changes in the prefrontal cortex of rats following blast overpressure exposure, where blast group is compared to corresponding sham group, *p<0.05.....84

Figure 5.4: Myo-inositol (Ins) in the prefrontal cortex of sham animals had a significant negative correlation (p<0.05) with working memory while this correlation was lost in overpressure exposed group of animals.....85

Figure 5.5: FluoroJade B positive (FJB+) stained neurons were significantly higher compared to shams at all time points. Representative histological images depict figures sham (A) and blast (B) groups in prefrontal cortex, *p<0.05; Arrows indicate FJB+ neurons.....85

Figure 5.6: GFAP positive-stained astroglia were measured using immunohistochemistry at various time points. Significant levels of FJB+ neurons were found at 168, but not 3 or 48, hours following blast compared to sham animals, *p<0.01. Representative figures sham (A) and blast (B) groups at 168 hours from prefrontal cortex; Arrows indicate GFAP positive astrocytes.....86

Figure 6.1: GABA shunt plays an important role in supporting Krebs’s cycle to regulate cellular energy metabolism and homeostasis.....103

Figure 6.2: Temporal evaluation of the programmed cell death marker, cleaved caspase-3 in hippocampus (HIP), amygdala (AMY), medial prefrontal cortex (PFC) and nucleus accumbens (NAC) ; 3h – 3 hours, 1d – 1 day, 2d – 2 day, 7d – 7 days, 1m – 1 month, 3m – 3 months; *p < 0.05 when compared to respective sham group.....105

Figure 6.3: Temporal evaluation of GFAP, a astrocyte marker, in hippocampus (HIPP), amygdala (AMY), medial prefrontal cortex (PFC) and nucleus accumbens (NAC) ; 3h – 3 hours, 1d – 1 day, 2d – 2 day, 7d – 7 days, 1m – 1 month, 3m – 3 months.....107

Figure 6.4: Chronic elevated microglia levels (measured using Iba1) were found in hippocampus (HIPP), amygdala (AMY), medial prefrontal cortex (PFC) and nucleus accumbens (NAC) following BOP. No changes were observed at an acute and sub-acute stage (3 hours – 7 days) following BOP; *p < 0.05 when compared to respective sham group.....108

Figure 6.5: Temporal evaluation of neurodegeneration using fluorojade B, in hippocampus (HIPP), amygdala (AMY), medial prefrontal cortex (PFC) and nucleus accumbens (NAC) ; 3h – 3 hours, 1d – 1 day, 2d – 2 day, 7d – 7 days, 1m – 1 month, 3m – 3 months; *p < 0.05 when compared to respective sham group.....109

Figure 6.6: Temporal evaluation of mature neurons measured by NeuN staining, in hippocampus (HIPP), amygdala (AMY), medial prefrontal cortex (PFC) and nucleus accumbens (NAC) ; 3h – 3 hours, 1d – 1 day, 2d – 2 day, 7d – 7 days, 1m – 1 month, 3m – 3 months; *p < 0.05 when compared to respective sham group.....110

Figure 6.7: Decreased SOD1 levels in medial prefrontal cortex (PFC) and nucleus accumbens (PFC), but no changes were observed at all-time points in hippocampus (PFC), amygdala (AMY) following BOP. In addition, no changes were observed at an acute and sub-acute stage (3hours – 48 hours) following BOP in all the regions.....111

Figure 6.8: Anxiety-like behavior was observed from 3 days – 3 months following blast overpressure exposure. 2d – 2 days, 7d – 7 days, 1m – 1 month, 3m – 3 months.....112

Figure 6.9: (A) Impaired working memory was observed from 7 days – 3 months following blast overpressure exposure. 3d – 3 day, 7d – 7 days, 1m – 1 month, 3m – 3 months.....113

Figure 6.10: (A) Positive correlation between impaired memory and elevated microglial levels in blast group showed microglial activation in hippocampus at 3 months could be involved tardive working memory issues; (B) Time spent in dark (indicator of anxiety)

was correlated with astrocyte activation in amygdular region of brain at 3 months following BOP exposure.....114

Figure 6.11: Myo-inositol (Ins) in the prefrontal cortex of sham animals had a significant negative correlation ($p < 0.05$) with working memory while this correlation was lost in overpressure exposed group of animals at 7 days post blast.....115

List of Tables

Table 4.1: Raw values of the neurochemicals that are altered at 48 and 72 hours following blast.....	61
Table 6.1: Raw data of various stains at 1 month and 3 months post blast in hippocampus (HIPPO), medial prefrontal cortex (PFC), amygdala (AMY) and nucleus accumbens (NAC), *p < 0.05.....	104

List of Abbreviations:

ALA	-	Alanine
ASP	-	Aspartate
BET	-	Betaine
BINT	-	Blast-induced neurotrauma
BOP	-	Blast over pressure
CHO	-	Choline
CRE	-	Creatine
FJB	-	FluoroJade B
GABA	-	γ - amino butyric acid
GFAP	-	Glial fibrillary acidic protein
GLN	-	Glutamine
GLU	-	Glutamate
GLY	-	Glycine
GPC	-	Glycerophosphocholine
GSH	-	Glutathione
HRMAS	-	High resolution magic angle spinning
INS	-	Inositol
LAC	-	Lactate
LD	-	Light and dark box
MRS	-	Magnetic resonance spectroscopy
NAA	-	N-acetyl aspartate
NAAG	-	N-acetyl aspartate glutamate
NAC	-	Nucleus accumbens
NOR	-	Novel object recognition
PBS	-	Phosphate buffered saline
PCH	-	Phosphocholine
PEA	-	Phosphorylethanolamine
PTSD	-	Posttraumatic stress disorder
PVDF	-	Polyvinylidene fluoride
TAU	-	Taurine
TBI	-	Traumatic brain injury

β -APP - Beta-amyloid precursor protein

Attribution

Several colleagues aided in the writing and research contained in this dissertation. A brief description of their contributions is included below.

Dr. Pamela VandeVord, Neural engineering lab, Virginia Polytechnic Institute and State University is the primary advisor and committee chair for this research. She provided extensive guidance and comments for the research. In addition, she provided extensive support with her blast research expertise, funds for research and with writing of this dissertation.

Chapter 3: Blast-induced neurotrauma leads to neurochemical changes and neuronal degeneration in the rat hippocampus

Dr. Matthew P. Galloway, Pre-clinical research of psychiatry and behavioral neurosciences, Wayne State University, advised and provided magnetic resonance spectroscopy (MRS) facility for neurochemical analysis and extensive editing with the manuscript preparation.

Farhad Ghoddoussi, Pre-clinical research of psychiatry and behavioral neurosciences, Wayne State University, advised with analyzing peaks resolved from MRS.

Dhananjeyan Thiruthalinathan, Neural engineering lab, Wayne State University, for assisting with FluoroJade B analysis.

Andrea Kepsel, Neural engineering lab, Wayne State University, assisted with western blotting assays.

Kathryn Hay, Neural engineering lab, Wayne State University, assisted with caspase-3 positive analysis.

Cynthia Bir, Sports medicine lab, Wayne State University advised with blast research expertise.

Chapter 4: Effects of blast-induced neurotrauma on the nucleus accumbens

Matthew P. Galloway, Pre-clinical research of psychiatry and behavioral neurosciences, Wayne State University, advised and provided magnetic resonance spectroscopy facility for neurochemical analysis.

Farhad Ghoddoussi, Pre-clinical research of psychiatry and behavioral neurosciences, Wayne State University, advised with analyzing peaks resolved from MRS.

Andrea Kepsel, Neural engineering lab, Wayne State University, assisted with western blotting assays.

Chapter 5: Blast neurotrauma impairs short-term memory and disrupts prefrontal *myo*-inositol levels in rats

Shane A. Perrine, Pre-clinical research of psychiatry and behavioral

neurosciences, Wayne State University, provided the facilities for behavioral experiments.

Farhad Ghoddoussi, Pre-clinical research of psychiatry and behavioral neurosciences, Wayne State University, advised with analyzing peaks resolved from MRS.

Christina S. Hall, Neural engineering lab, Virginia Polytechnic Institute and State University, assisted with counting GFAP staining.

Matthew P. Galloway, Pre-clinical research of psychiatry and behavioral neurosciences, Wayne State University, advised and provided magnetic resonance spectroscopy facility for neurochemical analysis.

Chapter 1

Introduction

Statement of problem

More than 25% of the veterans returning from Operation Iraqi Freedom (OIF) and Operation Enduring Freedom (OEF) are suffering from closed head injuries due to blast overpressure (BOP) exposure. Reports suggest that improvised explosive devices (IEDs) are the main weapon of the current wars. Blast induced neurotrauma (BINT) is the second most cause of injuries from BOP, next to amputations [1-12]. Clinical reports have indicated the development of cognitive associated disorders following BOP. Majority of these disorders are associated with anxiety, attention deficits, memory issues and problem solving skills [8, 13-16].

Most of these symptoms appear tardive in nature and often have overlapping indicators with post-traumatic stress disorder (PTSD) and impact associated traumatic brain injury (TBI). Although some sophisticated imaging techniques such as functional magnetic resonance imaging (fMRI) can identify severe forms of TBI, mild-to-moderate forms of BINT is still elusive for all the advanced techniques of imaging [5, 13, 17-20]. These factors make it difficult for the differential diagnosis of BINT as compared to TBI and PTSD. Thus far there is no effective diagnosis that is directed towards mild forms of BINT, and consequently patients suffering from BINT are often misdiagnosed with PTSD or TBI [14,16, 21-25].

In addition, molecular pathways associated with mild forms of BINT remain unclear. Fundamental studies are vital in order to understand the molecular pathways of BINT progression and associated neurological deficits.

Literature review

Mechanisms of primary blast injury

Mechanisms of BINT can be classified from either a biomechanical or a bio-molecular neuroscience point of view. Biomechanical mechanisms primary focus on interactions of BOP or shock waves with the skull whereas bio-molecular neuroscience investigates

the cellular injury cascades and cognitive impairment of the brain following BOP exposure. Both of these fields are important for the understanding of the primary blast injury mechanics and injury prognosis of BINT.

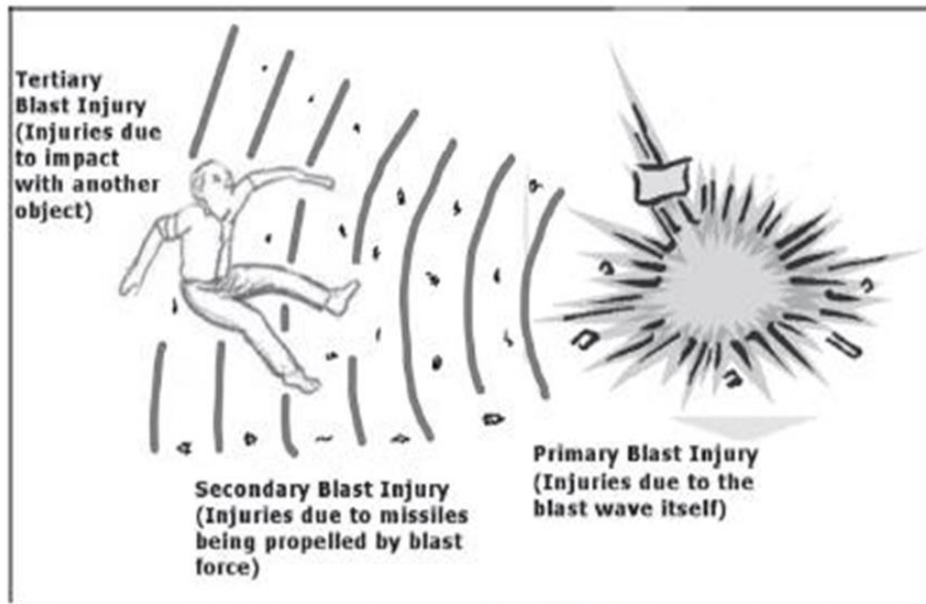


Figure 1.1: Classification of the blast overpressure induced neurotrauma.

Background

According to a report from Center for Disease Control (CDC) in 2011, more than 1.5 million people suffer from injuries related to blast overpressure from IEDs each year [1, 6, 7, 26-31]. Currently, there is still a need to identify the injury mechanisms of mild blast induced neurotrauma. IEDs, upon explosion, can cause deteriorating effects by various modes of injury which can be life-threatening. Injuries are classified as four types (Figure 1.1) [1, 27, 29, 32]:

1. Primary Blast Injury : Injuries which occur as a result of the blast overpressure wave
2. Secondary Blast Injury: Injuries from shrapnel propelled by the blast explosion
3. Tertiary Blast Injury: Injuries from impact of the body onto other objects as a result of the blast wind
4. Quaternary Blast Injury: Explosion-related injury or illness not due to any of the above such as burns and/or inhalational injuries

Effects of primary blast injury

Primary blast injury (PBI) is caused by direct overpressure exposure or a shock wave's impact on the body. One of the most important concerns of PBI is that resultant overpressure from IEDs can reach far beyond thermal and nuclear radiation that originates from the detonation area (Figure 1.2). The overpressure that results from the blast wave propagates on the order of Mach speed. PBI results in various injury, which can further be classified as mild, moderate and severe [1, 5, 8, 27, 32, 33].

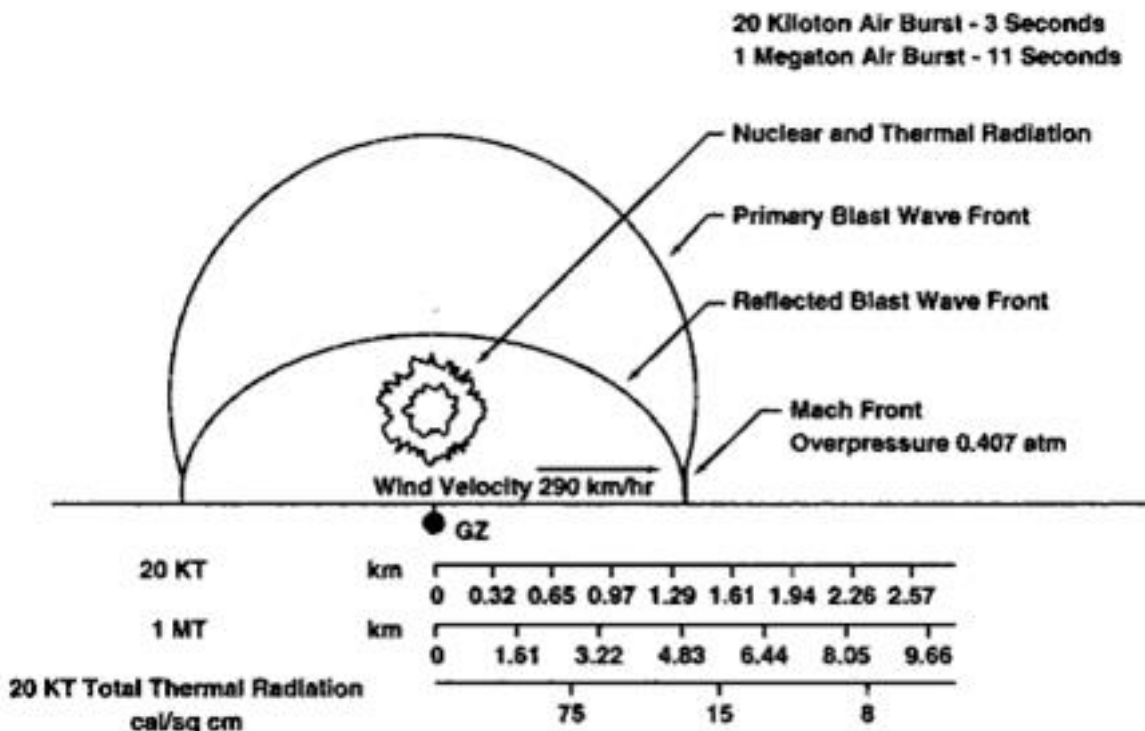


Figure 1.2: Chronological development of blast. Bellamy, R.F., et al., *Textbook of military medicine, conventional warfare: Ballistic, blast, and burn Injuries*, series on combat casualty care. Office of the Surgeon General, Dept. of the Army, Walter Reed Army Medical Center, Washington, DC, 1988, US government document.

Laboratory scale shock tubes which can generate a Friedlander waveform that resembles 'free field' shock wave profiles are currently used for animal models [24, 58, 59] (Figure 1.3). A Friedlander waveform occurs when a high explosive detonates in a free field, that is, with no surfaces nearby with which it can interact. The equation for a Friedlander waveform describes the pressure of the blast wave as a function of time:

$$P(t) = P_s e^{\frac{t}{t^*}} \left(1 - \frac{t}{t^*}\right).$$

where P_s is the peak pressure and t^* is the time at which the pressure first crosses the horizontal axis (before the negative phase) as shown in Figure 1.3.

A shock wave results in a sharp rise of pressure and temperature along its axis of propagation. Previous studies have shown duration of overpressure rise time play a very important role in PBI.

Propagation of blast wave

The shock which results from IEDs has two phases, a positive and negative phase in the waveform. The propagation and deteriorating effects of a shock wave are shown in Figure 1.4 [1, 29, 32, 48]. Compression of gasses in the atmosphere gives immediate rise to a positive phase, while a negative phase is created due to a sudden drop in the pressure along shock wave propagation [1, 32].

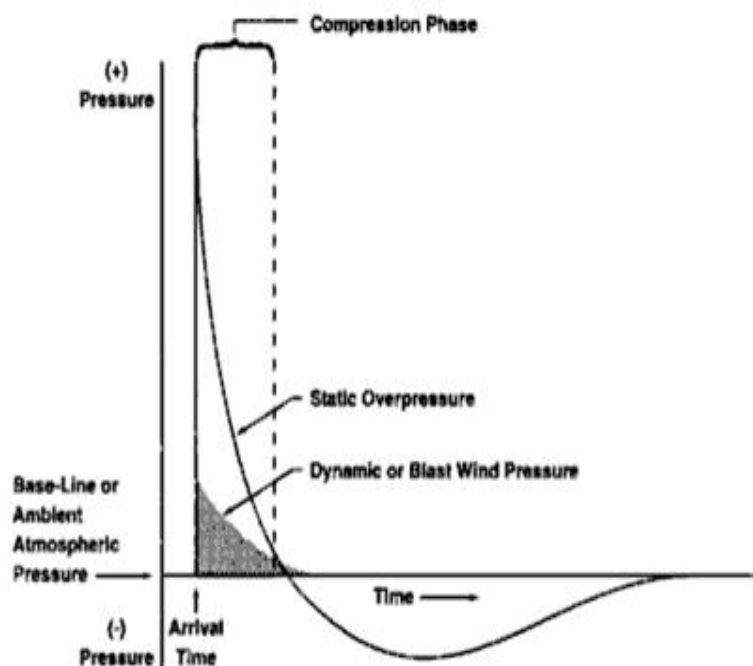


Figure 1.3: A schematic depicting the characteristic of Friedlander's wave that results from detonations. Bellamy, R.F., et al., Textbook of military medicine, conventional warfare: Ballistic, blast, and burn Injuries", series on combat casualty care. Office of the Surgeon General, Dept. of the Army, Walter Reed Army Medical Center, Washington, DC, 1988. US government document.

Biomechanical mechanisms underlying BINT

Several hypotheses have been proposed to identify the biomechanical mechanism of BINT. They are:

- (i) Skull flexure [58]
- (ii) Propagation of blast through orbitals in skull [60]
- (iii) Thoracic compression [30]
- (iv) Direct transmission of shock wave through skull [61]
- (v) Coup - contrecoup mechanism [62]

While research is still ongoing, the exact biomechanical response of blast is not clearly known. Experimental research has provided evidence that the shock wave interaction with the skull may cause skull flexure and transmission of shock wave through the skull could play a viable role in primary biomechanical mechanism of injury [24, 46, 58, 61]. In addition, compression of thoracic activity also may play a role in the injury mechanism, however, as a secondary mechanism of injury [63]. Compression of chest and thoracic cavity is usually caused due to the stress wave which precedes shock wave of blast. Studies have shown this form of injury can be mitigated using chest protective gear [64].

A pre-clinical study has shown protection to the orbital does not affect the injury to brain when exposed to blast overpressure [46]. Coup injury occurs under the site of impact with an object, and a contrecoup injury occurs on the side opposite the area that was impacted [62]. Limited studies are available to validate the coup and countrecoup mechanism in blast injury. Thus far, none of the studies have identified this biomechanical mechanism of injury to brain *via* blast overpressure exposure [15].

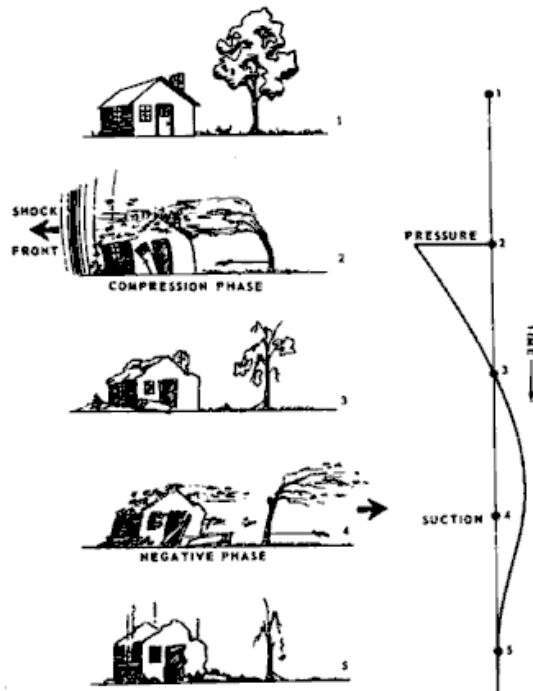


Figure 1.4: Effects and propagation of blast shock wave. Bellamy, R.F., et al., Textbook of military medicine, conventional warfare: Ballistic, blast, and burn Injuries”, series on combat casualty care. Office of the Surgeon General, Dept. of the Army, Walter Reed Army Medical Center, Washington, DC, 1988, US government document.

Bio-molecular mechanisms underlying blast injury

Human and animal studies have provided evidence of cognitive deficits following BINT. However the molecular cascades that are triggered by the blast energy transmission have not been identified. In contrast, impact-related traumatic brain injury is well described and is characterized by diffuse axonal injury and cell death. Alterations in neurochemistry are reported to play a key role in these negative outcomes in cognition [6, 11, 41, 47, 49, 65-70].

In addition to brain, moderate-to-severe PBI affect gas-filled organs like the auditory, pulmonary, and gastrointestinal systems as the pressure wave can rupture the tissues due to high energy transmission, contusions due to displacement of skeletal system onto the organs. Damage to lungs can lead to hypoxia due to decreased oxygen supply. However, this injury can be identified and effectively diagnosed to successfully treat lung damage and hypoxia to the tissues. Furthermore, using chest protection has been shown to mitigate lung injury [1,7, 33-37]. Tympanic membrane rupture has previously been used to identify and diagnose PBI. However, the main challenge lies in diagnosing

milder forms of PBI (when rupture of tympanic membrane or gross morphological lung injury is not identified). Conflicting reports exist in the literature about the likelihood of tympanic membrane rupture resulting from pressure as low as 5 pounds per square inch (psi), however there is no direct evidence from such cases [7, 9, 14, 17, 18, 26, 28, 38-44].

Many clinical reports have identified that low level overpressure exposure (multiple exposures of 30 KPa or 4.35 psi) result in primary blast induced neurotrauma. Most of these cases are dominant in mild-to-moderate forms of PBI resulting in mild blast induced neurotrauma (mBINT). The molecular cascades of PBI are still unclear as little is known about the pathways that are involved in this injury mechanism in order to develop effective treatment plans using pharmacological drugs. Due to the complexity, sophistication, and nature of PBI, the studies presented as part of this dissertation are focused on mild-moderate form of PBI (no visible injuries of lungs) [25, 27, 28, 34, 45-48].

Major concerns of mBINT, from the clinical standpoint, include no outward signs of injury, delayed on-set of symptoms, and overlapping symptoms with PTSD and TBI. Clinical reports have provided evidence that cognitive impairments such as memory deficits, anxiety, attention disorder, diminished problem solving skills, and substance abuse result from blast overpressure exposure [1, 12, 15, 24, 25, 49-55]. These cognitive disorders are associated with the hippocampus, prefrontal cortex, amygdala and nucleus accumbens in different pathological conditions [56, 57].

Ongoing research review

Several studies have reported glial activation using an astrocyte marker, glial fibrillary acidic protein (GFAP), during acute phases (up to 72 hours) of blast in both *in vitro* and *in vivo* studies. Although evidence suggests that cell death cascades are associated with glial activation, mechanisms that initiate these molecular cascades are currently unknown [5, 19, 24, 38, 51, 59]. Role of the protein caspase-3, a strong indicator of apoptosis, has shown to be increased following BINT [24, 59].

Additionally, increased intracranial pressure and blood brain barrier disruption have been identified by research groups [20, 24, 46, 71, 72,17, 27, 28]. Different biomolecular mechanisms are proposed that may be associated with behavioral deficits following cell death cascades.

Oxidative stress and cytokine release:

Oxidative Stress is primarily triggered by mitochondrial failure leading to compromised energy metabolism, inflammation due to cell membrane rupture, and irregular cellular homeostasis caused by the depletion of energy [5,8]. Few studies have demonstrated the role of oxidative stress following BOP. The role of reactive oxygen species (super oxide anion, hydrogen peroxide) and antioxidant systems (super oxide dismutase, glutathione) were proposed in literature thus far. Cernak et al., demonstrated an increase in oxidative stress followed BOP exposure at an acute phase in rat hippocampus [73].

Markedly decreased levels of glutathione and super oxide dismutase, major antioxidants in neurophil, support the evidence of oxidative stress. In addition, increased ROS generating enzymes, including NADPH oxidase (NOX) and inducible nitric oxide synthase (iNOS), and up-regulated oxidative/nitrosative damage markers such as 4-hydroxynonenal (4-HNE) and 3-nitrotyrosine (3-NT) were detected following BINT [38,73]. Moreover, increased ROS was directly detected using 2', 7'-dichlorofluorescein (DCF), another main indicator of ROS generation as early as one hour post BINT [35]. However, the temporal effect on oxidative system imbalance and oxidative stress on other cognitive regions such as amygdala, frontal cortex, nucleus accumbens is unknown. In hippocampus, some pre-clinical studies have shown oxidative stress is followed by pro-inflammatory cytokine release, that mediates cellular death [5,8].

Pro-inflammatory changes in BINT

The production of pro-inflammatory mediators regulates a cascade of inflammatory events. Enhanced expression of pro-inflammatory cytokines, chemokines, and other inflammatory-mediated molecules, and their close interactions facilitate pro-inflammatory pathways by recruiting and transmigrating inflammatory mediators to

tissues. Tumor necrosis factor- α (TNF- α), interleukin-1 β (IL-1 β), interferon- γ (IFN- γ) were shown to be elevated in BINT [74-78]. TNF- α , IL-1 β , and IFN- γ are essential pro-inflammatory cytokines and activators of macrophages by immunomodulatory effect, and monocyte chemoattractant protein-1 (MCP-1), a member of chemokine family playing a critical role in monocyte chemotaxis and transmigration [79] were shown to be elevated in BINT.

Furthermore, MCP-1 has been implicated in extensive neuronal loss and microglial/astroglial activation of brain injuries. Likewise, there are several other reports demonstrating that overexpression of various pro-inflammatory markers including C-reactive protein (CRP), TNF- α , interleukin-6 (IL-6) have been involved and associated with biomolecular changes in the brain after BINT [74-78].

Thus far, all animal models have shown diminished cognition following BOP exposure. A study by Saljo et al observed that overpressure as low as 60KPa can induce cognitive deficits [59]. Other studies have related diminished cognition with hippocampal injury, although the nature of BINT is diffusive and clinical symptom suggests that there is more than one cognitive region involved in BINT [5, 6, 8, 38, 59, 72, 73]. Limited studies have identified injury in the amygdala and motor cortex following BOP exposure [24].

When evaluating the gross cognitive dysfunction, researchers use a standard learning paradigm characterized with the Morris water maze. However, dysfunction in specific behavioral type (e.g., working memory) is important to understand different cognitive symptoms that are associated clinically [24, 38, 59, 81,82]. Behavioral stereotypes of memory include working memory, short term memory, executive memory and long term memory. Understanding behavioral stereotypes are useful tools which help unravel the key cognitive regions that are impaired following injury. Limited studies have been reported with a primary focus on the hippocampus. However, in order to fully appreciate the complexity of BINT, there is need to study other cognitive regions following BOP exposure.

Anatomy of major cognitive regions in brain of humans and rats

The brain is a complex system networked with axonal fibers, which signal *via* neurotransmission from one cognitive region to the other in order to perform well organized thought processes and decision making. Learning and behavior is an outcome of this communication process among these cognitive structures. Learning, memory, decision making, attention, and coordination signals that comes from limbic system and cortical signaling is well understood in both primates and rodents. The primary regions that play a role in memory potentiation are hippocampus and frontal cortex of the brain [76-79]. The anxiety and reward system is gated by the amygdala and nucleus accumbens respectively. For the simplicity in understanding the molecular injury mechanisms following BOP exposure, the signaling network between these cognitive regions is not taken into consideration, instead molecular pathways are assayed and studied individually in each cognitive region [56, 87-91].

Hippocampus

Anatomy:

The hippocampus is the gateway for emotions and memory potentiation. It belongs to the limbic system and plays important roles in long-term memory and spatial navigation. Like the cerebral cortex, with which it is closely associated, it is a paired structure, with mirror-image halves in the left and right sides of the brain. In humans and other primates, the hippocampus is located inside the medial temporal lobe, beneath the cortical surface. The hippocampus as a whole has the shape of a curved tube, which has been analogized variously to a seahorse, a ram's horn (Cornu Ammonis, hence the subdivisions CA1 through CA4) [56, 83, 84, 92-96]. Hippocampus organization is very similar in both rodents and humans.

The entorhinal cortex (EC), the greatest source of hippocampal input and target of hippocampal output, is strongly and reciprocally connected with many other parts of the cerebral cortex, and thereby serves as the main "interface" between the hippocampus and other parts of the brain. The superficial layers of the EC provide the most prominent input to the hippocampus, and the deep layers of the EC receive the most prominent output [97-98].

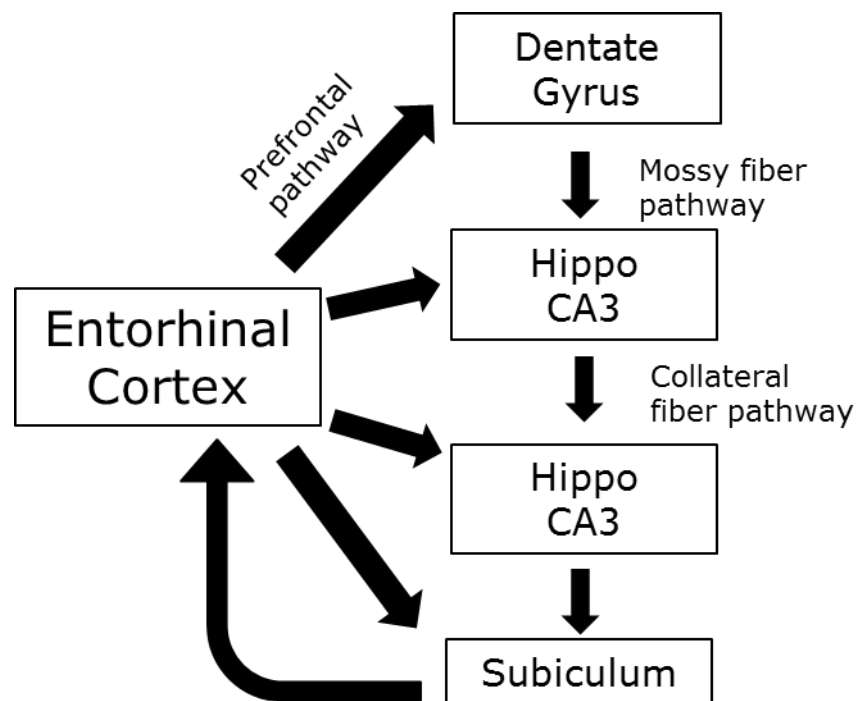


Figure 1.5: Signaling of subfields of hippocampus with entorhinal cortex and subiculum

Within the hippocampus, the flow of information is largely unidirectional, with signals propagating through a series of tightly packed cell layers, first to the dentate gyrus, then to the CA3 layer, to the CA1 layer, to the subiculum, and then out of the hippocampus to the EC (Figure 1.5) . Each of these layers also contains complex intrinsic circuitry and extensive longitudinal connections.

The dentate gyrus is convoluted with hippocampus and is one of the few regions in brain that can regenerate neurons in an adult brain. It is understood the role of dentate gyrus helps in maintaining the neuronal capacity in hippocampus and potentiate glial response in hippocampal injury upon injury to minimize the damage after injury [96-100].

Function and pathology:

Some researchers view the hippocampus as part of a larger medial temporal lobe memory system responsible for general declarative memory (memories that can be explicitly verbalized such as memory for facts in addition to episodic memory) [92-96]. Damage to the hippocampus does not affect specific types of memory, such as the ability to learn new motor or cognitive skills (playing a musical instrument or solving certain types of puzzles) [97, 98].

This fact suggests that such abilities depend on different types of memory (procedural memory) and different brain regions. Recent clinical imaging studies have shown decision making, executive memory and working memory is responsible for short term and long term memory potentiation is gated by prefrontal cortex of brain *via* innervations to hippocampus. Direct axonal afferent and efferent fibers are used to for signaling from prefrontal cortex and hippocampus, and consolidate the process memory and plasticity (Figure 1.6) [106-109].

The classic diseases that are associated with hippocampus are vascular dementia, and amnesia. Entire hippocampal volumes are identified to be reduced in all these classic diseases upon the onset of the diseases. Various clinical reports have shown that the aging brain has reduced volumes of hippocampus. In addition, diseased conditions like schizophrenia and Parkinson’s disease have also had negative effects on the hippocampus [109-116].

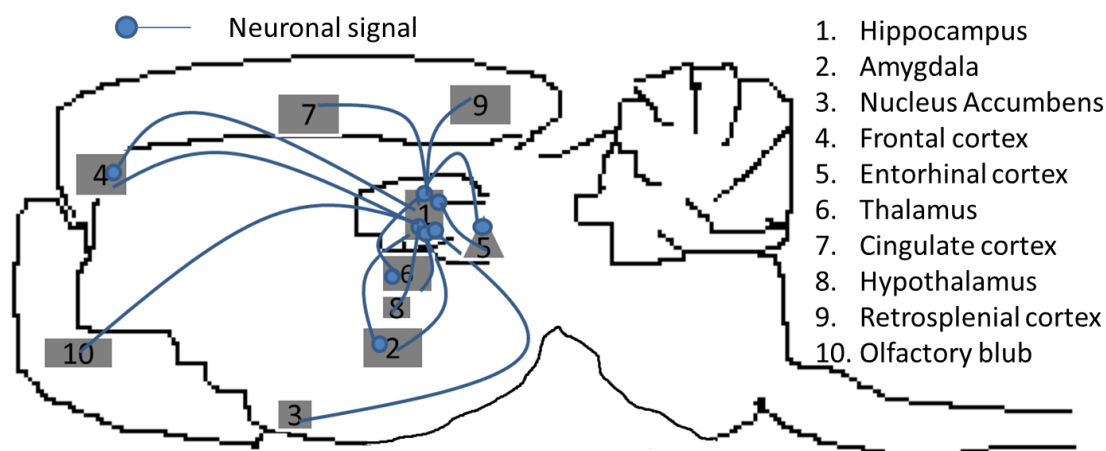


Figure 1.6: Main afferent and efferent connection of hippocampal signaling

Role of hippocampus in BINT:

Cell death was shown in association with traumatic brain injury and with correlations between negative cognition effects and hippocampal dysfunction. Studies using BOP exposure have shown hippocampal injury following BINT in association with cognition; however, the injury mechanisms remain unclear. Multiple exposures to BOP as low as 30KPa, has shown injury to the hippocampus and cognitive impairment [38, 59].

Apoptotic cascades studied by various research groups have shown the involvement of caspase-3 associated cell death in the hippocampus [22, 44, 59, 71]. However the mechanism that leads to the caspase-3 apoptotic cascade in BINT is unknown. More studies are needed to better understand the regulation and pathways of injury that are involved in the hippocampal dysfunction [24, 46, 61, 73]. In addition other cognition regions such as prefrontal cortex should be examined in order to understand the complete account of BINT.

Prefrontal cortex:

Anatomy:

The prefrontal cortex (PFC) is located in frontal cortex of the brain and has dorsal, ventral, lateral, medial regions. Unlike the hippocampus, the organization of the prefrontal cortex is less complicated and relays information to various cognitive regions in the brain [113].

Function and pathology:

The PFC governs the executive control of information processing and behavioral expression, including the ability to selectively attend and maintain information, inhibit irrelevant stimuli and impulses, and evaluate and select the appropriate response [107, 108]. This cognitive and behavioral control facilitates successful achievement of complex goal-directed behaviors. Some evidence suggests that all regions of the PFC (dorsal, ventral, lateral, medial) have the capacity to perform the same type of executive control functions. However, the primary focus of this research is on the medial PFC because this region regulates working memory (memory regulated at the moment of certain action), decision making and executive memory (higher order functions that can influence attention and motor skills) [114-117].

Studies with PTSD support the idea that the ventromedial PFC is an important component for reactivating past emotional associations and events, therefore essentially mediating pathogenesis of PTSD. Treatments geared to the inhibition of the ventromedial prefrontal cortex are suggested for PTSD [118-120]. The right half of the ventrolateral prefrontal cortex, being active during emotion regulation, was activated when participants were offered an unfair offer in a scenario [121-123].

Specific deficits in reversal learning and decision-making have led to the hypothesis that the ventromedial PFC is a major locus of dysfunction in the mild stages of the behavioral variant of fronto-temporal dementia. In addition, studies have shown that PFC can invoke fear and anxiety with its efferent axon fibers to amygdala [124,125] .

Role of prefrontal cortex in BINT:

Many studies have shown the role of hippocampal impairment in conjunction with cognitive impairment [24, 46]. However, other major cognitive regions such as the PFC play an important role in memory related cognitive functions in brain. In addition to working memory, PFC plays a major role in potentiation of long term memories due to its direct innervation of axonal fibers to hippocampus. Although the animal behavioral tests showed impaired cognition in an acute phase, paradigms specific for working and short term memory issues has not been evaluated.

Thus far no animal studies have evaluated the injury crisis in PFC after BOP exposure, although there is a recent clinical report showing evidence of injury in the PFC after blast exposure [17]. In addition, the critical role to evoke fear and anxiety (a typical symptom in BINT) signals to the amygdala makes the PFC an important region in cognition.

Amygdala:

Anatomy:

The amygdaloid complex, located in the medial temporal lobe, is structurally diverse and comprises 13 nuclei. These are further divided into subdivisions that have extensive internuclear and intranuclear connections. In this classification, the amygdala nuclei are divided into three groups [2, 126] (Figure 1.7):

- 1) The deep or basolateral group, which includes the lateral nucleus, the basal nucleus, and accessory basal nucleus
- 2) The superficial or cortical-like group, which includes the cortical nuclei and nucleus of the lateral olfactory tract
- 3) The centromedial group composed of the medial and central nuclei

There is a separate set of nuclei that do not fall into any of these three groups; these include the intercalated cell masses and the amygdalohippocampal area.

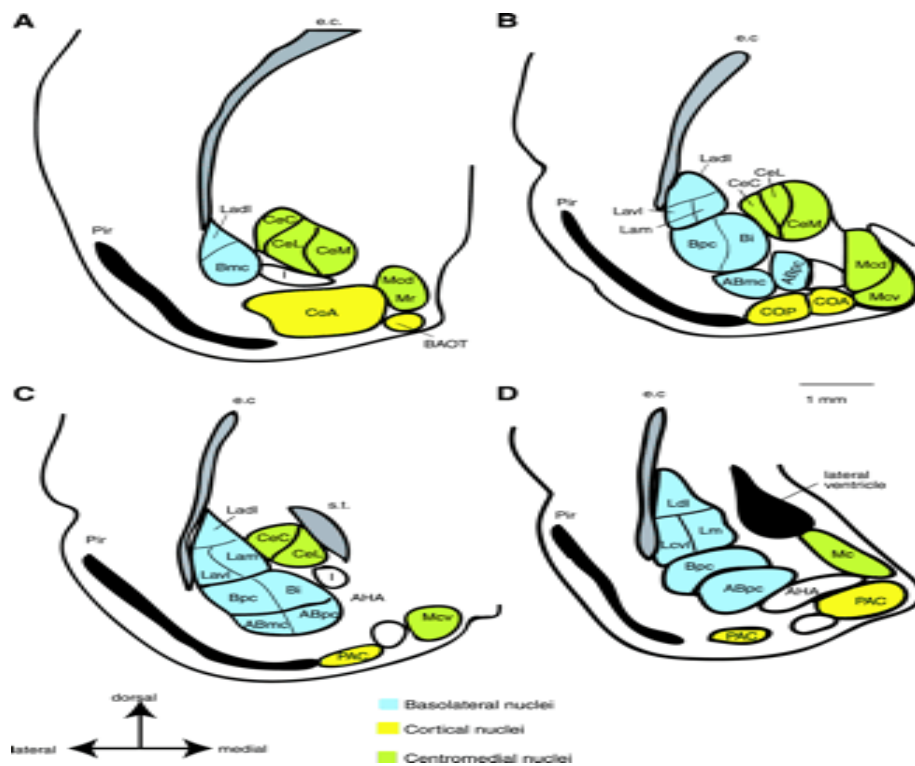


Figure 1.7: Different nuclei of amygdala

ABmc, accessory basal magnocellular subdivision; ABpc, accessory basal parvocellular subdivision; Bpc, basal nucleus magnocellular subdivision; e.c., external capsule; Ladi, lateral amygdala medial subdivision; Lam, lateral amygdala medial subdivision; Lavi, lateral amygdala ventrolateral subdivision; Mcd, medial amygdala dorsal subdivision; Mcv, medial amygdala ventral subdivision; Mr, medial amygdala rostral subdivision; Pir, piriform cortex; s.t., stria terminalis. Sah, P., et al., The amygdaloid complex: anatomy and physiology. physiological reviews, 2003. 83(3):803-834, and used under fair use, 2013.

Functions and pathology:

Inputs to the amygdala can be separated into those arising in cortical and thalamic structures and those arising in the hypothalamus or brain stem. Cortical and thalamic inputs supply information from sensory areas and structures related with memory systems. Hypothalamic and brain stem inputs arise from regions involved in behavior and autonomic systems. The major source of sensory information to the amygdala is the cerebral cortex [127-129]. These projections are glutamatergic, predominantly arising from layer V pyramidal neurons. Most of the sensory information arises from frontal cortex and olfactory lobe of brain (primarily in animals) [3] (Figure 1.8).

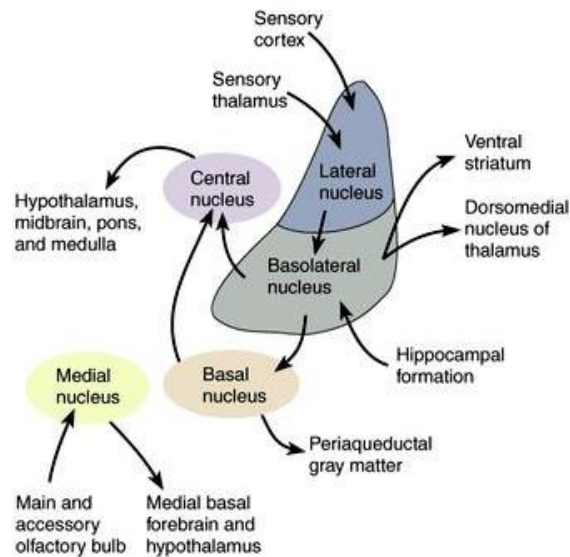


Figure 1.8: Amygdaloid efferent and afferent signals. Mahan, A.L. and K.J., Ressler, Fear conditioning, synaptic plasticity and the amygdala: implications for posttraumatic stress disorder. Trends in Neurosciences, 2012. 35(1):24-35, and used under fair use, 2013.

Efferents of amygdaloid nuclei have widespread projections to cortical, hypothalamic, and brain stem regions. In general, projections from the amygdala to cortical sensory areas are light and originate in cortical and basolateral areas of the amygdala. The perirhinal area, along with other areas in the frontal cortex that project to the amygdala, receive reciprocal connections from periamygdaloid cortex [130-133].

Amygdala is involved in emotional responses, especially in fear and fear conditioning. These responses are characterized by freezing, potentiated startle, release of stress hormones, and changes in blood pressure and heart rate which are elicited by activation of the autonomic and hormonal systems [127, 128]. Damage to this system can potentially initiate the cascades of fear and anxiety in conditions such as PTSD, epilepsy, depression disorders, and TBI [3, 130, 136-138].

Role of amygdala in BINT:

Although clinical research reports showed anxiety as one of the main concerns in BINT, damage to amygdala has not been examined yet in the field of blast over pressure exposure in animal models [10, 11, 27, 28]. Only one animal study showed caspase-3 associated cell injury in amygdala following blast overpressure. However, no assessment of behavioral outcome was done [24].

Nucleus accumbens

Anatomy:

The human nucleus accumbens (NAC), which belongs to the basal ganglia of the brain, is the main part of the ventral striatum. NAC is typically divided into two major subdivisions, the shell and the core (Figure 1.9) [139]. The primary output neurons of both of these areas are medium spiny neurons (MSNs), which are quiescent at rest and depend on the relative input of excitatory and inhibitory synapses to determine when they fire action potentials. These synaptic inputs are, in turn, regulated by a number of neurochemical signaling agents that can ultimately influence information processing in the NAC [140, 141].

Functions and pathology:

NAC is mainly involved in motivation, reward, motor function, and learning. Drugs of abuse increase dopamine release in the NAC and also changes in locomotor activity. Recent studies have demonstrated that the NAC may play an important role in the etiology and pathophysiology of depression [142-145]. Damage to NAC leads to distress, which often times is the cause of substance abuse. The reward system recognizes diminished distress due to substance abuse, which eventually leads to addiction [146-147].

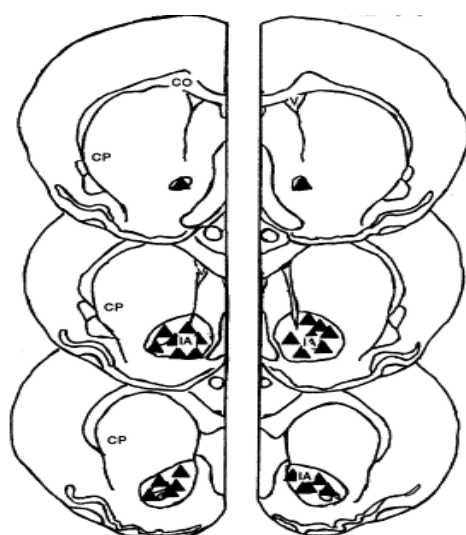


Figure 1.9: Anatomy of nucleus accumbens in coronal view

The NAC contains small populations of γ -aminobutylic acid (GABA)-containing and cholinergic interneurons, in addition to a large number of efferent GABAergic medium spiny projecting neurons. The activity of projecting medium spiny neurons is regulated

by glutamatergic afferents arising from the prefrontal cortex, hippocampus and amygdala, by dopaminergic afferents from the ventral tegmental area, by serotonergic afferents from the raphe nucleus, and by noradrenergic afferents from the locus ceruleus as shown in Figure 1.10 [148-151]. These afferents converge primarily on GABA neurons, the main output cells of this region. In addition, GABAergic projection neurons receive inhibitory input, primarily from a small population of GABAergic and cholinergic interneurons but also through feedforward inhibition and axon collaterals of neighboring medium spiny neurons [151-153].

Role of nucleus accumbens in BINT:

Ongoing clinical research has shown abuse of alcohol and addition to drugs in order to reduce biological distress in relation to BOP exposure [153-156]. Thus far no injury mechanism to understand NAC pathology after BOP exposure is known. Despite the intensive concern over the veterans abusing drugs and involvement of psychosis in NAC role is associated in blunt TBI. However, very limited number of animal studies are available on NAC in order to compare the clinical symptoms of BINT to TBI. NAC plays a very important role in rehabilitation in psychosis, recovery after distress and depression. In order to potentially diagnose and rehabilitate patients suffering from BINT, the role of NAC has to be understood.

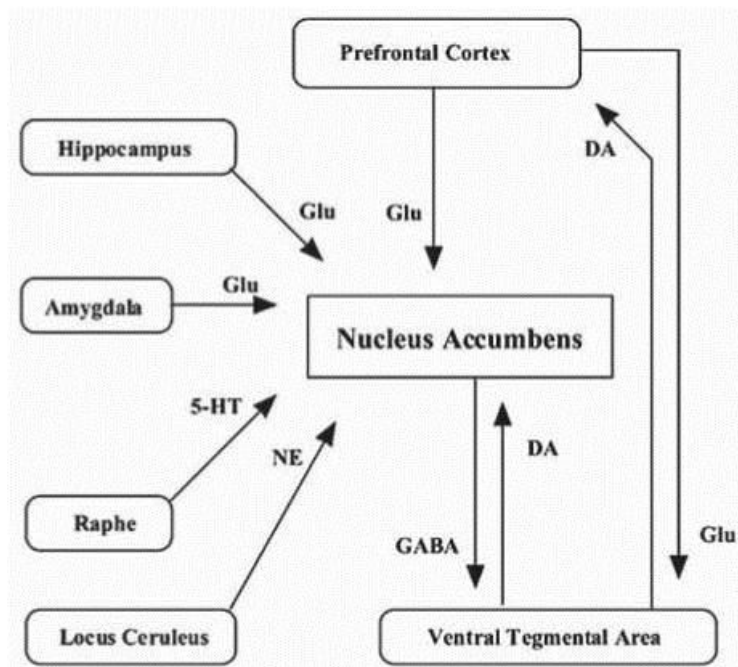


Figure 1.10: Nucleus accumbens afferent and efferent connections to other regions of brain. γ -amino butyric acid, GABA; Glutamate, Glu; Dopamine, DA; Serotonin, 5-HT.

Overall, in order to assess the extent of injury after BOP, studies related to behavioral deficits such as anxiety and memory issues has to be understood at both acute and long term time points. In addition, the neurochemical changes help the understanding of the basic molecular changes and mechanisms for the prognosis of injury. Cell death cascades have to be studied to understand mean peak activation period of the cascade and implication on behavioral deficits. Understanding the cascades of cell death helps in the treatment strategies to diagnose the individuals suffering from BINT.

Chapter 2

Specific Aims and Hypothesis

Hypothesis

Behavioral deficits are caused by acute oxidative stress coupled with acute neurochemical changes following mild blast overpressure exposure.

Specific Aims

The molecular mechanisms and behavioral deficits in accordance with this hypothesis were investigated using an animal model of mild blast induced neurotrauma:

Specific Aim 1:

Neurochemical profiling of the hippocampus, prefrontal cortex, nucleus accumbens and amygdala was determined using magnetic resonance spectroscopy

Hypothesis: Neurochemical changes are triggered in various regions of brain following BOP exposure

Specific Aim 2:

Progression of cell death and astrogliosis was assayed using immunohistochemistry

Hypothesis: Functional deficits at cellular level are caused by oxidative stress resulting active cell death and neurodegeneration along with glial scarring following BOP exposure

Specific Aim 3:

Memory deficits and anxiety behavioral paradigms were used to evaluate functional outcomes.

Hypothesis: Behavioral deficits such as short term memory deficits and anxiety are associated with BOP exposure

Specific Aim 4:

Behavioral changes were correlated with neurochemical, histological, and biomarker results in order to better understand the injury and recovery progression.

Hypothesis: Behavioral deficits such as short term memory deficits and anxiety are associated with neurochemical changes or/and cell death or/and glial scarring

Materials and methods

Blast exposure:

The testing parameters were same for all the molecular and behavioral studies. The shock front and dynamic overpressure was generated by a custom-built shock tube (ORA Inc. Fredericksburg, VA.) as described by VandeVord et al. (2011) [24]. Briefly, a positive phase of peak static overpressure of 117kPa will be produced with compressed helium and calibrated Mylar or Acetate sheets (GE Richards Graphics Supplies Inc., Landsville, PA). Exposure pressures were determined by sensors placed within the tube and one placed inside a sling holding the rat.

Pressure measurements were collected at 250 kHz using a Dash 8HF data acquisition system (Astro-Med, Inc, West Warwick, RI) and shock wave profiles were verified to maintain consistent exposure pressures between subjects. Rats were anesthetized with 3% isoflurane, positioned in the shock tube in a rostral cephalic orientation towards the shock wave. Blast group rats will be exposed to a single incident pressure profile resembling a 'free-field' blast exposure (Figure 2.1 & 2.2). Sham animals were anesthetized with the same isoflurane induction but did not experience the shock wave exposure.

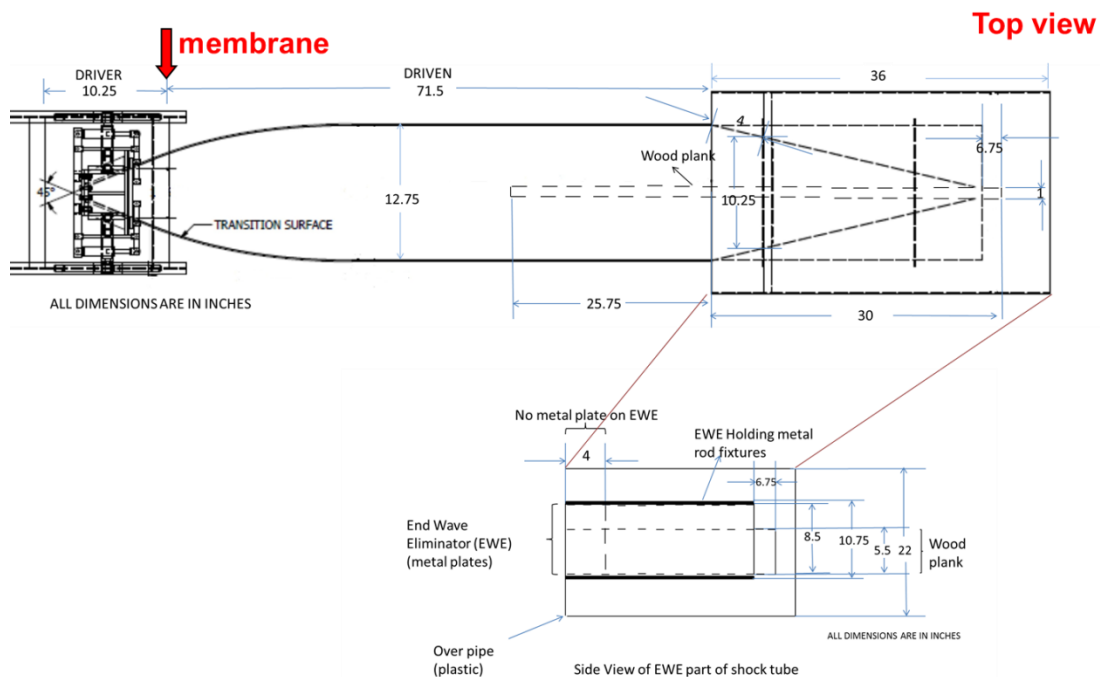


Figure 2.1: Schematic of shock tube with a pressure center calibration set up at the animal location.

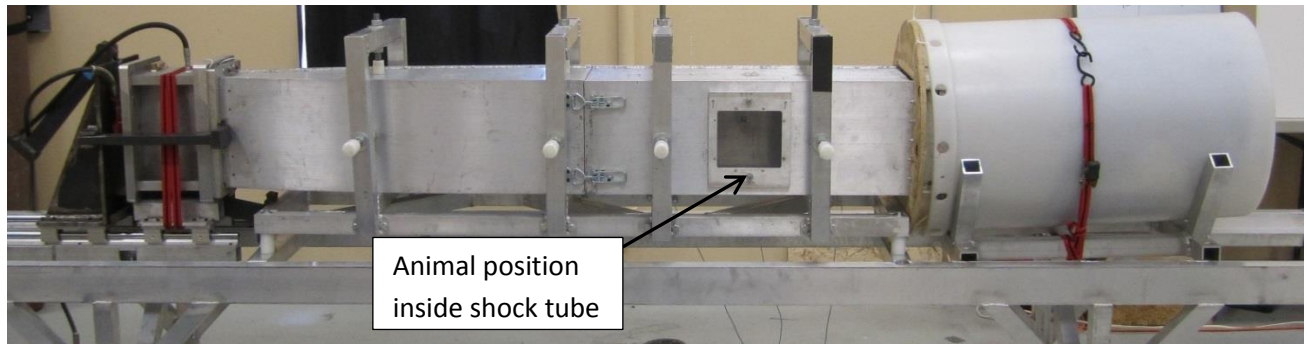


Figure 2.2: Virginia Tech shock tube with an arrow pointing at animal location.

Specific Aim 1:

Neurochemical profiling of hippocampus, prefrontal cortex, nucleus accumbens and amygdala using magnetic resonance spectroscopy (MRS).

Materials and methods:

Proton magnetic resonance spectroscopy (1H-MRS) analysis

After decapitation, whole brains were immediately removed, placed in a chilled brain matrix (ASI, Warren, MI), and cut in 2 mm coronal slices. Slices were frozen on solid CO₂, then two contralateral, 1.5 mm (diameter) punches were taken from the individual slices that contained region of interest. Frozen punches were transferred to micro-centrifuge tubes and stored at -80°C until high resolution magic angle spectroscopy (HRMAS ¹H MRS).

Frozen intact tissue samples were weighed and placed directly into a Bruker zirconium rotor (4 mm diameter, 10 µL capacity) containing 5 µL buffer (pH= 7.4; 100 mM potassium phosphate, 200 mM sodium formate, 1 g/L NaN₃ and 3mM trimethylsilyl-propionate (TSP, Sigma; St Louis, MO) diluted with an equal volume of D₂O containing 0.75% TSP). TSP serves as an internal chemical shift reference (0.00 ppm), formate (8.44 ppm) for phase corrections, and D₂O to lock on the center frequency. The rotor (with sample) was placed into a Bruker magic angle spinning probe maintained at 4°C in a vertical wide-bore (8.9 cm) Bruker 11.7 T magnet with an AVANCETM DRX-500 spectrometer (Bruker Biospin Corp., Billerica, MA). Rotors were spun at 4200 + 2Hz at 54.7° relative to the static magnetic field B₀.

Field inhomogeneities were compensated using first and second order manual and semi-automated shimming. After a pre-saturation pulse for water suppression, tissue

spectra was acquired with a rotor-synchronized 1-D Carr-Purcell-Meiboom-Gill (CPMG) pulse sequence [90-(τ -180- τ) n -acquisition] [32]. The inter-pulse ($\tau = 150 \mu\text{s}$) and the 180° echo pulse was applied ($n=12$ times) for a total echo time $TE = 3.6 \text{ ms}$. The 90 degree pulse length was $6 \mu\text{s}$, 16384 complex data points, $TR = 6.21 \text{ s}$, and a spectral band width of 7 kHz (14 ppm) was used. The number of transients (number of samplings) was 64 with total acquisition time of 3 minutes and 48 seconds.

Signals were acquired with Bruker-XWINNMR (v 3.6 software) and the identical brain regions from all animals in an experimental cohort was analyzed in the same session. Spectra was analyzed with a custom LCModel software package version 6.1-4, utilizing a linear combination of 27 individual neurochemical model spectra (basis set) as well as non-specific lipid signals to fit the tissue spectrum and calculate absolute concentration values for neurochemicals with signals between 1.0 – 4.2 ppm (32) (Figure 2.3).

The precision of the LCModel fit to the spectral data was estimated with Cramér-Rao bounds (CRB); CRB were typically <10% and metabolites with CRB > 25% was not considered for further analysis. LCModel analyzes of sample spectrum as a linear combination of model spectra obtained from the individual standard solutions of known concentrations. Advantages of the LCModel are spectral complexity since multiple chemical shifts (from J-coupling) was used for each compound.

LCModel is also automatic (non-interactive), it adapts to the data and seeks the smoothest line shape and baseline consistent with data. All the data in the 1-4ppm range was used simultaneously in a least squares analysis obtain concentrations, line shapes, referencing shifts, baseline, and phasing (33-35). To account for variations in the mass of individual samples, absolute concentrations of MR visible metabolites was corrected for tissue weight and was expressed as nmol/mg of wet tissue weight; variance associated with means suggests a substantial degree of analytical reproducibility [68, 157, 158].

Peak assignments were based on identical chemical shifts of standards dissolved in the same buffer (identical pH, temperature) which were used for tissue analysis (see methods). The basis set for the customized LCModel used for rat brain also compensated for non-specific lipid resonances at 1.2, 1.4, 1.6, and 1.7 ppm. Lactate,

LAC; Alanine, ALA; γ - amino butyric acid, GABA; N-acetyl aspartate, NAA; N-acetyl aspartate glutamate, NAAG; Glutamate, GLU; Glutamine, GLN; Glutathione, GSH; Succinate, SUC; Aspartate, ASP; Choline, CHO; Phosphocholine, PCH; Glycerophosphocholine, GPC; Betaine, BET; Inositol, INS; Taurine, TAU; Glycine, GLY; Creatine, CRE; Phosphorylethanolamine, PEA.

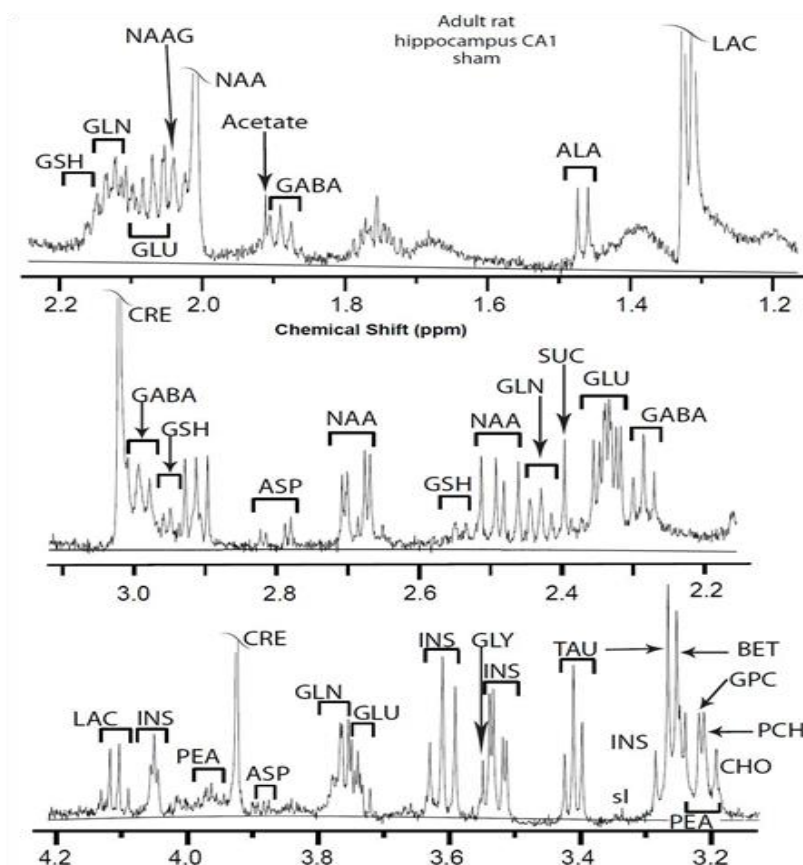


Figure 2.3: Representative HR-MAS ¹H-MRS chemical shift spectrum from ~ 2 mg rat brain hippocampus (256 averages) demonstrates resolution of constituents and sensitivity at 500 MHz.

Specific Aim 2:

Progression of cell death and astrogliosis was assayed using immunohistochemistry

Materials and methods:

Tissue sectioning:

Animals were sacrificed using transcardial perfusion with 4% paraformaldehyde. Fixed brains were embedded with optimal cutting temperature compound (OCT), and were frozen on solid CO₂. Sections were obtained from the area of interest (Hippocampus, Medial prefrontal cortex, amygdala and nucleus accumbens). 40 μ m tissue sections were prepared with a microtome.

Fluoro-Jade B (FJB) analysis:

FJB is a fluorescein dye with high specificity for neuronal degeneration. Sections were stained with Fluoro-Jade B as described [152]. Briefly, brain slices were incubated in 1% NaOH-80% ethanol, hydrated in 70% ethanol, and then washed in distilled water. The sections were subsequently incubated in 0.006% potassium permanganate (Sigma-Aldrich, St. Louis MO) on a rotating stage, rinsed in distilled water, and incubated in a 0.0004% solution of FJB (Histochem Inc., Jefferson, AR). They were then rinsed in distilled water, air-dried and placed on slide warmer until fully dry. The dry slides were cleared in xylene and mounted with 1,3-diethyl-phenylxanthine (Sigma-Aldrich; St. Louis, MO). An observer blind to the experimental conditions carried out counting counts which were based on the morphology, fluorescent intensity, size and location of specific neurons using a Zeiss epifluorescence microscope. The number of FJB+ neurons reported was determined in the entire hippocampus using multiple coronal slices.

GFAP, Iba1, SOD1, NeuN and caspase-3:

Sections (40µm thick) obtained from a microtome were stained with GFAP (astrogliosis) or cleaved caspase-3 (apoptosis). Briefly, tissue sections were first washed in phosphate saline buffer (PBS) and incubated in 0.5% gelatin blocking buffer. Sections were incubated with a primary antibody, anti-GFAP or anti-cleaved caspase-3 (Invitrogen, Grand Island, NY) or anti- Iba-1 (Biocompare, Carsland, CA) or NeuN (Invitrogen, Grand Island, NY) or SOD1 (Biocompare, Carsland, CA), (1:100) overnight at 4°C.

Following PBS wash, the samples were incubated for one and half hour with fluorescent tagged FITC-secondary anti-rat IgG antibodies ((Vector Laboratories, Burlingame, CA), (1:100)) or Alexa flour-555 anti-rabbit IgG antibody (Cell signaling technology Inc, Danvers, MA, (1:100)) avoiding light in the surrounding environment. After a PBS wash, samples were mounted on slides, air dried and coverslipped with prolong anti-fade gold antifade reagent with 4',6-diamidino-2-phenylindole (DAPI) (Invitrogen, Grand Island, NY) avoiding light in the surrounding environment [24].

Sections were examined under Zeiss fluorescence microscope at 20X magnification under appropriate fluorescent filters avoiding light in the surrounding environment. An observer blinded to the experimental conditions carried out cell counting.

Specific Aim 3:

Memory deficits and anxiety behavioral paradigms was used to evaluate functional outcomes.

Materials and methods:

Novel object recognition test:

An opaque black acrylic box with dimensions 80 x 80 x 36 cm was used for the task.

Animals were acclimated to the box for 3 days before BOP exposure. The animals that were subjected to the testing will undergo two tasks with a delay of 20 minutes between each trial for working memory evaluation.

The first task (T1) involved the exposure of animal to identical “familiar” objects for 5 minutes. In the second the task (T2), animals were exposed to a “familiar” object (same object used in the first task) and a novel object with which the animal was never exposed (Figure 2.4).

To eliminate the bias towards the objects, orientation of the animal when placed into the chamber was done such that animals does not get a first look on any of the objects as shown in the Figure 2.4. The tracking of the tasks were done by EthoVision™ tracking software. Precautions were taken by cleaning the chamber between the trails and the experimenter leaving the room when the experiment is underway [160].

Data collection and exclusion criteria:

The data is collected when the animal “nose point” is facing towards the object with in 1.5x radius of object from the measured from center of the object (arena settings were done EthoVision™ tracking software). The animal that spent more than 75% of its time in T1 at one object will be excluded in the study in order to avoid the animal preferences in the one particular location in the experimental chamber.

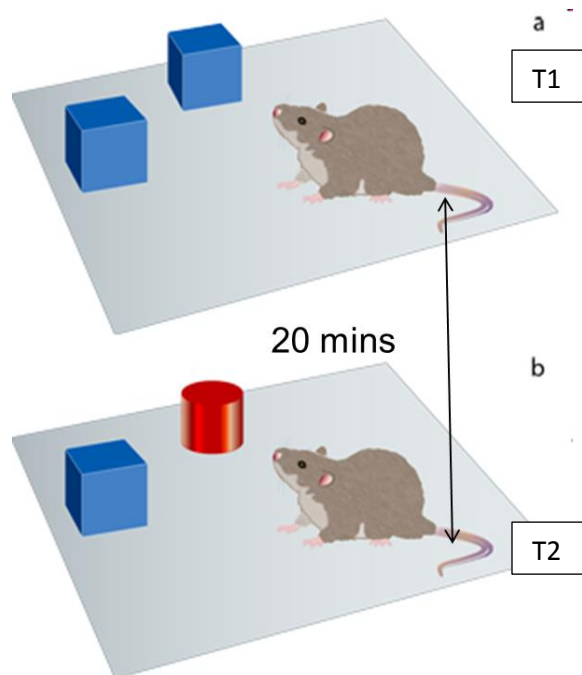


Figure 2.4: Schematic of NOR for working memory.

Light/dark box:

The apparatus consisted of two equal acrylic compartments, one dark side closed with a lid and one light side (Figure 2.5). Rats were placed in the light area, facing away from the dark one, and were allowed to explore the novel environment for 5 min. The number of transfers from one compartment to the other along with the time spent in the light and dark side were measured. This test exploited the conflict between the animal's tendency to explore an open environment (non-anxiety like effect) and to stay in a defensive mode (anxiety like effect) [161].

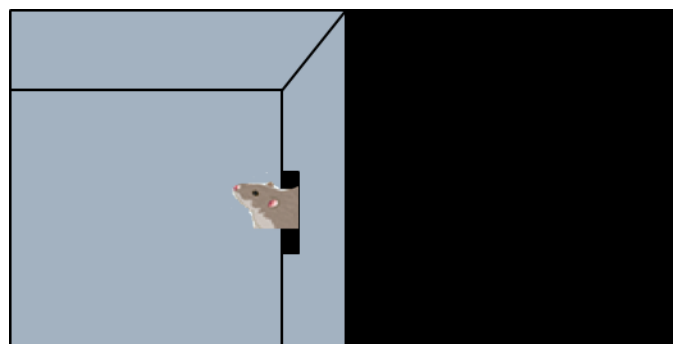


Figure 2.5: Schematic representing an aerial view of light and dark

Specific Aim 4:

Behavioral changes were correlated with neurochemical, histological, and biomarker results in order to better understand the injury and recovery progression.

Materials and methods:

The data obtained from specific aims 1-3 is correlated with specific aim 4 data using Pearson correlation or linear regression analysis.

Statistics:

Effects of blast exposure were measured in separate experiments. In each experiment, separate sham animals served as respective comparison groups to control for unknown influences (e.g. residual effects of isoflurane). Thus, statistical differences between sham and blast exposed rats were assessed with two tailed Student's t-test with $p < 0.05$ considered significant. A two tailed repeated measured ANOVA is used for the behavioral testing to find the differences associated with learning in novel object recognition paradigm with Bonferroni post hoc test. $p < 0.05$ was considered statistically significant. Pearson correlation or linear regression is used to correlate levels of neurochemical with behavior outcome following blast overpressure exposure. Unless indicated otherwise, data were presented as mean \pm standard error of the mean (SEM).

Chapter 3

Blast-induced neurotrauma leads to neurochemical changes and neuronal degeneration in the rat hippocampus

Venkata Siva Sai Sujith Sajja¹, Matthew P. Galloway², Farhad Ghoddoussi², Dhananjeyan Thiruthalinathan³, Andrea Kepsel³, Kathryn Hay³, Cynthia A. Bir³ and Pamela J. VandeVord^{3,4}

¹School of Biomedical Engineering and Sciences, Virginia Polytechnic Institute and State University, Blacksburg, VA

²Psychiatry and Behavioral Neurosciences, and ³Anesthesiology, Wayne State University, Detroit, MI

³Department of Biomedical Engineering, Wayne State University, Detroit, MI

⁴Veterans Affairs Medical Center, Detroit, MI

Abstract

Blast-induced neurotrauma (BINT) is a major concern due to the complex expression of neuropsychiatric disorders after exposure. Disruptions in neuronal function, proximal in time to the blast exposure, may eventually contribute to the late emergence of the clinical deficits. Using magic angle spinning ^1H magnetic resonance spectroscopy and a rodent model of blast-induced neurotrauma, we find acute (24-48 hrs) decreases in succinate, glutathione, glutamate, phosphorylethanolamine, and GABA, no change in N-acetylaspartate, and increased glycerophosphorylcholine, alterations consistent with mitochondrial distress, altered neurochemical transmission, and increased membrane turnover. Increased levels of apoptotic markers Bax and caspase-3 suggested active cell death, consistent with increased Fluorojade B staining in hippocampus. Elevated levels of glial fibrillary acidic protein suggested ongoing inflammation without diffuse axonal injury measured by no change in β -amyloid precursor protein. In conclusion, BINT induces a metabolic cascade associated with neuronal loss in the hippocampus in the acute period following blast-induced neurotrauma.

Keywords: neurotrauma, apoptosis, ^1H -MRS, blast, hippocampus

Introduction

Blast-induced neurotrauma (BINT) or blast-induced traumatic brain injury is a serious health concern of individuals exposed to blast during their combat experience [1,2]. Cognitive functions, such as attention, memory, language and problem solving skills are negatively affected as a result of BINT [3,4]. These neurological disorders have a higher incidence in blast environments as compared to other BINT associated symptoms such as tinnitus [5]. Furthermore, late-emerging behavioral deficits in mood, anxiety, impulsivity, and emotional outbursts often confound a differential diagnosis because of similar symptoms associated with posttraumatic stress disorder (PTSD) [6-11]. Thus, due to the tardive nature of symptoms and comorbidity with PTSD, BINT-related deficits are substantially under-diagnosed [12,13]. The delayed appearance of symptoms is a critical factor in the underreporting of BINT and therefore discovery of predictive biomarkers around the time of exposure might enhance treatment strategies. Besides complications with differential clinical diagnosis, the biomolecular mechanism underlying BINT that gives rise to cognitive deficits is poorly understood.

Human and animal studies have provided evidence of cognitive deficits following BINT [5,6, 14-17]. However the molecular cascades that are triggered by the blast energy transmission have not been identified. In contrast, impact-related traumatic brain injury is well described and is characterized by diffusion axonal injury and cell death. Alterations in neurochemistry are reported to play a key role in these negative outcomes [18-20]. Therefore, investigating if similar neurochemical shifts occur in blast neurotrauma will allow for clinically translatable research.

Magnetic resonance spectroscopy (MRS) offers a unique non-invasive approach for assessing the metabolic status of brain in vivo both in humans and animals, therefore this approach may provide a best fit to study neurotrauma. Recent studies have demonstrated the importance of MRS in the field of traumatic brain injury [21-23]. The number of MR-visible neurochemicals in MRS at clinical field strengths up to 4 Tesla include N-acetyl aspartate (NAA—which also includes some signal from N-acetyl-aspartylglutamate), total choline (tCho—a combination of free choline (CHO), glycerophosphorylcholine (GPC) and phosphorylcholine (PCH)), creatine (Cre—

including phosphocreatine) glutamate (GLU), glutamine (GLN), γ - amino butyric acid (GABA) , and myo-inositol (INS) [24,25]. NAA is a major peak in the 1H-MRS spectrum and is localized to adult neuronal mitochondria. It has been used as a clinical marker of neuronal integrity in different neurological disorders such as Amyolateral Sclerosis ALS and stroke [26,27]. Glutamate is the main excitatory neurotransmitter in brain and is implicated in excitotoxicity which is a probable cause in traumatic brain injury (TBI) etiology.

In this study, we used a special application of MRS, high resolution magic angle spinning (HR MAS) MRS for studying intact brain tissue excised from the rat. Although this particular technique is invasive and performed ex vivo, it has several advantages such as providing considerable anatomic resolution and increasing the number of neurochemicals (about 25) measured with more accuracy as a result of better spectral resolution. Furthermore, it requires no physical disruption of the brain tissue. Thus, the results have direct translational capability since the chemical shift spectral region is identical to that measured in clinical scanners.

The objective of this study was to investigate both the neurochemical and cellular responses in the acute (24 and 48 hours) period after exposure to low level blast waves. Given the cognitive impairments and mood disorders associated with BINT, we focused on potential effects in the rat hippocampus [4, 5, 28, 29].

Furthermore, we determined levels of protein markers for apoptosis (Bax, Bcl-2, caspase 3), diffuse axonal injury (β -amyloid precursor protein), neurodegeneration (FluoroJade B) and inflammation (GFAP) using Western blotting and immunohistochemistry to investigate potential biochemical cascades associated with neurodegeneration. Overall, the data are consistent with the hypothesis that mitochondrial oxidative stress and an active neurodegenerative process occur in the hippocampus in the acute period following BINT.

Materials and methods

Animals and testing parameters

The Wayne State University Institutional Animal Care and Use Committee approved experimental protocols described herein. Prior to all experiments, male Sprague Dawley rats (~250 g, Harlan Labs, San Diego) were acclimated for at least three days (12 hr light/dark) and food and water provided ad lib. The shock front and dynamic overpressure was generated by a custom-built shock tube (0.305 m diameter, 6 m shock-producing tube attached to 1 m compression chamber, ORA Inc. Fredericksburg, VA.) located at the Wayne State University Bioengineering Center. A peak static overpressure was produced with compressed helium and calibrated Mylar sheets (GE Richards Graphics Supplies Inc., Landsville, PA). Exposure pressures were determined by sensors placed within the tube (2.4 m apart) and one placed on the platform holding the rat. Pressure measurements were collected at 250 kHz using a Dash 8HF data acquisition system (Astro-Med, Inc, West Warwick, RI) and shock wave profiles were verified to maintain consistent exposure pressures between subjects. Rats were harnessed and positioned in the tube 1.09 m from the open end with a rostral cephalic orientation towards the shock wave (Figure 3.1). Rats were exposed to a single incident pressure profile resembling a 'free-field' blast exposure. Additionally, the harness was attached to a sled to reduce the dynamic pressure load and prevent translation of the entire body [30]. The animals were anesthetized with 3% isoflurane and exposed to peak overpressure of 117 kPa for 7.5 msec duration, while control animals were anesthetized with 3% isoflurane but did not experience the overpressure. Given that we were interested in the enduring effects of the blast, that there were no fatalities, and that the animals (including controls) were anesthetized during blast exposure, we deemed that collection of physiological parameters at the time of the blast was not germane to the tested hypothesis. Animals (histology group; n=5 sham and 5 blast at 24 hours and 48 hours. 1H-MRS group; n=5 sham and n = 5 blast at 24 hours, n= 9 sham and n=10 blast at 48 hours) were sacrificed by decapitation (MRS studies) or cardiac perfusion (histology studies) at either 24 or 48 hours following blast.

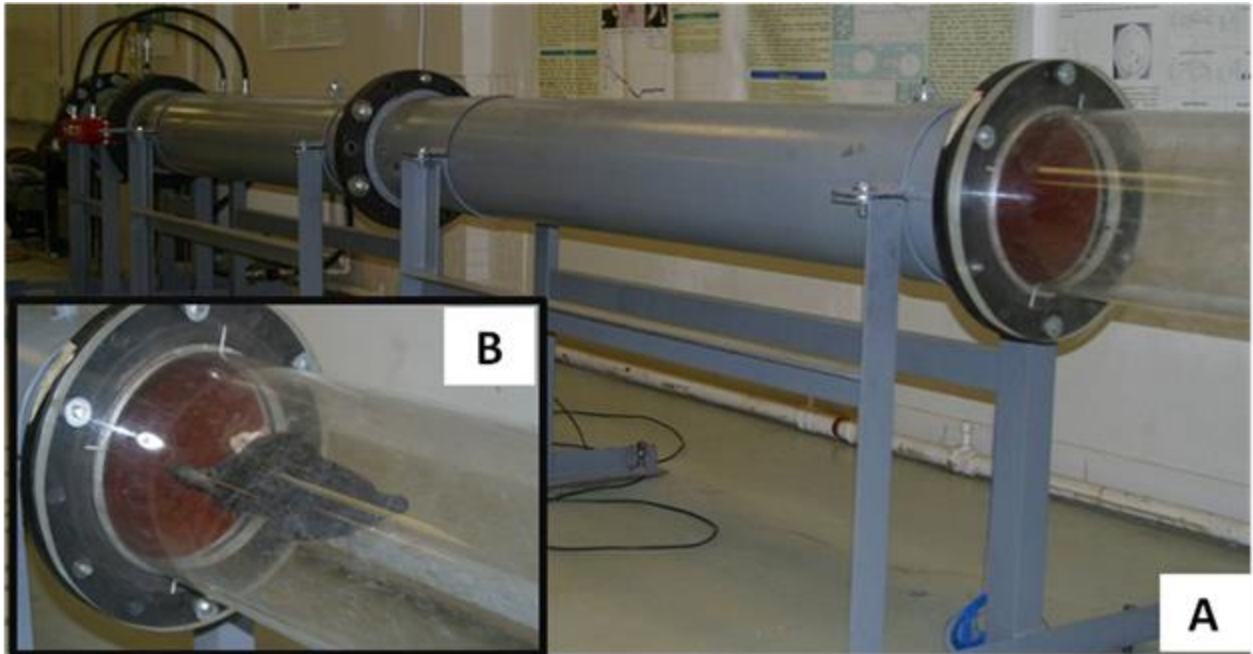


Figure 3.1: (A) The Wayne State University Bioengineering shock tube generates a consistent shock wave profile. (B) The placement of the animals is 1.09 m into the shock tube

1H-MRS analysis

After decapitation, whole brains were immediately removed, placed in a chilled brain matrix (ASI, Warren, MI), and cut in 2 mm coronal slices. Slices were frozen on solid CO₂, then two contralateral, 1.5 mm (diameter) punches taken from the individual slices that contained the regions of interest. The 1.5 mm diameter punch was centered approximately 2 mm from the midline with the dorsal border tangential to the cortical-hippocampal fissure and contained elements of CA1, CA2, and CA3 as well as dentate gyrus [31]. Frozen punches were transferred to micro-centrifuge tubes and stored at -80°C until HR-MAS 1H MRS.

Frozen intact tissue samples were weighed (~2 mg) and placed directly into a Bruker zirconium rotor (4 mm diameter, 10 μ L capacity) containing 5 μ L buffer (pH= 7.4; 100 mM potassium phosphate, 200 mM sodium formate, 1 g/L NaN₃ and 3mM trimethylsilyl-propionate (TSP Sigma; St Louis, MO) diluted with an equal volume of D₂O containing 0.75% TSP). TSP serves as an internal chemical shift reference (0.00 ppm), formate (8.44 ppm) for phase corrections, and D₂O to lock on the center frequency. The rotor (with sample) was placed into a Bruker magic angle spinning probe maintained at 4°C in a vertical wide-bore (8.9 cm) Bruker 11.7 T magnet with an

AVANCETM DRX-500 spectrometer (Bruker Biospin Corp., Billerica, MA). Rotors were spun at 4200 + 2Hz at 54.7° relative to the static magnetic field B₀.

Field inhomogeneities were compensated using first and second order manual and semi-automated shimming. After a pre-saturation pulse for water suppression, tissue spectra were acquired with a rotor-synchronized 1-D Carr-Purcell-Meiboom-Gill (CPMG) pulse sequence [90-(τ -180- τ)n-acquisition] [32]. The inter-pulse ($\tau = 150 \mu\text{s}$ and the 180° echo pulse was applied n=12 times) for a total echo time TE = 3.6 ms. The 900 degree pulse length was 6 μs , acquisition time = 1.169 s, 16384 complex data points, TR = 6.21 s, and a spectral band width of 7 kHz (14 ppm) was used. The number of transients (number of samplings) was 64 with total acquisition time of 3 minutes and 48 seconds.

Signals were acquired with Bruker-XWINNMR (v 3.6 software) and the identical brain regions from all animals in an experimental cohort were analyzed in the same session. Spectra were analyzed with a custom LCModel software package version 6.1-4, utilizing a linear combination of 27 individual neurochemical model spectra (basis set) as well as non-specific lipid signals to fit the tissue spectrum and calculate absolute concentration values for neurochemicals with signals between 1.0 – 4.2 ppm [32] (Figure 3.2).

The precision of the LCModel fit to the spectral data was estimated with Cramér-Rao bounds; CRB were typically <10% and metabolites with CRB > 25% were not considered for further analysis. LCModel analyzes of sample spectrum as a linear combination of model spectra obtained from the individual standard solutions of known concentrations. Advantages of the LCModel are spectral complexity since multiple chemical shifts (from J-coupling) are used for each compound. LCModel is also automatic (non-interactive), it adapts to the data and seeks the smoothest line shape and baseline consistent with data. All the data in the 1-4ppm range are used simultaneously in a least squares analysis obtain concentrations, line shapes, referencing shifts, baseline, and phasing [33-35]. To account for variations in the mass of individual samples, absolute concentrations of MR visible metabolites were corrected for tissue weight and are expressed as nmol/mg of wet tissue weight; variance associated with means suggests a substantial degree of analytical reproducibility [36].

Immunohistochemistry

Fluoro-Jade B (FJB) analysis

FJB is a fluorescein dye with high specificity for neuronal degeneration (Schmued and Hopkins, 2000). Fixed brains were embedded with optimal cutting temperature compound (OCT) (Sakura Finetek USA, Inc., Torrance, CA) then frozen on solid CO₂. Starting at the rostral pole of the hippocampus and ending at the caudal pole, 40 μm tissue sections were prepared with a microtome. Sections were obtained from the area ranging from bregma -2.04 to bregma -4.08. Sections were stained with Fluoro-Jade B as described [37]. Briefly, brain slices were incubated in 1% NaOH-80% ethanol, hydrated in 70% ethanol, and then washed in distilled water. The sections were subsequently incubated in 0.006% potassium permanganate (Sigma-Aldrich, St. Louis MO) on a rotating stage, rinsed in distilled water, and incubated in a 0.0004% solution of FJB (Histochem Inc., Jefferson, AR). They were then rinsed in distilled water, air-dried and placed on slide warmer until fully dry. The dry slides were cleared in xylene and mounted with 1,3-diethyl-phenylxanthine (Sigma-Aldrich; St. Louis, MO). An observer blind to the experimental conditions carried out cell counting; counts were based on the morphology, fluorescent intensity, size and location of specific neurons using a Zeiss epifluorescence microscope. The number of FJB+ neurons reported was determined in the entire hippocampus using multiple coronal slices.

β-Amyloid precursor protein (β-app), and caspase-3

Microtome slices were obtained as noted above and tissue sections evaluated for levels of β-APP and caspase-3. Brain slices were washed with phosphate buffered saline (PBS), placed in citrate buffer and incubated at 70-80°C for 1 hour. The samples were thoroughly washed with PBS, placed in 0.3% H₂O₂ at room temperature for 1 hour and then washed with PBS. Slices were incubated overnight in goat serum containing primary antibodies for β-APP (1:250) (Invitrogen Inc., Carlsbad, CA) or cleaved caspase-3 (1:100) (Cell Signaling, Danvers, MA). Following a PBS wash, the samples were incubated for 1 hour with secondary anti-rabbit IgG antibodies (Vector Laboratories, Burlingame, CA). After a PBS wash, samples were placed for 1 hour in avidin biotin conjugate (Vector Laboratories, Burlingame, CA), washed with PBS, then incubated in

DAB peroxidase substrate (Vector Laboratories, Burlingame, CA) for 5 min. The samples were cleared in xylene, air dried and coverslipped with Permount (Fisher Inc., Fair Lawn, NJ). Sections were examined at 200X on a Zeiss AxioVision microscope by a blinded observer and analysis was conducted with 200x magnification.

Western blotting

A contralateral punch from the same brain slice used for 1H-MRS was weighed then homogenized in a lysis buffer (40mM Tris-HCl, pH 7.5, 150 mM NaCl, 2.5 mM EDTA, pH 8.0, 1% v/v Triton X-100, and 1:10 diluted protease inhibitor cocktail (Sigma-Aldrich Inc. St. Louis, MO). Protein samples (5 µg) were separated on a 12% polyacrylamide gel (Bio-Rad Inc), and transferred electrophoretically to a PVDF membrane (Bio-Rad, Hercules, CA) [38]. The membrane was blocked with 5% nonfat dry milk in TRIS buffered saline (TBS)-Tween 20 (0.1%) then incubated with primary antibodies (anti-Bax (1:500), anti-Bcl2 (1:250) (Santa Cruz Inc., Santa Cruz, CA), anti-β actin (1:5000) (Sigma-Aldrich Inc. St. Louis, MO), or anti-GFAP (1: 500) (Millipore, Billerica, MA) at 4°C overnight. The antibodies were detected using HRP-conjugated anti-rabbit IgG or anti-mouse secondary antibodies (1:2000) (Santa Cruz, Inc., Santa Cruz, CA) as appropriate. Image J software is used to perform densitometry after the blots were developed using chemiluminescence [39].

Statistics

Effects of blast exposure were measured in two separate experiments (i.e. 24 and 48 hours). In each experiment, separate sham-treated animals served as respective comparison groups to control for unknown influences (e.g. residual effects of isoflurane). Thus, statistical differences between sham and blast exposed rats were assessed with Student's t-test or ANOVA with $p < 0.05$ considered significant. Unless indicated otherwise, data are presented as mean + standard error of the mean (SEM).

Results

Neurochemical assessment by 1H-MRS

Given the relatively short period (24-48 hr) between blast exposure and tissue analysis, we focused on metabolome changes as they relate to disrupted energy homeostasis

rather than long term neurotoxicity and loss of neuropil. This approach is reinforced by the observation that disrupted mitochondrial energy status and the resultant oxidative stress is a key pathway that is activated in the early stages after brain injury [40,45]. The levels of succinate, glutamate, GABA, glutathione, alanine, and phosphorylethanolamine (PEA) decreased significantly 24 hours after BINT (Figure 3.2). Levels of N-acetylaspartate, lactate, creatine, taurine, betaine, myo-inositol and glutamine were not significantly different from their respective sham-treated subjects when measured either at 24 or 48 hours post-BINT.

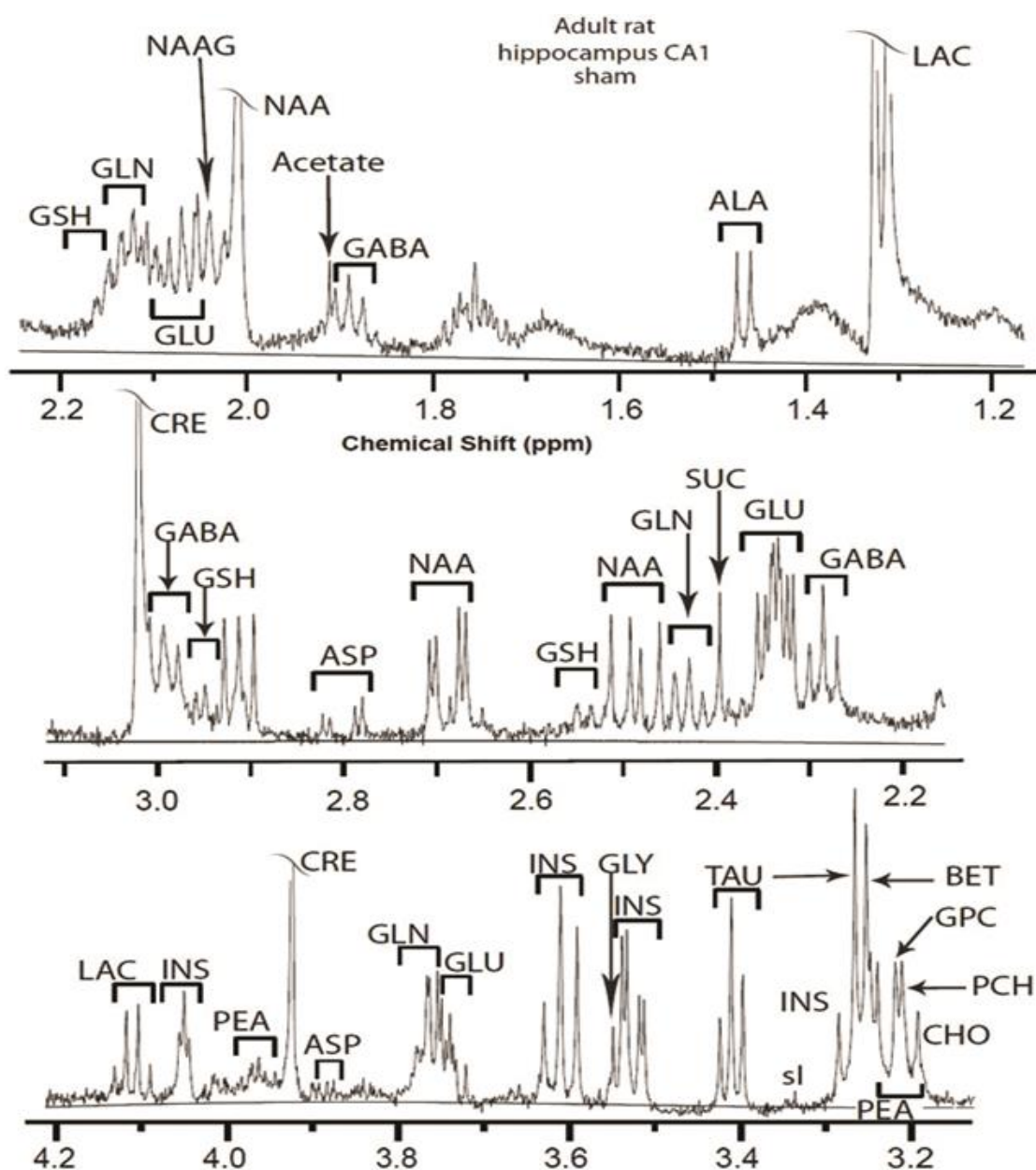


Figure 3.2: Chemical shift spectrum from ~2 mg of rat brain hippocampus (256 averages) demonstrates the resolution of constituents and sensitivity at 500 MHz. Peak assignments are based on identical chemical shifts of standards dissolved in the same buffer (identical pH, temperature) as used for tissue analysis (see Materials and

methods). The basis set for the customized LCModel used for rat brain also compensates for nonspecific lipid resonances at 1.2, 1.4, 1.6 and 1.7 ppm

Lactate, LAC; Alanine, ALA; γ - amino butyric acid, GABA; N-acetyl aspartate, NAA; N-acetyl aspartate glutamate, NAAG; Glutamate, GLU; Glutamine, GLN; Glutathione, GSH; Succinate, SUC; Aspartate, ASP; Choline, CHO; Phosphocholine, PCH; Glycerophosphocholine, GPC; Betaine, BET; Inositol, INS; Taurine, TAU; Glycine, GLY; Creatine, CRE; Phosphorylethanolamine, PEA.

There were significant decreases in glutathione (GSH), PEA, and succinate at 48 hours (Figure 3.3). Glycerophosphorylcholine (GPC) levels tended to increase at 24 hours, a trend that was significant when determined at 48 hours post-BINT. Similar to observations with absolute values of neurometabolites, ratios of glutathione, glutamate, succinate, and PEA to creatine decreased 24 hours after BINT; PEA, GSH, and GPC ratios to creatine significantly altered at 48 hours post-BINT. The lactate/succinate ratio significantly increased 24 (but not 48) hours after BINT.

Immunohistochemistry

β -Amyloid precursor protein

Incubation of hippocampal slices with an antibody directed against β -amyloid precursor protein revealed no staining in either the sham or blast exposed animals, suggesting that diffuse axonal injury had not occurred in this brain region in response to blast overpressure (data not shown).

FluoroJade B (FJB)

Analysis of hippocampal neuronal degeneration as determined by FJB staining revealed increased FJB-positive neurons in the CA1 and CA2/ CA3 subfields of the hippocampus (Figure 3.4). The mean of the FJB+ neurons was 116.2 ± 11.3 neurons/mm² and 191.8 ± 68.4 neurons/mm² at 24 and 48 hours after BINT compared to 3.2 ± 0.2 neurons/mm² and 14.8 ± 1.59 neurons/mm² in the 24 and 48 hour sham controls in the total hippocampal region (Figure 3.4).

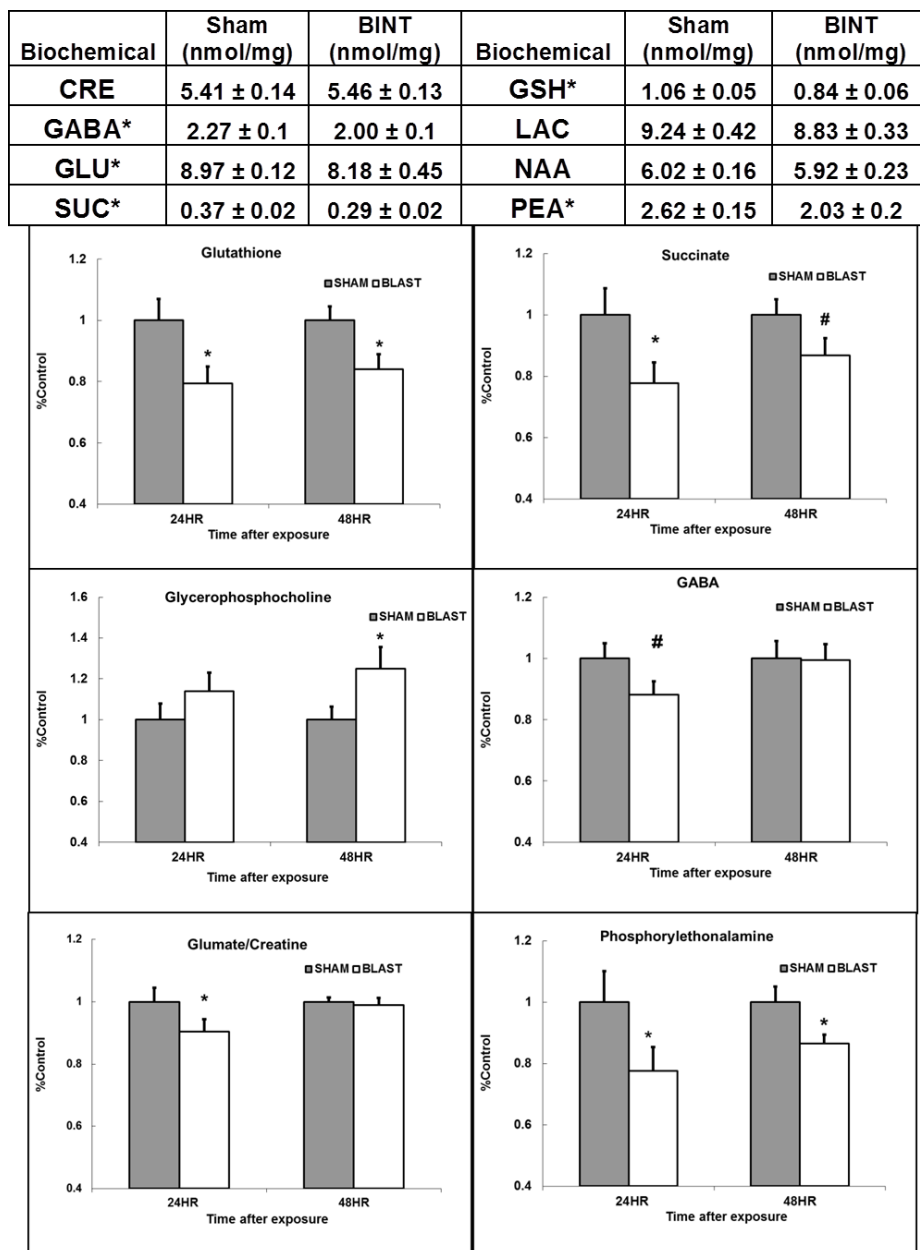


Figure 3.3: Summary of statistically significant changes in MR-visible neurochemical profiles 24 h after blast-induced neurotrauma (BINT). Each bar is the mean and standard error of the mean (SEM) from separate experiments at 24 and 48 h; absolute concentrations are presented in the table. CRE, creatine; GABA, g-aminobutyric acid; GLU, glutamate; GSH, glutathione; LAC, lactate; NAA, N-acetylaspartate; PEA, phosphorylethanolamine; SUC, succinate. *p < 0.05; #p = 0.08

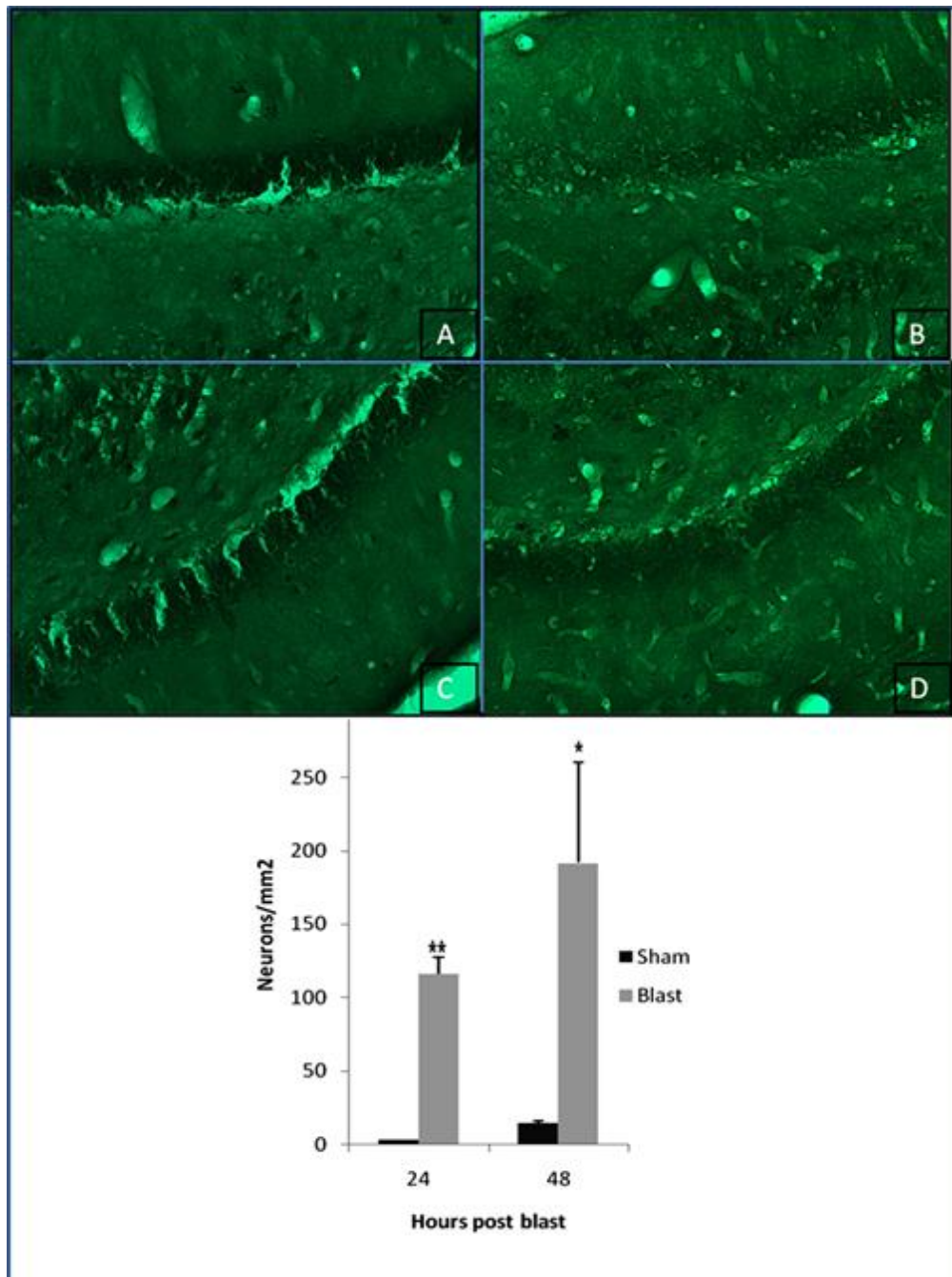


Figure 3.4: Active neurodegeneration in the hippocampus, indicated by positive FluoroJade B (FJB) staining, increased substantially after blast-induced neurotrauma (BINT). Forty-eight hours after BINT, FJB-positive neurons indicate active degeneration in CA1 (A) and CA3 (C) subfields of the hippocampus, whereas sham-treated animals showed minimal FJB-positive staining in CA1 (B) or CA3 (D). Graph depicts the quantification of FJB-positive neurons, revealing a significant increase at both 24 and 48 h after blast overpressure (mean \pm standard error of the mean; * $p < 0.05$; ** $p < 0.001$).

Caspase-3

Expression of the apoptotic marker cleaved caspase-3 showed an increasing trend 24 hours after BINT (289 \pm 86 vs 153 \pm 22 neurons/mm²) and by 48 hours after BINT the trend was significant (370 \pm 17 vs. 66 \pm 20 neurons/mm² $p < 0.001$) (Figure 3.5).

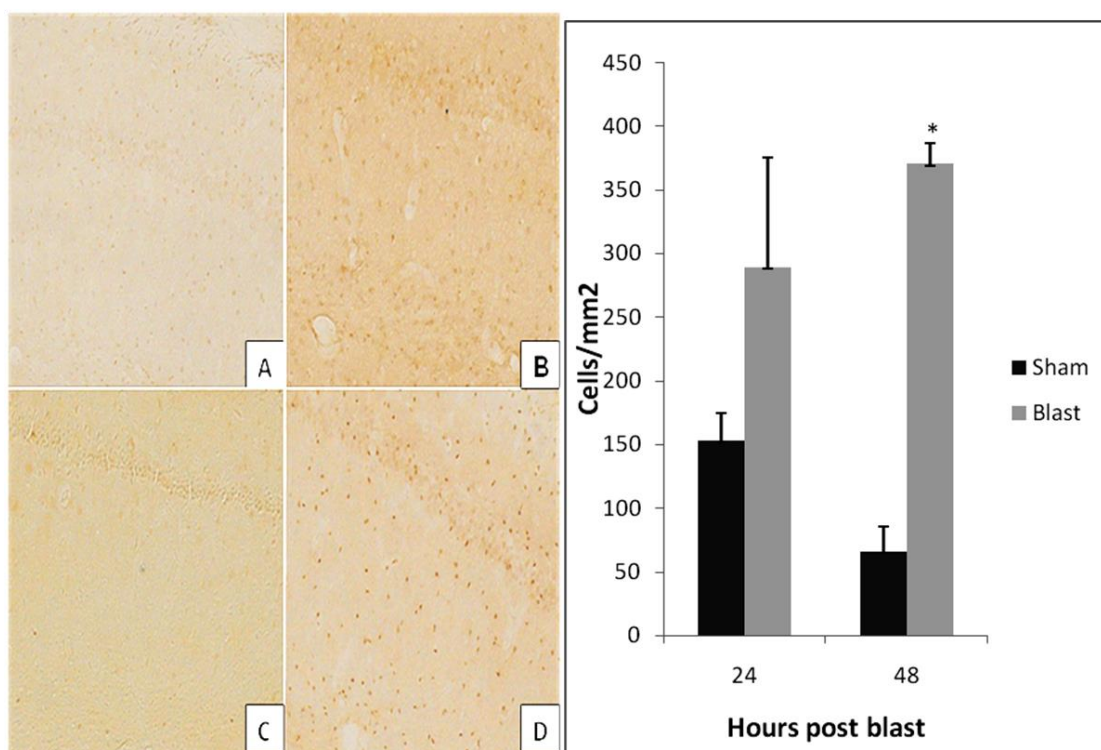


Figure 3.5: Cleaved caspase-3-positive neurons in the CA1 subfield of the hippocampus were increased significantly 48 h after blast-induced neurotrauma (BINT).

Representative sections from the sham group at 24 h (A) and 48 h (C). Although levels of cleaved caspase-3 were increased after 24 h (B), the effect only achieved statistical significance 48 h after BINT (D). Widespread caspase-3-positive cells are observed in the hippocampus (D). The graph depicts the quantification of caspase-3 across experimental groups, revealing a significant increase 48 h after BINT (mean \pm standard error of the mean; * $p < 0.001$).

Western blotting

Additional indices of neurodegeneration in the hippocampal subfields were determined by measuring protein levels of GFAP, Bax and Bcl-2 (all normalized to actin levels). The GFAP- actin ratio increased by 85% ($p < 0.02$) at 24 hours (0.098 ± 0.0013) when compared to the 24 hours sham group (0.053 ± 0.010); there were no significant differences between groups 48 hours after BINT (Figure 3.6). The Bax-actin ratio increased significantly ($P < 0.02$) at 48 (but not 24) hours in animals exposed to overpressure (1.50 ± 0.35) when compared to the sham group (0.65 ± 0.10) (Figure 3.7). Bcl-2/actin ratios were not significantly different from shams when measured either 24 or 48 hours after BINT (data not shown).

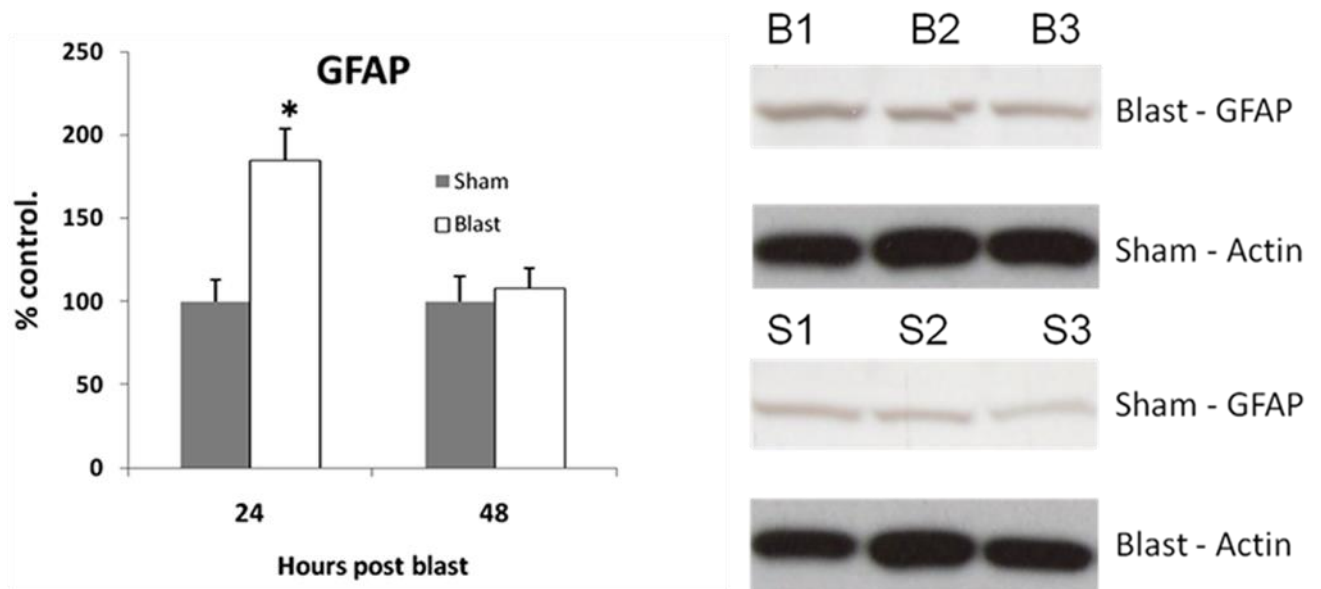


Figure 3.6: Early increase in glial fibrillary acidic protein (GFAP) is followed by a delayed increase in hippocampal Bax. Compared with the respective controls, GFAP, a measure of astrogliosis, increased significantly 24 h (representative blots show blast groups B1–B3 and sham groups S1–S3), but not 48 h, after blast-induced neurotrauma (BINT).

Bars represent mean standard error of the mean (* $p < 0.02$)

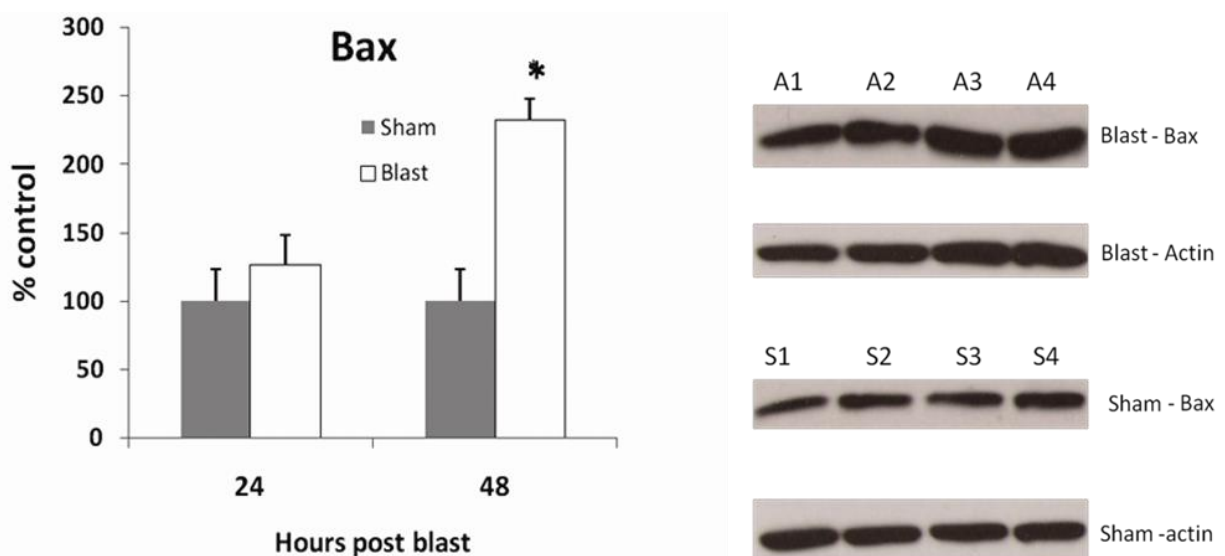


Figure 3.7: Levels of Bax, unchanged at 24 hours, were significantly increased 48 hours after BINT (mean \pm SEM, * $p < 0.01$). Representative blots (A1-A5 are from blast exposed subjects) show increased levels of the apoptotic marker Bax in the blast group as compared to the shams (S1-S5).

Discussion:

Our results demonstrate that exposure to a calibrated blast overpressure induces a neurodegenerative process in the hippocampus of rats when measured in the early period (24-48 hours) after blast. Based on changes in metabolic intermediaries, we

suspect that the neurodegenerative process was a consequence of oxidative stress and mitochondrial dysfunction. Although our observations were determined in the acute phase after BINT, the early vulnerability of the hippocampus may portend behavioral deficits that emerge long after the BINT. Moreover, the degree of hippocampal injury suggests that the common reference to 'low-level' blast may be an inaccurate moniker.

Metabolic response to BINT

Twenty four hours after blast exposure, hippocampal succinate was significantly decreased by 22%, a deficit that lessened to 13% at 48 hours post BINT. This perturbation of a key intermediate in the tricarboxylic acid cycle (TCA) one or two days after blast is consistent with a disruption in the efficiency of oxidative phosphorylation and hence energy status in the hippocampus. Moreover, decreased TCA efficacy will lead to a deficit in NADH and other reducing equivalents and eventually contribute to a milieu of oxidative stress and the increased lactate to succinate ratio (at 24 hr) is consistent with impaired mitochondrial oxidative phosphorylation. Mitochondrial failure is often linked to stimulation of anaerobic glycolysis and change in lactate. However mitochondrial failure is not limited to change in lactate levels. Regulation of succinate and glutathione is highly associated with mitochondrial failure when TCA cycle is compromised and alternative energy pathways (Pentophosphate pathway and GABA shunt) are in function to maintain energy status. Wide range of literature also suggests the role of glutathione and succinate as surrogate marker for mitochondrial dysfunction [41-44].

The mechanism responsible for decreased succinate, either decreased synthesis from α -ketoglutarate or increased conversion to fumarate remains to be determined; however, decreases in succinate, glutamate, and GABA are consistent with decreased activity of the GABA shunt that depends on α -ketoglutarate as a starting substrate.

Compromised activity in the GABA shunt may be a particular concern for maintenance of proper neurotransmission in hippocampal GABA-containing neurons. The absence of change in glutamine levels (or glutamine/glutamate ratios) at 24 or 48 hours indicates a resistance of astroglial mitochondria to the insult and/or a return to equipoise of any potential disruptions in the glutamate-glutamine cycle. Although NAA levels may reflect

acute changes in mitochondrial integrity, levels were unchanged under the present conditions [45-49]. Neither NAA levels nor those of creatine were altered at this early stage after BINT, however the GSH/NAA ratio was significantly decreased at 24 (but not 48) hours, consistent with the relationship of mitochondrial damage posited by Clark [46]. Besides its role in mitochondrial acetate homeostasis, the high concentration of NAA and its localization to neuronal mitochondria make it a surrogate marker of neuronal density in clinical 1H-MRS. The absence of an effect on NAA at these early time points suggests that NAA is not a suitable marker of early hippocampal disruption. Alternatively, the large NAA reserve (~ 5-10 mM) may buffer against significant alterations at this early stage of insult.

Blast-induced decreases in GSH, a major anti-oxidant in neurons, is consistent with a cellular response to increased reactive oxygen species and/or a compromised ability to reduce oxidized glutathione by glutathione:NADPH reductase [41]. Decreased GSH and compromised TCA would also be expected to increase the pentose phosphate pathway in an attempt to maintain NADPH for glutathione reductase. As GSH levels fall, an inability to neutralize oxidized species would also contribute to lipid peroxidation and membrane turnover, as indicated by an increased GPC/PEA ratio at both 24 and 48 hours. Since GPC is the final catabolic species of phospholipase A2 mediated breakdown of membrane PtdCho to produce inflammatory mediators (such as arachidonic acid, prostaglandins, leukotrienes, and platelet activating factor), increased GPC at 24 and 48 hours after blast may reflect an elevated state of inflammation. Ultimately, the loss of energy status may activate apoptotic pathways leading to hippocampal neuronal loss and related clinical deficits.

Cellular response to BINT

Within 24 hours after BINT, GFAP levels increased in the hippocampus, an effect that subsided by 48 hours. Since GFAP is a marker of reactive astrogliosis, the increase at 24 hours is consistent with an early activation of inflammatory astrocytic pathway. GFAP is also commonly unregulated in glial scarring which acts as a physical and interactive barrier for neuronal signaling [50,51]. Reports by Svetlov et al. and Cernak et al. note similar increases in GFAP at 24 hours post insult. Labeling with Fluoro Jade-B, a

marker of neuronal degeneration, also increased at 24, and to a greater extent at 48 hours after BINT suggesting an acute neurodegenerative process in the hippocampus [52, 53]. The absence of change in β -amyloid precursor protein levels after primary blast injury is consistent with other blast related studies and does not support an active diffuse axonal injury typically associated with blunt force trauma to the head [19,54]. To assess for potential cell death after BINT, we evaluated the pro-apoptotic and anti-apoptotic markers caspase-3, Bax, and Bcl-2, respectively. The significant rise in Bax combined with no change in Bcl-2 at 48 hours post exposure indicates an ongoing initiation of apoptosis. The increased expression of caspase-3 suggests an active apoptotic process at 48 hours post blast.

A limitation of our study is animals were anesthetized with isoflurane during the short blast exposure. Isoflurane is neuroprotective could acutely modify levels of glutamate and glutamine by facilitating GABAA receptor mediated inhibition. As such, the effect of blast exposure in a non-anesthetized individual would be predicted to be more extensive than the present observations. Also, neuronal changes (e.g. glutamate release) in the acute period (i.e. <24 hours) after blast as well as the anatomical specificity of the effects, remain to be determined.

Conclusions

Overall the results suggest that exposure to an overpressure from a blast is deleterious to hippocampal cells in the rat. In particular, the metabolic response determined with 1H-MRS is consistent with mitochondrial distress and this loss of mitochondrial integrity is accompanied by histological and molecular evidence of neuronal degeneration and apoptosis. Although the long term effect of overpressure on hippocampal function remains to be determined, the early response noted herein may be related to tardive emergence of clinical symptoms such as depression, emotional outbursts and anxiety associated issues could be addressed. The results also highlight the potential utility of clinical 1H-MRS imaging in the treatment of BINT.

Acknowledgements

The authors thank James Kopacz, Drs. Li Mao and Bin Wu for their expert technical assistance. The expert consultation of Drs. Gregory J Moore and Stanley T. Fricke is greatly appreciated.

Disclosures

No competing financial interests exist.

References

1. Okie S. Traumatic Brain Injury in the War Zone. *New England Journal of Medicine*. 2005; 352:2043-2047.
2. Leung LY, VandeVord PJ, Dal Cengio AL, Bir C, Yang KH, King AI. Blast related neurotrauma: a review of cellular injury. *Molecular Cellular Biomechanics* 2008; 5:155–168.
3. Fausti SA, Wilmington DJ, Gallun FJ, Myers PJ, Henry JA. Auditory and vestibular dysfunction associated with blast-related traumatic brain injury. *Journal of Rehabilitation, Research and Development* 2009; 46:97–810.
4. Trudeau DL, Anderson J, Hansen LM, Shagalov DN, Schmoller, J, Nugent S, Barton S. Findings of mild traumatic brain injury in combat veterans With PTSD and a history of blast concussion. *J. Neuropsychiatry Clinics in Neuroscience* 1998; 10:308-313.
5. Hoge CW, McGurk, D, Thomas JL, Cox AL, Engel CC, Castro CA. Mild traumatic brain injury in U.S. soldiers returning from Iraq. *N. Engl. J. Med.* 2008; 358:453-463.
6. Svetlov SI, Larner SF, Kirk DR, Atkinson J, Hayes RL, Wang KK. Biomarkers of blast-induced neurotrauma: Profiling molecular and cellular mechanisms of blast brain injury. *Journal of Neurotrauma* 2009; 26:913-921.
7. Warden D. Military TBI during the Iraq and Afghanistan wars. *Journal of head Trauma and Rehabilitation* 2006; 21:398-402.
8. Jeffrey VR, Nick LF. Bomb blast, mild traumatic brain injury and psychiatric morbidity: A review. *Injury* 2010; 41:437-443.
9. Bremner JD. The relationship between cognitive and brain changes in posttraumatic stress disorder. *Annals of New York Academy of Sciences* 2006; 1071:80-86.
10. McNally RJ. Cognitive abnormalities in post-traumatic stress disorder. *Trends in Cognitive Sciences* 2006; 10:271-277.

11. Nemeroff CB, Bremner JD, Foa EB, Mayberg HS, North CS, Stein MB. Posttraumatic stress disorder: A state-of-the-science review. *Journal of Psychiatry Research* 2006; 40:1-21.
12. Kochanek PM, Bauman AR, Long JB, Dixon CE, Jenkins LW. Blast-induced traumatic brain injury and polytrauma--a critical problem begging for new insight and new therapies. *Journal of Neurotrauma* 2009; N/A
13. Säljö A, Svensson B, Mayorga M, Hamberger A, Bolouri H. Low-level blasts raise intracranial pressure and impair cognitive function in rats. *Journal of Neurotrauma* 2009; 26:1345-1352.
14. Cernak I, Wang Z, Jiang J, Bian X, Savic J. Cognitive deficits following blast injury-induced neurotrauma: possible involvement of nitric oxide. *Brain Inj.* 2001; 15:593-612.
15. Gottshall KR, Hoffer ME. Tracking recovery of vestibular function in individuals with blast-induced head trauma using vestibular-visual-cognitive interaction tests. *Journal of Neurology and Physical Therapy* 2010; 34:94-97.
16. Pascual JM, Solivera J, Prieto R, Barrios L, López-Larrubia P, Cerdán S, Roda JM. Time course of early metabolic changes following diffuse traumatic brain injury in rats as detected by (1)H NMR spectroscopy. *Journal of Neurotrauma* 2007; 24:944-959.
17. Vandevord PJ, Bolander R, Sajja VS, Hay K, Bir CA. Mild neurotrauma indicates a range-specific pressure response to low level shock wave exposure. *Annals of Biomedical Engineering* 2012; 40(1):227-236
18. Royo NC, Schouten JW, Fulp CT, Shimizu S, Marklund N, Graham DI, McIntosh TK. From cell death to neuronal regeneration: building a new brain after traumatic brain injury. *Journal of Neuropathological and Experimental Neurology* 2003; 62:801-811.
19. Xie M, Tobin JE, Budde MD, Chen CI, Trinkaus K, Cross AH, McDaniel DP, Song SK, Armstrong RC. Rostrocaudal analysis of corpus callosum demyelination and axon damage across disease stages refines diffusion tensor imaging correlations with

pathological features. *Journal of Neuropathological and Experimental Neurology* 2010; 69:704-716.

20. Patel AD, Gerzanich V, Geng Z, Simard JM. Glibenclamide reduces hippocampal injury and preserves rapid spatial learning in a model of traumatic brain injury. *Journal of Neuropathological and Experimental Neurology* 2010; 69:1177-1190.

21. Brooks WM, Friedman SD, Gasparovic C. Magnetic resonance spectroscopy in traumatic brain injury. *J Head Trauma Rehabilitation* 2001; 16(2):149-164

22. Marino S, Ciurleo R, Bramanti P, Federico A, De Stefano N. 1H-MR spectroscopy in traumatic brain injury. *Neurocritical Care* 2011; 14(1):127-133

23. Hunter JV, Wilde EA, Tong K, Holshouser BE. Merging imaging tools for use with traumatic brain injury research. *Journal of Neurotrauma* 2011; 29(4):654-671.

24. Stanley JA, Pettegrew JW, Keshavan MS. Magnetic resonance spectroscopy in schizophrenia: methodological issues and findings—part I. *Biological Psychiatry* 2000; 48:357–368.

25. Moore GJ and Galloway MP. Magnetic resonance spectroscopy: neurochemistry and treatment effects in affective disorders. *Psychopharmacological Bulletin* 2000; 36(2):5-23.

26. Rooney WD, Miller RG, Gelinas D, Schuff N, Maudsley AA, Weiner MW. Decreased N-acetylaspartate in motor cortex and corticospinal tract in ALS. *Neurology* 1998; 50(6):1800-1805.

27. Cirstea CM, Brooks WM, Craciunas SC, Popescu EA, Choi IY, Lee P, Bani-Ahmed A, Yeh HW, Savage CR, Cohen LG, Nudo RJ. Primary motor cortex in stroke: a functional MRI-guided proton MR spectroscopic study. *Stroke* 2011; 42(4):1004-1009

28. Matthews SC, Strigo IA, Simmons AN, O'Connell RM, Reinhardt LE, Moseley SA. A multimodal imaging study in U.S. veterans of Operations Iraqi and Enduring Freedom with and without major depression after blast-related concussion. *Neuroimage* 2011; 54:S69-S75.

29. Macqueen G, Frodl T. The hippocampus in major depression: evidence for the convergence of the bench and bedside in psychiatric research? *Molecular Psychiatry* 2011; 16:252-264.
30. Dal Cengio Leonardi A, Bir CA, Ritzel DV, VandeVord PJ. Intracranial pressure increases during exposure to a shock wave. *Journal of Neurotrauma* 2011; 28:85-94.
31. Franklin KBJ. *The mouse brain in stereotaxic coordinates*, 3rd ed. Amsterdam: Elsevier Academic Press 2008.
32. Cheng LL, Ma MJ, Becerra L, Ptak T, Tracey I, Lackner A, González RG. Quantitative neuropathology by high resolution magic angle spinning proton magnetic resonance spectroscopy. *Proceedings of National Academy of Sciences United States of America* 1997; 94:6408-6413.
33. Provencher SW. Estimation of metabolite concentrations from localized in vivo proton NMR spectra. *Magnetic Resonance in Medicine* 1993; 30:672-679.
34. Provencher SW. Automatic quantification of localized in vivo ¹H spectra with LCModel. *NMR in Biomedicine* 2001; 14:260-264.
35. Cavassila S, Deval S, Huegen C, van Ormondt D, Graveron-Demilly D. Cramer-Rao bounds: an evaluation tool for quantification. *NMR in Biomedicine* 2001; 14:278-283.
36. Ghoddoussi F, Galloway MP, Jambekar A, Bame M, Needleman R., Brusilow WS. Methionine sulfoximine, an inhibitor of glutamine synthetase, lowers brain glutamine and glutamate in a mouse model of ALS. *Journal of Neurological Sciences* 2010; 290:41-47.
37. Schmued LC, Hopkins KJ. Fluoro-Jade B: a high affinity fluorescent marker for the localization of neuronal degeneration. *Brain Research* 2000; 874:123-130.
38. Towbin H, Staehelin T, Gordon J. Electrophoretic transfer of proteins from polyacrylamide gels to nitrocellulose sheets: procedure and some applications. *Proceedings of National Academy of Sciences United States of America* 1979; 76:4350-4354.

39. Haan C, Behrmann I. A cost effective non-commercial ECL-solution for western blot detections yielding strong signals and low background. *Journal of Immunological Methods* 2007; 318:11-19.
40. Cernak I, Wang Z, Jiang J, Bian X, Savic, J. Ultrastructural and functional characteristics of blast injury-induced neurotrauma. *Journal of Trauma* 2001; 50:695-706.
41. Bolaños JP, Almeida A, Moncada S. Glycolysis: a bioenergetic or a survival pathway? *Trends in Biochemical Sciences* 2010; 35:145-149.
42. Keller JN, Guo Q, Holtsberg FW, Brucekeller AJ, Mattson MP. Increased sensitivity to mitochondrial toxin-induced apoptosis in neural cells expressing mutant presenilin-1 is linked to perturbed calcium homeostasis and enhanced oxyradical production. *The Journal of Neuroscience* 1998; 18:4439–4450.
43. Greco T, Fiskum G. Neuroprotection through stimulation of mitochondrial antioxidant protein expression. *Journal of Alzheimers Disease* 2010; 20(2):S427-S437.
44. Brustovetsky N, Dubinsky JM. Dual responses of CNS mitochondria to elevated calcium. *The Journal of Neuroscience* 2000 ;20(1):103-113.
45. Singh IN, Sullivan PG, Deng Y, Mbye LH, Hall ED. Time course of post-traumatic mitochondrial oxidative damage and dysfunction in a mouse model of focal traumatic brain injury: implications for neuroprotective therapy. *Journal of Cerebral Blood Flow Metabolism* 2006; 26:1407-1418.
46. Clark JB. N-acetyl aspartate: a marker for neuronal loss or mitochondrial dysfunction. *Developmental Neuroscience* 1998; 20:271-276.
47. Barker PB. N-acetyl aspartate--a neuronal marker? *Annals of Neurology* 2001; 49:423-424.
48. Moffet JR, Tieman SB, Weinberger DR, Coyle JT, Namboodiri AM A. N-Acetyl aspartate: An unique molecule in central nervous system. New York: Springer 2006.

49. Salek RM, Xia J, Innes A, Sweatman BC, Adalbert R, Randle S, McGowan E, Emson PC, Griffin JL. A metabolomic study of the CRND8 transgenic mouse model of Alzheimer's disease. *Neurochemical International* 2010; 56:937-47.
50. Sofroniew MV. Molecular dissection of reactive astrogliosis and glial scar formation. *Trends in Neurosciences*. 2009; 32:638-647.
51. Buffo A, Rolando C, Ceruti S. Astrocytes in the damaged brain: Molecular and cellular insights into their reactive response and healing potential. *Biochemical Pharmacology* 2010; 79:77-89.
52. Svetlov SI, Prima V, Kirk DR, Gutierrez H, Curley KC, Hayes RL, Wang KK. Morphologic and biochemical characterization of brain injury in a model of controlled blast overpressure exposure. *Journal of Trauma* 2010; 69:795-804.
53. Cernak I, Merkle AC, Koliatsos VE, Bilik JM, Luong QT, Mahota TM, Xu L, Slack N, Windle D, Ahmed FA. The pathobiology of blast injuries and blast-induced neurotrauma as identified using a new experimental model of injury in mice. *Neurobiology of Disease* 2011; 41:538-551.
54. Risling M, Plantman S, Angeria M, Rostami E, Bellander BM, Kirkegaard M, Arborelius U, Davidsson J. Mechanisms of blast induced brain injuries, experimental studies in rats," *Neuroimage* 2011; 54:S89-S97.

Chapter 4

Effects of Blast-Induced Neurotrauma on the Nucleus Accumbens

Venkata Siva Sai Sujith Sajja¹, Matthew P. Galloway², Farhad

Ghoddoussi², Andrea Kepsel³, and Pamela J. VandeVord^{1,3}

¹ School of Biomedical Engineering and Sciences, Virginia Polytechnic Institute and State University, Blacksburg, Virginia

² Department of Psychiatry and Behavioral Neurosciences, and Anesthesiology, Wayne State University, Detroit, MI, USA

³ John D. Dingell Veteran's Administration Medical Center, Detroit, MI, USA

Introduction

Exposure to blast overpressure has been reported to trigger various neurological problems and is often associated with more than one symptom of traumatic brain injury (TBI) such as headaches, tinnitus, distress, irritability, and nausea [1-6]. These outcomes often involve dysfunction in various centers of the brain such as the limbic system, nucleus accumbens (NAC), basal ganglia and frontal lobes. These dysfunctions most likely result from direct damage to the cognitive centers or indirectly through the circuits which connect them. While blast overpressure has been extensively studied in association with injury to the hippocampus [6-11], blast brain injury has been labeled as diffuse [3, 12-14]. As such, damage to other regions of the brain should be thoroughly examined in order to characterize the global effect of blast overpressure on the brain.

Several psychiatric outcomes such as mood, anxiety, impulsivity, and emotional outbursts, have been linked to individuals who have been exposed to blast [15-18]. Blast induced neurotrauma (BINT) has also been reported to be associated with aggression, suicidal tendency and irritability [9, 19]. Further evidence suggests that personnel associated with BINT are more likely to become dependent on alcohol and/or other drugs to diminish the distress which is evoked after blast exposure [20-24]. Cellular injury effects can directly evoke stress-related responses and there is a high risk of substance abuse to counteract the stress [20]. These effects are reported to be caused by changes in neurochemical levels, mainly the monoamine, serotonin and dopamine systems [21, 22].

Few studies have attempted to address the negative neurological outcomes which are a consequence of blast exposure. Moreover, research has been limited to evaluating potential damage to the hippocampus. The need to understand the vulnerability of other cognitive centers is vital to determine the widespread effect that blast has on the brain.

The NAC plays an important role in reward pathways, addiction, aggression and fear which are consequences reported in those suffering from BINT. Furthermore, NAC has direct circuitry connections with the anxiety (amygdala), emotion and memory (hippocampus and prefrontal cortex) centers of the brain [23, 24]. The current study focused on possible injury to the NAC after blast overpressure pressure using an animal

model. Furthermore, studies for pro- and anti-apoptotic markers to further elucidate the cascade of events that may be associated with the neurochemical alternations were conducted. Understanding key centers, such as the NAC, can reduce confounds involved with the differential diagnosis following BINT. It is hypothesized that blast overpressure causes inflammation and neurochemical changes that triggers apoptosis in NAC. This could negatively affect the functional outcome of NAC. These events may lead to stress-related behavioral outcomes and subsequent psychiatric sequelae.

In order to identify and measure alterations in neurochemicals associated with brain injury, high resolution magic angle proton magnetic resonance spectroscopy (HRMAS ¹H-MRS) along with high performance liquid chromatography (HPLC) for monoamine systems is used. The non-invasive nature of clinical ¹H-MRS provides an ideal modality to assess pathological changes in neurochemistry [25]. Despite the extensive use of ¹H-MRS for clinical neuroscience, a definitive understanding of disease-induced alterations in the neurochemical profile is in a nascent stage. Therefore, preclinical ¹H-MRS studies with relevant animal models provide a basis for understanding neurobiological processes as well as informing the interpretation of clinical ¹H-MRS observations. The overall goal of the study was to investigate pathological effects blast overpressure has on the NAC in order to elucidate reports of subsequent adverse changes in behavioral and cognition.

Methods

Animal handling and care

The Wayne State University Institutional Animal Care and Use Committee approved experimental protocols described herein. Prior to all experiments, male Sprague Dawley rats (~250 g, Harlan Labs, San Diego) were acclimated for at least three days (12 hour light/dark) and food and water provided ad lib. Animals (n=5 sham and n=5 blast at 24 hours, n=10 sham and n=10 blast at both 48 and 72 hours) were sacrificed by decapitation.

Testing parameters

The shock front and dynamic overpressure was generated by a custom-built shock tube (0.305 m diameter, 6 m shock-producing tube attached to 1 m exposure chamber, ORA Inc. Fredericksburg, VA.). Previous research by VandeVord et al (2012) determined that an overpressure of 117kPa significantly caused neurological deficits in this rodent model of blast [10]. Briefly, a positive phase of peak static overpressure of 117kPa (7.5 msec duration) was produced with compressed helium and calibrated Mylar sheets (GE Richards Graphics Supplies Inc., Landsville, PA). Exposure pressures were determined by sensors placed within the tube and one placed on the platform holding the rat. Pressure measurements were collected at 250 kHz using a Dash 8HF data acquisition system (Astro-Med, Inc, West Warwick, RI) and shock wave profiles were verified to maintain consistent exposure pressures between subjects. Rats were anesthetized with 3% isoflurane, harnessed and positioned in the tube 1.09 m from the open end with a rostral cephalic orientation towards the shock wave. Blast group rats were exposed to a single incident pressure profile resembling a ‘free-field’ blast exposure (Figure 4.1). Sham animals were anesthetized with the same isoflurane induction but did not experience the shock wave exposure. Animals were sacrificed at 24, 48 and 72 hours following blast exposure for analysis.

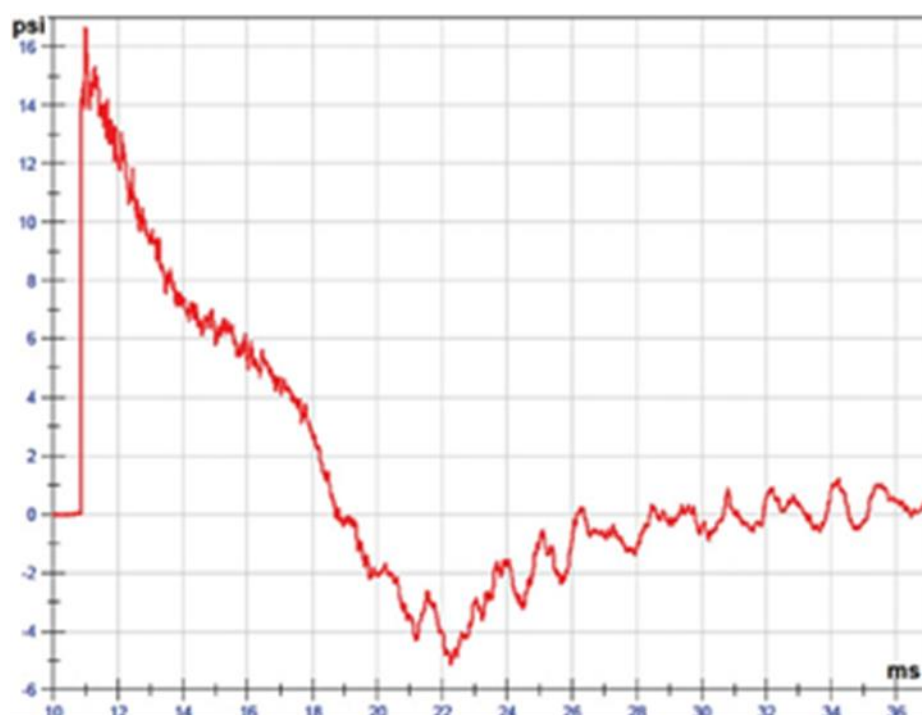


Figure 4.1: Representative pressure profile of the shock wave that is generated from the shock tube.

1H-MRS analysis

After decapitation, whole brains were immediately removed, placed in a chilled brain matrix (ASI, Warren, MI), and cut in 2 mm coronal slices. Slices were frozen on solid CO₂, then two contralateral, 1.5 mm (diameter) punches taken from the individual slices that contained NAC. Frozen punches were transferred to micro-centrifuge tubes and stored at -80°C until HRMAS 1H MRS.

Frozen intact tissue samples were weighed (~2 mg) and placed directly into a Bruker zirconium rotor (4 mm diameter, 10 µL capacity) containing 5 µL buffer (pH= 7.4; 100 mM potassium phosphate, 200 mM sodium formate, 1 g/L NaN₃ and 3mM trimethylsilyl-propionate (TSP Sigma; St Louis, MO) diluted with an equal volume of D₂O containing 0.75% TSP). TSP serves as an internal chemical shift reference (0.00 ppm), formate (8.44 ppm) for phase corrections, and D₂O to lock on the center frequency. The rotor (with sample) was placed into a Bruker magic angle spinning probe maintained at 4°C in a vertical wide-bore (8.9 cm) Bruker 11.7 T magnet with an AVANCETM DRX-500 spectrometer (Bruker Biospin Corp., Billerica, MA). Rotors were spun at 4200 + 2Hz at 54.7° relative to the static magnetic field B₀.

Field inhomogeneities were compensated using first and second order manual and semi-automated shimming. After a pre-saturation pulse for water suppression, tissue spectra were acquired with a rotor-synchronized 1-D Carr-Purcell-Meiboom-Gill (CPMG) pulse sequence [90-(τ-180-τ)n-acquisition] [32]. The inter-pulse (τ = 150 µs and the 180° echo pulse was applied n=12 times) for a total echo time TE = 3.6 ms. The 900 degree pulse length was 6 µs, acquisition time = 1.169 s, 16384 complex data points, TR = 6.21 s, and a spectral band width of 7 kHz (14 ppm) was used. The number of transients (number of samplings) was 64 with total acquisition time of 3 minutes and 48 seconds.

Signals were acquired with Bruker-XWINNMR (v 3.6 software) and the identical brain regions from all animals in an experimental cohort were analyzed in the same session. Spectra were analyzed with a custom LCModel software package version 6.1-4, utilizing a linear combination of 27 individual neurochemical model spectra (basis set) as well as non-specific lipid signals to fit the tissue spectrum and calculate absolute concentration values for neurochemicals with signals between 1.0 – 4.2 ppm [32].

The precision of the LCModel fit to the spectral data was estimated with Cramér-Rao bounds (CRB); CRB were typically <10% and metabolites with CRB > 25% were not considered for further analysis. LCModel analyzes of sample spectrum as a linear combination of model spectra obtained from the individual standard solutions of known concentrations. Advantages of the LCModel are spectral complexity since multiple chemical shifts (from J-coupling) are used for each compound. LCModel is also automatic (non-interactive), it adapts to the data and seeks the smoothest line shape and baseline consistent with data. All the data in the 1-4ppm range are used simultaneously in a least squares analysis obtain concentrations, line shapes, referencing shifts, baseline, and phasing [33-35]. To account for variations in the mass of individual samples, absolute concentrations of MR visible metabolites were corrected for tissue weight and are expressed as nmol/mg of wet tissue weight; variance associated with means suggests a substantial degree of analytical reproducibility [11].

High performance liquid chromatography (HPLC)

Contralateral NAC punch from was weighed, sonically disrupted in 200 μ L of 0.2M HClO₄ and then centrifuged for 15 min to remove cellular debris. A 100 μ L aliquot of the clear supernatant was added to sample vials that were placed in an ESA 542 auto injector. 10 μ L of the sample was injected onto a C18-RP column (300C) with ESA MD-TM mobile phase running at a flow rate of 0.6 ml/min. Coulometric detection was accomplished with an ESA 5011A dual electrode cell and the signal analyzed on a EZChrome Elite data processing platform. Absolute tissue values of (ng/mg) norepinephrine (NE), 3,4-dihydroxyphenylacetic acid (DOPAC), dopamine (DA), 5-hydroxyindoleacetic acid (5HIAA), homovanillic acid (HVA) and serotonin (5HT) were calculated by comparison to external standard curves determined with each batch of tissue samples.

Western blotting

A contralateral punch from the same brain slice used for 1H-MRS was weighed then homogenized in a lysis buffer (40mM Tris-HCl, pH 7.5, 150 mM NaCl, 2.5 mM EDTA, pH 8.0, 1% v/v Triton X-100, and 1:10 diluted protease inhibitor cocktail (Sigma-Aldrich Inc. St. Louis, MO). Protein samples (5 μ g) were separated on a 12% polyacrylamide

gel (Bio-Rad Inc), and transferred electrophoretically to a polyvinylidene fluoride (PVDF) membrane (Bio-Rad, Hercules, CA). The membrane was blocked with 5% nonfat dry milk in TRIS buffered saline (TBS)-Tween 20 (0.1%) then incubated with primary antibodies (anti-Bax (1:500), anti-Bcl-2 (1:250) (Santa Cruz Inc., Santa Cruz, CA), anti- β actin (1:5000) (Sigma-Aldrich Inc. St. Louis, MO), or anti-GFAP (1: 500) (Millipore, Bedford, MA) at 4 °C overnight. The antibodies were detected using HRP-conjugated anti-rabbit IgG or anti-mouse secondary antibodies (1:2000) (Santa Cruz, Inc., Santa Cruz, CA) as appropriate. Blot intensity was determined with chemiluminescence [26].

Statistics

Effects of blast exposure were measured in separate experiments (i.e. 24, 48 and 72 hours). In each experiment, separate sham-treated animals served as respective comparison groups to control for unknown influences (e.g. residual effects of isoflurane). Thus, statistical differences between sham and blast exposed rats were assessed with Student's t-test with $p < 0.05$ considered significant. Unless indicated otherwise, data are presented as mean + standard error of the mean (SEM).

Results

Neurochemical profiling using 1H-MRS

At 48 hours following exposure, glycerophosphocholine (GPC), N-acetyl aspartyl glutamate (NAAG), and creatine (CRE) were found to be significantly ($p < 0.05$) increased in the exposed as compared to the sham group. At 72 hours following exposure, the glutamate (GLU) –CRE ratio along with sum of the cholines (Glycerophosphocholine (GPC) + Choline (CHO) + Phosphocholine (PCH) - CRE ratio increased significantly compared to the control group, no changes observed in creatine at 72 hours following exposure ($p < 0.05$) (Table 1, Figure 4.2).

Neurochemical profiling using HPLC

There was a selective loss of monoamines and their breakdown products at 24 hours following exposure. 5HT level in blast group was significantly decreased at 24 hours post blast (0.29 + 0.10 ng/mg vs 0.095 + 0.010 ng/mg, respectively) ($p < 0.01$). Additionally, the ratio of 5-hydroxyindoleacetic acid (5 HIAA)/5HT was significantly

elevated in exposed group as compared to the sham (1.57 + 0.38 ng/mg (sham) vs 4.63 + 1.38 ng/mg) ($p < 0.01$) (Figure 4.3).

		48 hours following blast exposure			
Neurochemical →	Cre (nmol/ml)	GPC (nmol/ml)	NAAG (nmol/ml)	Glu/cre	
Sham	5.79	1.07	1.25	1.85	
Blast	6.44	1.39	1.9	1.72	
		72 hours following blast exposure			
Neurochemical →	Cre (nmol/ml)	GPC (nmol/ml)	NAAG (nmol/ml)	Glu/cre	
Sham	5.88	1.02	1.54	1.77	
Blast	5.37	1.92	1.6	1.95	

Table 4.1: Raw Values of the Neurochemicals That Are Altered at 48 and 78 Hours Following Blast.

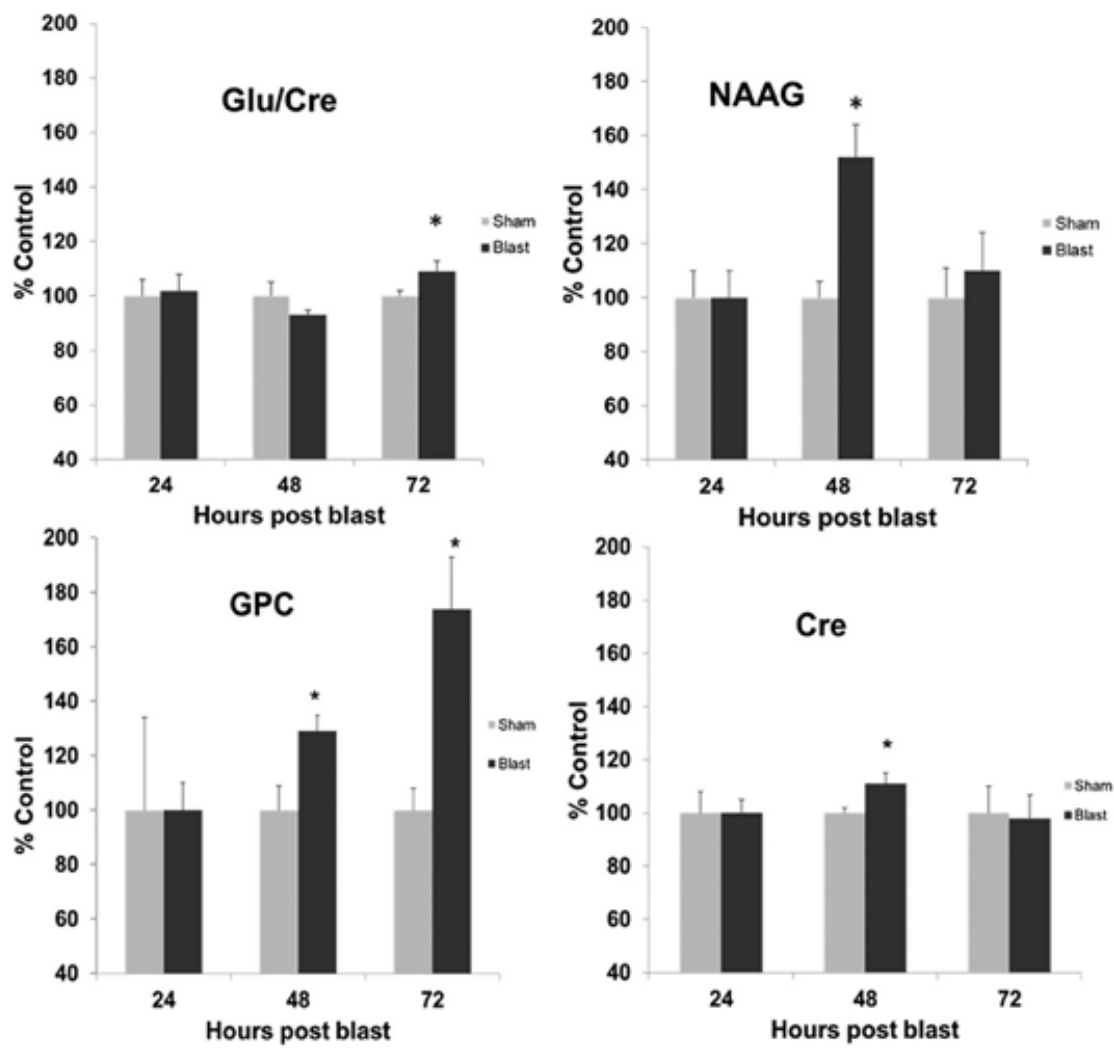


Figure 4.2: Graphs depict the temporal neurochemical response following blast exposure. Elevated levels of Glu/Cre were observed, suggesting a potential excitotoxic effect at 72 hr postblast (* $p < 0.05$). Elevated levels of NAAG and Cre were observed at 48 hr following blast, demonstrating an ongoing neuroprotective effect. GPC, an inflammatory marker, was significantly increased at 48 and 72 hr postblast compared with sham.

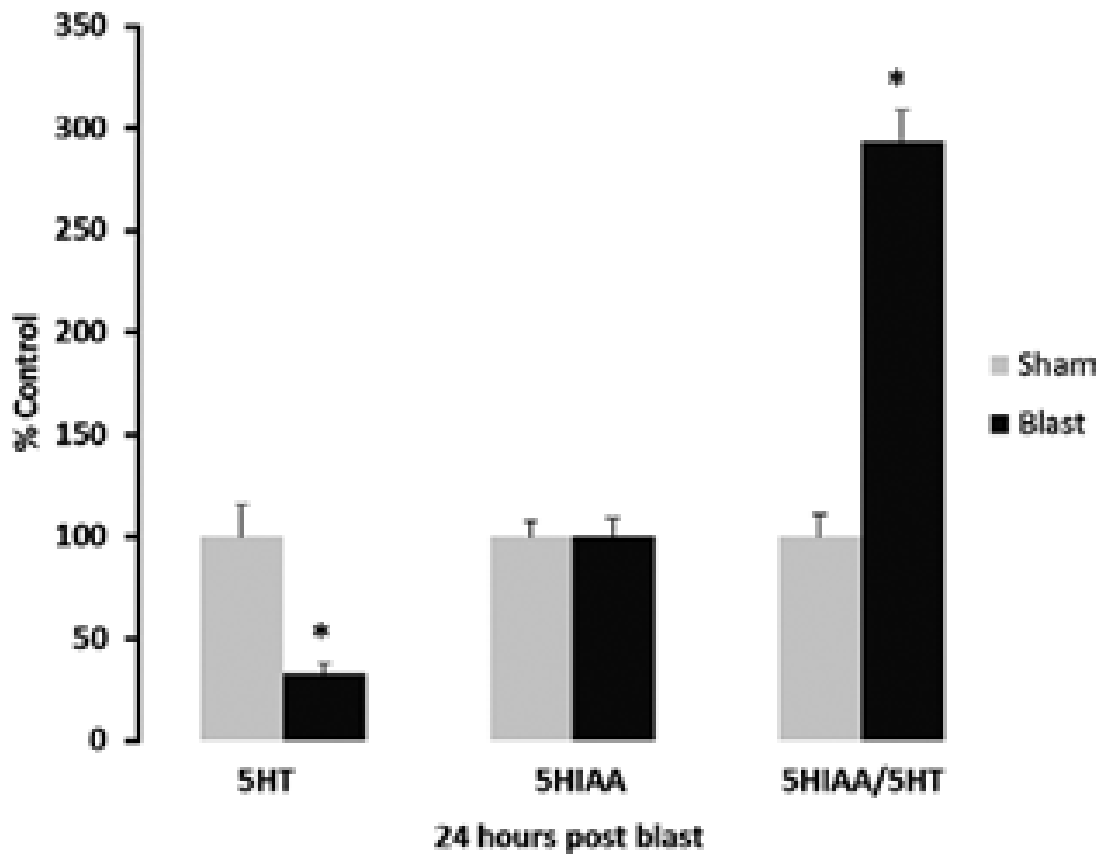


Figure 4.3: Selective loss of 5-HT levels. *p < 0.01

Levels of homovanillic acid (HVA) increased significantly in exposed (0.51 ± 0.09 ng/mg) vs sham (0.38 ± 0.05 ng/mg) ($p < 0.05$) and the ratio of HVA/dopamine (DA) increased in exposed (0.102 ± 0.017 ng/mg) vs sham (0.082 ± 0.005 ng/mg) ($p < 0.05$) (Figure 4.4). No changes in norepinephrine (NE) or 3,4-dihydroxyphenylacetic acid (DOPAC) were observed at the 24 hour time point.

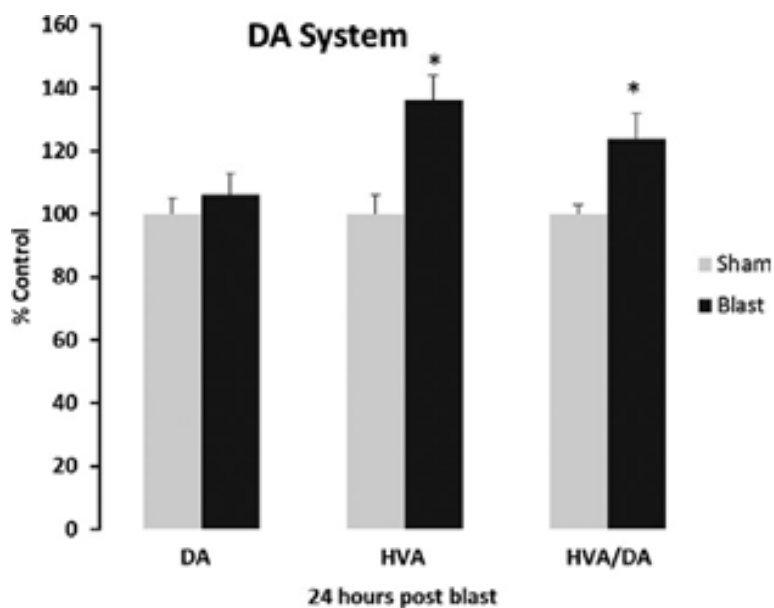


Figure 4.4: Increased levels of HVA and HVA/DA at 24 following blast, with no change in levels of DA suggest increased CA turnover. *P < 0.05.

Western blotting

The protein levels of apoptotic markers (Bax, Bcl-2) and astrogliosis (GFAP) were assessed at 24, 48 and 72 hours following exposure. The Bcl-2 (0.75 ± 0.101 vs 0.421 ± 0.036) ($p < 0.01$) and GFAP-actin ratio (0.171 ± 0.005 vs 0.130 ± 0.011) ($p < 0.05$) was significantly increased in the BINT group compared to the sham at 24 hours following exposure (Figures 4.5, 4.6). The Bax-actin ratio significantly elevated in the exposed group as compared to sham at 48 hours group (0.641 ± 0.073 vs 0.36 ± 0.056) ($p < 0.01$) (Figure 4.7). Overall β -actin levels significantly decreased at 72 hours in exposed group compared to sham (59894 ± 6984 vs 81314 ± 5046) ($p < 0.05$) (Figure 4.8).

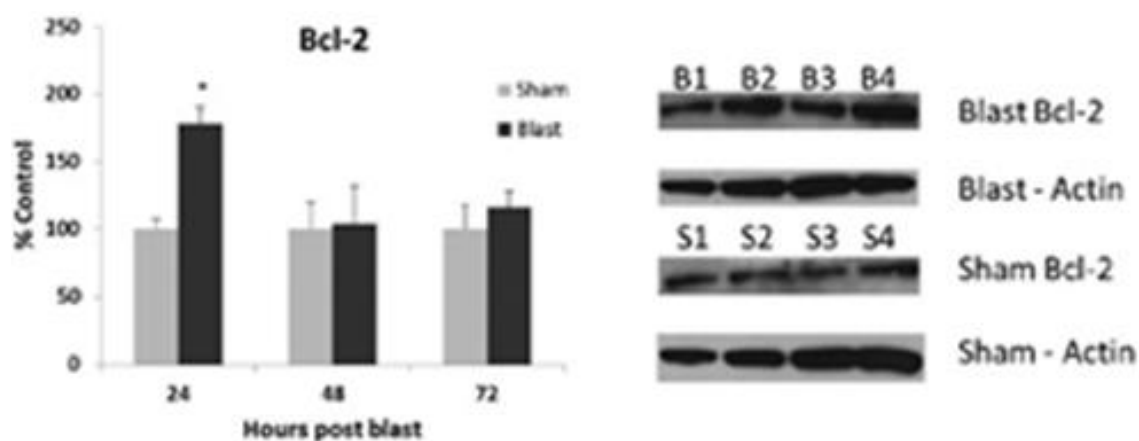


Figure 4.5: At 24 h following blast, increased levels of the antiapoptotic marker Bcl-2 were found, indicating an ongoing neuroprotective effect in the NAC. Representative blot. B1–B4, blast group; S1–S4, sham group. * $p < 0.01$.

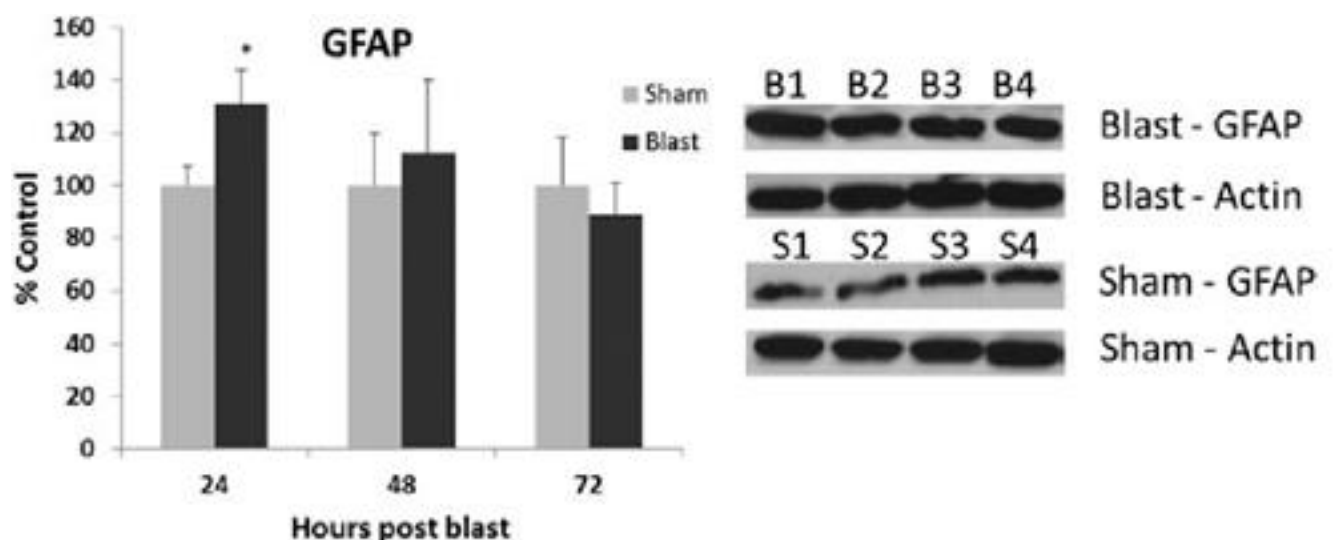


Figure 4.6: GFAP, a marker of astrogliosis, was increased at 24 hr following blast, showing ongoing astrocyte reactivity in the NAC. Representative blot. B1–B4, blast group; S1–S4, sham group. * $p < 0.05$.

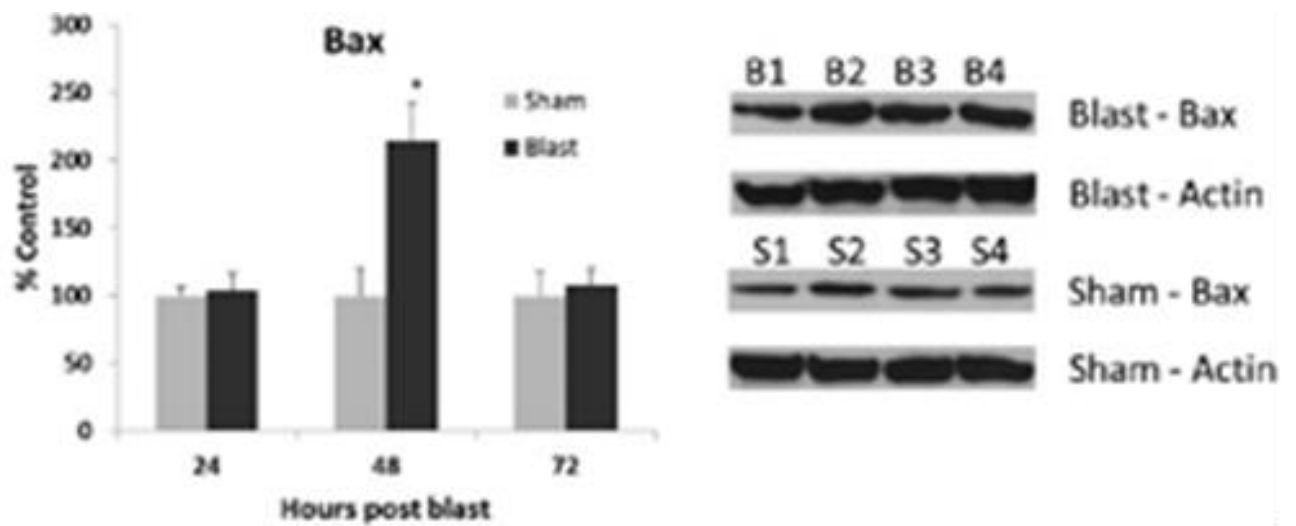


Figure 4.7: Increased levels of the proapoptotic marker Bax at 48 hr post-blast, indicating triggering of the apoptotic pathway. Representative blot. B1–B4, blast group; S1–S4, sham group. *p < 0.01.

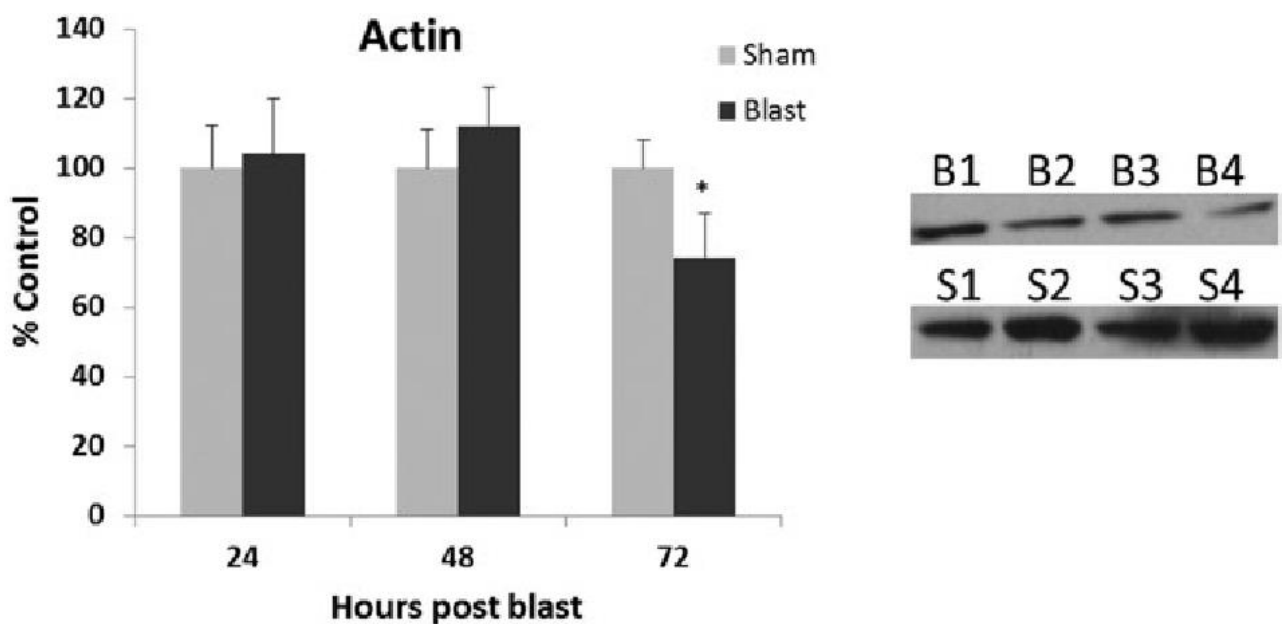


Figure 4.8: β -Actin, a major protein in the cytoskeleton and microtubules of the cell, was significantly decreased at 72 hr postblast. Representative blot. B1–B4, blast group; S1–S4, sham group. *p < 0.05.

Discussion

The clinical symptoms associated with blast exposure indicate that various primary cognitive centers are affected and that the injury to the brain is diffuse. Damage to the cognitive centers of the brain is known to evoke stress related responses and high metabolic energy demands are required for repairing mechanisms [8, 23, 27].

Therefore, acute neurological changes following blast exposure are likely to initiate

pathological cascades at the cellular level. These undetectable injuries could lead to late-emerging clinical disorders such as mood and anxiety disorders [28-30]. The pathological consequence of damage to the NAC has been shown to result in dysfunction to other cognitive centers such as substantia nigra, ventral tegmental area, frontal cortex, hippocampus and amygdala (regions that are directly involved in signaling via neurotransmission) [31].

NAC is an important region in brain associated with cognition, reward, motivation and addiction. Afferents of the NAC arrive from the prefrontal cortex, a key decision making center, and the amygdala, which is the center for anxiety and fear. Injury to NAC can significantly affect behavioral outcomes and the thought process due to its relative projections to these other key brain regions in humans [22, 32, 33]. Furthermore, anxiety and fear with or without substance abuse could be easily triggered. Our results support the hypothesis that exposure to blast overpressure causes neuropathology in the NAC by triggering the cascade of apoptotic pathways through inflammation and neurochemical imbalance.

Neurochemical changes

Twenty four hours following exposure, a selective loss of monoamine-5HT was observed. In addition, the ratio of 5-HIAA, the breakdown product of 5HT, to 5HT was increased suggesting an increased clearance of 5HT in the NAC. However, decrease in 5HT levels could also be due to impaired synthesis of 5HT in NAC neurons. Importantly, the early loss of 5HT (70%) may reflect a selective insult to this monoaminergic system involved with the maintenance of mood and sleep [34]. Clinical reports have documented BINT personnel who are experiencing sleep and mood disorders [35-37]. The low level of 5HT could explain these symptoms at the acute phase following injury.

HVA, the biodegradation product of DA, along with HVA-DA ratio increased substantially without changes in absolute concentrations of DA, DOPAC and NE. This observation could indicate an increased synthesis or release and clearance rate of DA (HVA/DA ratio) from the synapses. Increased functional activity of DA in mesolimbic pathway, where NAC plays a major role, is linked with alteration/impairment of mood, memory, processing fine tuning motor function, motivational reward [38-40]. The

combined effect of 5HT and DA system in NAC has also been shown to play a crucial role in evoking substance abuse, an unfavorable outcome linked to individuals exposed to blast [40-43].

NAAG is an agonist of glutamate autoreceptors as well as a potential source of free glutamate. NAAG also plays a key role in regulating glutamate homeostasis by either buffering excessive glutamate or releasing glutamate upon demand. When injury/stress occurs, the level of glutamate is maintained by NAAG, which can potentially reduce the effect of glutamate excitotoxicity [44, 45]. An increase of NAAG at 48 hours after blast overpressure exposure indicates a neuroprotective effect in response to glutamate homeostasis [46]. With the advancement of recent techniques to resolve the level of NAAG clinically in addition to the traditionally observable peaks such as lactate, glutamate, NAA, and creatine, this data could potentially give insight into the diagnosis and treatment of the personnel suffering from BINT [47, 48].

Ongoing inflammation/membrane turnover is evident from the significant increase of GPC at 48 and 72 hours combined with the increase of Cre and Glu in the blast over pressure exposed group [48]. GPC is the breakdown product of arachnoid acid by the action of phospholipase A2 enzyme. Arachnoid acid is an abundant fatty acid present in brain helps in the maintenance of cell and cell membrane integrity. Consequently GPC is considered an inflammatory marker for the membrane breakdown and integrity [49]. Increases in glutamate levels potentially suggest an excitotoxic effect with dysregulation of creatine, which maintains energy homeostasis. Hence increased GPC, glutamate, and creatine levels are indicators of compromised cellular activities within the NAC with an inflammatory role.

Cellular injury response

Increased levels of GFAP, a marker of astrogliosis, and Bcl-2, an anti-apoptotic protein, at 24 hours following exposure could represent the beginning stage of neuronal damage. Due to this initial phase, increased Bcl-2 levels could mark a subsequent counteractive mechanism against the ongoing cellular damage. This counteractive process generally requires a large amount of energy. Kosten et al (2007) demonstrated that external stress to various brain regions caused changes in both in the Bcl-2 and

5HT levels [34]. Moreover, BINT animal models established dramatic acute changes in neurochemical, inflammatory, and apoptotic response in cortical, hippocampal and amygdular regions [24, 45-47].

An increased vulnerability of the NAC is further supported by increased Bax (a pro-apoptotic marker) at 48 hours and decrease of β -actin, a major protein in cytoskeleton and dendritic spines. As a consequence, dysfunction of the NAC can lead to various pathological and psychiatric disorders. Additionally, NAC's direct association with mood, addiction associated behavior, and also indirectly association in developing fear, anxiety and memory associated disorders plays an important role in BINT.

Clinical studies that are directed towards NAC have not evaluated although psychiatric outcomes such as sleep disturbances, mood disorders, stress, substance abuse and aggressive have been some of the predominant symptoms which are directly associated with NAC. This study is the first to address the pathological changes and importance of NAC in the field of blast injury. Overall, majority of the neurochemical changes that were found (namely cholines, creatine, and glutamate) can also be detected using nuclear magnetic resonance (NMR) on clinical patients. Overall, the results demonstrated highly active inflammation which appear to trigger apoptotic cascades leading to cell death at an acute stage following blast overpressure exposure in NAC.

Acknowledgements

This research work is supported by Thomas C. Rumble fellowship, National Institute of Drug Abuse (NIDA R01-DA16736), and the Joe Young Research Fund in Psychiatry.

Conflict of interest

The authors declare that they have no financial or other conflict of interests.

References

1. Helfer TM, Jordan NN, Lee RB, Pietrusiak P, Cave K, Schairer K. Noise-induced hearing injury and comorbidities among postdeployment U.S. Army Soldiers: April 2003-June 2009. *American Journal of Audiology*. 2011;20:33-41.
2. Mao J, Pace E, Pierozynski P, Kou Z, Shen Y, VandeVord PJ, Haacke EM, Zhang X, Zhang J. Blast-induced tinnitus and hearing loss in rats: Behavioral and Imaging Assays. *Journal of Neurotrauma*. 2011; 29(2):430-444.
3. Warden DL, French LM, Shupenko L, Fergus J, Riedy G, Erickson ME, Jaffee MS, Moore DF. Case report of a soldier with primary blast brain injury. *NeuroImage*. 2009;47, Supplement 2:T152-T153.
4. McAllister TW, Stein MB. Effects of psychological and biomechanical trauma on brain and behavior. *Annals of the New York Academy of Sciences*. 2010;1208:46-57.
5. Hicks RR, Fertig SJ, Desrocher RE, Koroshetz WJ, Pancrazio JJ. Neurological Effects of Blast Injury. *The Journal of Trauma*. 2010;68:1257-1263.
6. Bazarian JJ, Cernak I, Noble-Haeusslein L, Potolicchio S, Temkin N. Long-term neurologic outcomes after traumatic Brain Injury. *The Journal of Head Trauma Rehabilitation*. 2009;24:439-451
7. Säljö A, Svensson B, Mayorga M, Hamberger A, Bolouri H. Low levels of blast raises intracranial pressure and impairs cognitive function in rats. *Journal of Neurotrauma*. 2009.
8. Taber KH, Warden DL, Hurley RA. Blast-related traumatic brain injury: What is known? *J Neuropsychiatry Clinical Neuroscience*. 2006;18:141-5.
9. Cernak I, Noble-Haeusslein LJ. Traumatic brain injury: An overview of pathobiology with emphasis on military populations. *J Cerebral Blood Flow Metabolism*. 2009;30:255-266.
10. VandeVord P, Bolander R, Sajja V, Hay K, Bir C. Mild neurotrauma indicates a range-specific pressure response to low level shock wave exposure. *Annals of Biomedical Engineering*. 2012; 40(1):227-236.

11. Hayes JP, Morey RA, Tupler LA. A case of frontal neuropsychological and neuroimaging signs following multiple primary-blast exposure. *Neurocase*. 2012;18(3):258-269.
12. Kocsis JD, Tessler A. Pathology of blast-related brain injury. *Journal of rehabilitation research & development*. 2009;46:667-672.
13. Mac Donald CL, Johnson AM, Cooper D, Nelson EC, Werner NJ, Shimony JS. Detection of blast-related traumatic brain injury in U.S. military personnel. *New England Journal of Medicine*. 2011;364:2091-2100.
14. Rosenfeld JV, Ford NL. Bomb blast, mild traumatic brain injury and psychiatric morbidity: A review. *Injury*. 2010;41:437-443.
15. Hoge CW, McGurk D, Thomas JL, Cox AL, Engel CC, Castro CA. Mild traumatic brain injury in U.S. soldiers returning from Iraq. *New England Journal of Medicine*. 2008;358:453-463.
16. Dobscha SK, Clark ME, Morasco BJ, Freeman M, Campbell R, Helfand M. Systematic review of the literature on pain in patients with polytrauma including traumatic brain injury. *Pain Medicine*. 2009;10:1200-17.
17. Thompson JM, Scott KC, Dubinsky L. Battlefield brain. *Canadian Family Physician*. 2008;54:1549-51.
18. Chew E, Zafonte RD. Pharmacological management of neurobehavioral disorders following traumatic brain injury-A state-of-the-art review. *Journal of rehabilitation research & development*. 2009;46(6):851-79.
19. Ryding E, Lindström M, Träskman-Bendz L. The role of dopamine and serotonin in suicidal behaviour and aggression. In: Giuseppe Di Giovanni VDM, Ennio E, editors. *Progress in Brain Research*: Elsevier; 2008. p. 307-15.
20. van Erp AMM, Miczek KA. Aggressive behavior, increased accumbal dopamine, and decreased cortical serotonin in rats. *The Journal of Neuroscience*. 2000;20:9320-5.
21. Self DW, Nestler EJ. Relapse to drug-seeking: neural and molecular mechanisms. *Drug and Alcohol Dependence*. 1998;51:49-60.

22. Yeo RA, Phillips JP, Jung RE, Brown AJ, Campbell RC, Brooks WM. Magnetic resonance spectroscopy detects brain injury and predicts cognitive functioning in children with brain injuries. *Journal of Neurotrauma*, 2006. 23(10):1427-1435.
23. Belujon P, Grace AA. Hippocampus, amygdala, and stress: interacting systems that affect susceptibility to addiction. *Annals of the New York Academy of Sciences*. 2011;1216:114-21.
24. Commons KG. Neuronal pathways linking substance P to drug addiction and stress. *Brain Research*. 2010;1314:175-82.
25. Paxinos G, Watson C. *The rat brain in stereotaxic coordinates*, 2nd edition. San Diego; Academic Press. 1986.
26. Ghoddoussi F, Galloway MP, Jambekar A, Bame M, Needleman R, Brusilow WSA. Methionine sulfoximine, an inhibitor of glutamine synthetase, lowers brain glutamine and glutamate in a mouse model of ALS. *Journal of the Neurological Sciences*. 2010;290:41-7
27. Stetler RA, Gan Y, Zhang W, Liou AK, Gao Y, Cao G. Heat shock proteins: Cellular and molecular mechanisms in the central nervous system. *Progress in Neurobiology*. 2010;92:184-211.
28. Terrio H, Brenner LA, Ivins BJ, Cho JM, Helmick K, Schwab K, Scally K, Bretthauer R, Warden D. Traumatic brain injury screening: Preliminary findings in a US army brigade combat team. *The Journal of Head Trauma Rehabilitation*. 2009; 24(1):14-23.
29. Gavett B, Stern R, Cantu R, Nowinski C, McKee A. Mild traumatic brain injury: a risk factor for neurodegeneration. *Alzheimer's Research & Therapy*. 2010; 2(3):18.
30. Elder GA, Mitsis EM, Ahlers ST, Cristian A. Blast-induced mild traumatic brain injury. *The Psychiatric clinics of North America*. 2010;33:757-81.
31. Kim E-M, Quinn JG, Levine AS, O'Hare E. A bi-directional μ -opioid–opioid connection between the nucleus of the accumbens shell and the central nucleus of the amygdala in the rat. *Brain Research*. 2004;1029:135-9.

32. Sesack SR, Grace AA. Cortico-basal ganglia reward network: Microcircuitry. *Neuropsychopharmacology*. 2009;35:27-47.
33. Kosten TA, Galloway MP, Duman RS, Russell DS, D'Sa C. Repeated unpredictable stress and antidepressants differentially regulate expression of the Bcl-2 family of apoptotic genes in rat cortical, hippocampal, and limbic brain structures. *Neuropsychopharmacology*. 2007;33:1545-58.
34. Ruff RL RS, Wang XF. Improving sleep: initial headache treatment in OIF/OEF veterans with blast-induced mild traumatic brain injury. *Journal of rehabilitation research & development*. 2009;46:1074-81.
35. Vasterling JJ, Verfaellie M, Sullivan KD. Mild traumatic brain injury and posttraumatic stress disorder in returning veterans: Perspectives from cognitive neuroscience. *Clinical Psychology Review*. 2009;29:674-84.
36. Elder GA, Cristian A. Blast-related mild traumatic brain injury: mechanisms of injury and impact on clinical care. *Mount Sinai Journal of Medicine: A Journal of Translational and Personalized Medicine*. 2009;76:111-8.
37. Stuber GD, Sparta DR, Stamatakis AM, van Leeuwen WA, Hardjoprajitno JE, Cho S, et al. Excitatory transmission from the amygdala to nucleus accumbens facilitates reward seeking. *Nature*. 2011;475:377-80.
38. Qi Z, Kikuchi S, Tretter F, Voit EO. Effects of dopamine and glutamate on synaptic plasticity: A computational modeling approach for drug abuse as comorbidity in mood disorders. *Pharmacopsychiatry*. 2011;44:S62,S75.
39. Galloway MP. Regulation of dopamine and serotonin synthesis by acute administration of cocaine. *Synapse*. 1990;6:63-72.
40. Blum K, Chen TJH, Chen ALH, Madigan M, Downs BW, Waite RL, et al. Do dopaminergic gene polymorphisms affect mesolimbic reward activation of music listening response? Therapeutic impact on Reward Deficiency Syndrome (RDS). *Medical Hypotheses*. 2010;74:513-520.

41. Quinlan JD. Care of the returning veteran. *American Family Physician*. 2010;82:42-49.
42. MacManus D, Dean K, Al Bakir M, Iversen AC, Hull L, Fahy T, et al. Violent behaviour in UK military personnel returning home after deployment. *Psychological Medicine*. 2011;FirstView:1-11.
43. Jessen F, Fingerhut N, Sprinkart AM, Kühn KU, Petrovsky N, Maier W, Schild HH, Block W, Wagner M, Träber F. N-acetylaspartylglutamate (NAAG) and N-acetylaspartate (NAA) in patients with Schizophrenia. *Schizophrenia Bulletin*. 2013; 39(1):197-205.
44. Benarroch EE. N-acetylaspartate and N-acetylaspartylglutamate. *Neurology*. 2008;70:1353-1357.
45. Thomas AG, Olkowski JL, Slusher BS. Neuroprotection afforded by NAAG and NAALADase inhibition requires glial cells and metabotropic glutamate receptor activation. *European Journal of Pharmacology*. 2001;426:35-38.
46. Edden RAE, Pomper MG, Barker PB. In vivo differentiation of N-acetyl aspartyl glutamate from N-acetyl aspartate at 3 Tesla. *Magnetic Resonance in Medicine*. 2007;57:977-982.
47. Moore GJ, Galloway MP. Magnetic resonance spectroscopy: neurochemistry and treatment effects in affective disorders. *Psychopharmacology bulletin*. 2002;36:5-23.
48. Walter A, Korth U, Hilgert M, Hartmann J, Weichel O, Hilgert M, Fassbender K, Schmitt A, Klein J. Glycerophosphocholine is elevated in cerebrospinal fluid of Alzheimer patients. *Neurobiology of Aging*. 2004; 25(10):1299-303.

Chapter 5

Blast neurotrauma impairs working memory and disrupts prefrontal myo-inositol levels in rats

Venkata Siva Sai Sujith Sajja¹, Shane A. Perrine², Farhad Ghoddoussi^{2,3}, Christina S. Hall¹, Matthew P. Galloway^{2,3}, and Pamela J. VandeVord^{4,5}

¹School of Biomedical Engineering and Sciences, Virginia Polytechnic Institute and State University, Blacksburg, VA

²Psychiatry and Behavioral Neurosciences, and ³Anesthesiology, Wayne State University, Detroit, MI

⁴Department of Biomedical Engineering, Wayne State University, Detroit, MI

⁵Salem VA Medical Center, Research & Development Service, Salem, VA

Blast neurotrauma impairs working memory and disrupts prefrontal myo-inositol levels in rats

Venkata Siva Sai Sujith Sajja¹, Shane A. Perrine², Farhad Ghoddoussi^{2,3}, Christina S. Hall¹, Matthew P. Galloway^{2,3}, and Pamela J. VandeVord^{1,4}

¹School of Biomedical Engineering and Sciences, Virginia Polytechnic Institute and State University, Blacksburg, VA, ²Psychiatry and Behavioral Neurosciences, and ³Anesthesiology, ⁴Salem VA Medical Center, Research & Development Service, Salem, VA, USA.

Submitted for Publication

Abstract:

Working memory, which is dependent on higher-order executive function in the prefrontal cortex, is often disrupted in patients exposed to blast overpressure. In this study, we evaluated working memory and medial prefrontal neurochemical status in a rat model of blast neurotrauma. Adult male sprague dawley rats were anesthetized with 3% isoflurane and exposed to calibrated blast overpressure (17 psi, 117 kPa) while sham animals received only anesthesia. Early neurochemical effects in the prefrontal cortex included a significant decrease in betaine (trimethylglycine) and an increase in GABA at 24 hours, and significant increases in glycerophosphorylcholine, phosphorylethanolamine, as well as glutamate/creatine and lactate/creatine ratios at 48 hours. Seven days after blast, only *myo*-inositol levels were altered showing a 15% increase. Compared to controls, working memory in the novel object recognition task was significantly impaired in animals exposed to blast overpressure. Working memory in control animals was negatively correlated with *myo*-inositol levels ($r = -.759$, $p < 0.05$), an association that was absent in blast exposed animals. Increased *myo*-inositol may represent tardive glial scarring in the prefrontal cortex, a notion supported by GFAP changes in this region after blast overexposure as well as clinical reports of increased *myo*-inositol in disorders of memory.

Keywords: Working memory, *myo*-inositol, Glia, Prefrontal cortex, Blast neurotrauma

Introduction

Blast-induced neurotrauma (BINT) has been shown to have deteriorating effects on cognition. Previous animal and clinical studies have shown irreversible damage in cognitive centers of the brain, namely the hippocampus [1-6]. Commonly associated clinical issues with BINT include memory deficits and anxiety [5,7-10]. Studies mainly have focused on the role of hippocampal impairment in conjunction with cognitive impairment. These studies have demonstrated neurodegeneration, glial response and inflammation in hippocampus following blast overpressure exposure. However, other major cognitive regions such as the medial prefrontal cortex (PFC), which plays an important role in memory-related cognitive functions, may also be affected [11-15].

The association of PFC, perirhinal cortex and hippocampus plays an important role in working memory, decision making, and short term memory. In addition, PFC contributes to the potentiation of long term memories due to its direct innervation of axonal fibers with the hippocampus [16-23]. Although animal behavioral tests demonstrated impaired cognition in an acute phase, paradigms specific for working and short term memory issues have not been evaluated following blast neurotrauma. Recent pre-clinical and clinical reports have shown injury in PFC after blast exposure [13,15,24]. These factors indicate the need for behavioral studies that test cognition and working memory governed by the PFC.

It is hypothesized that working memory impairment after blast exposure is due to acute metabolic neurochemical changes and neurodegeneration in the medial prefrontal cortex. To test this hypothesis, novel object recognition paradigm was used to evaluate working memory and the PFC tissue from these animals was used to assess metabolic and neurochemical changes by high-resolution magic angle spinning (HRMAS) proton magnetic resonance spectroscopy (^1H -MRS) *ex vivo* and neurodegeneration using fluorojade B staining. Collectively, these data address memory impairment issues mediated by early neurochemical alterations, neurodegeneration and gliosis in the PFC following blast overpressure exposure and thereby provide novel insight that is amenable to clinical translation.

Materials and methods

Animals and blast overpressure exposure

The Wayne State University Institutional Animal Care and Use Committee approved the experimental procedures described herein. Prior to all experiments, animals were acclimated for at least three days (12 hour light/dark; on at 6 AM) and normal rat chow and tap water provided ad libitum. Male Sprague Dawley rats (Charles River Labs., Portage, MI) weighing ~250 g were briefly anesthetized with isoflurane (3%), then positioned in a shock tube 1.09 m from the open end with a rostral cephalic orientation towards the shock wave and exposed to a 117 kPa overpressure for a 7.5 ms duration. Sham animals did not experience the overpressure but were anesthetized and placed in the shock tube. The shock tube generates a single free field pressure (Figure 1). Time profile is determined with a piezoelectric sensor axial to the blast pressure source and recorded at 250 kHz (per channel) as described previously [6].



Figure 5.1: Representative pressure profile of calibrated shock wave to which animals are exposed with a resultant peak positive overpressure at 117 KPa

Novel object recognition test (NOR):

The NOR test was used to measure working memory, specifically object recognition [26,27]. Animals were tested at 72 hours (3 days) and 168 hours (7 days) following blast exposure (n = 8/group). Testing occurred in 3 phases, including: acclimation = acclimate to novel environment, trial 1 (T1) = presentation of two similar objects, trial 2 (T2) = presentation of a novel and familiar object. In the first phase, rats were

acclimated to a custom-made open field testing chamber (79 x 79 x 35 cm; Formtech Plastics, Oak Park, MI) with dim lighting by allowing them to explore the empty chamber for 5 min (time used in all phases) for two consecutive days prior to testing. On days 3 and 7 rats underwent T1 where they were placed in the chamber with 2 identical objects residing in opposite corners. Different objects were used for day 3 and 7. After a 20 min interval, object recognition was determined in T2 on each day. During T2, rats were returned to the testing chamber, where one of the familiar objects was substituted with a novel object. For T1 and T2 phases (5 min each), rats were placed in the chamber directed away from the objects. The rats were monitored for time spent exploring the familiar objects, which was defined as the nose-point of the animal being directed toward an object and also located within 1.5x radius of the object measured from center of the object. Memory recognition behavior was quantified as the fraction of time spent exploring the novel object relative to the familiar object during T1 and T2 phases. An animal that spent 75% or more time in T1 exploring one of the objects was excluded from the study to avoid an initial object bias; also, the placement of objects within the chambers was counterbalanced among animals to reduce the potential of a place bias. Arena settings were set and behaviors were analyzed using Ethovision™ tracking software (Noldus Information Technology, Leesburg, VA). The testing chamber was located in a closed room and behavior was digitally recorded with a camera located above the chamber and linked to a computer outside the room. After placing an animal in the chamber, the experimenter exited the room and viewed the animal on the computer linked to the camera. Automated tracking and scoring was verified by a rater blind to the treatment conditions. The testing chamber was cleaned with 70% ethanol in water between each use.

Fraction of time spent = Time of animal spent at novel object location / (Time spent at novel object location + familiar object location).

High resolution magic angle spinning proton-magnetic resonance spectroscopy (HRMAS ¹H-MRS) analysis:

¹H-MRS analysis was performed as described previously using a HRMAS modified technique at high magnetic field (Sajja et al., 2012). Brains (n=8/group at 3, 24, 48 and

168 hours; 168 hours group animals underwent NOR test prior extraction of brains for ^1H -MRS analysis) were rapidly excised after decapitation, placed into a chilled brain matrix, and cut into 2 mm coronal slices. Slices were immediately frozen on solid CO_2 and then contralateral, 1.5 mm diameter punches were taken from the medial prefrontal cortex according to Paxinos & Watson brain atlas (Paxinos and Watson, 1997). Tissues were stored at -80°C until ^1H MRS neurochemical analysis.

Frozen intact tissue samples were weighed (2-3 mg) then placed into a Bruker zirconium rotor (2.9 mm diameter, 10 μL capacity) containing 2.5 μL PO_4 buffer (pH = 7.4), formate, NaN_3 , 3-(trimethylsilyl)-propionic acid (TSP) and 2.5 μL of D_2O . TSP served as an internal chemical shift reference (0.00 ppm), formate (8.44 ppm) for auto-phasing, and D_2O to lock on the center frequency. Once prepared, the rotor was promptly placed into a Bruker 11.7T Avance 500 MHz spectrometer maintained at 4°C and was allowed to spin at a rate of 4.2k Hz; the spatial orientation of the rotor was 54.7° (the magic angle) relative to the longitudinal (or main) magnetic field (B_0). Field inhomogeneities were adjusted using a semi-automatic shimming procedure (Bruker). Tissue spectra were acquired with a CPMG rotor-synchronized pulse sequence [29].

Each spectrum was analyzed using LCModel software utilizing a linear combination of a custom set of 27 neurochemical model spectra (basis set) to fit known MR-visible neurochemicals and calculate absolute concentration values for each neurochemical. The goodness of fit for each compound was determined with Cramer-Rao bounds $< 15\%$ being required for further analysis [30,31]. Absolute concentrations of MR visible metabolites were corrected for tissue weight and were expressed as nmol/mg tissue weight.

Immunohistochemistry:

For immunohistochemistry, animals ($n = 5/\text{group}$ at 3, 48 and 168 hours) were perfused transcardially with 4% paraformaldehyde and then fixed in 30% sucrose solution prior to sectioning. Fixed brains were embedded within optimal cutting temperature compound (Sakura Finetek USA, Inc., Torrance, CA) then frozen on solid CO_2 . Starting at +2.76 Bregma of the PFC and ending at +1.76 Bregma, 40 μm tissue sections were prepared

with a microtome at -20°C. Brain slices were further stained and analyzed for neurodegeneration (FluoroJade B) and astrogliosis (Glial fibrillary acidic protein, GFAP).

FluoroJade B (FJB) analysis:

Brain slices were incubated in 1% NaOH-80% ethanol, hydrated in 70% ethanol, and washed in distilled water. The sections were subsequently incubated room temperature in 0.006% potassium permanganate (Sigma-Aldrich, St. Louis MO) on a rotating stage, rinsed in distilled water, and incubated in a 0.0004% solution of FJB (Histochem Inc., Jefferson, AR) [32]. All solutions were made in dH₂O. The brain sections were then rinsed in distilled water, air-dried and placed on a slide warmer until fully dry. The dry slides were cleared in xylene and mounted with 1,3-diethyl-phenylxanthine (Sigma-Aldrich; St. Louis, MO). An observer blind to the experimental conditions carried out cell counting. Counts were based on the morphology, fluorescent intensity, size and location of specific neurons using a Zeiss epifluorescence microscope. The number of FJB+ neurons was determined for the entire PFC using multiple coronal slices (every 3rd slice).

GFAP analysis:

Effects of blast exposure were measured in separate experiments (i.e. 3, 24, 48 and 168 hours following blast overpressure exposure). In each experiment, separate sham-treated animals served as respective comparison groups for unknown influences (e.g. residual effects of isoflurane). Thus, for neurochemical experiments statistical differences between sham and blast-exposed rats were assessed with independent two-tailed Student's t-test with $p < 0.05$ considered significant. Immunohistochemistry studies were treated as two separate experiments to avoid the unknown influences and were assessed using independent two-tailed Student's t-test with $p < 0.05$ considered significant. A two-factorial repeated measured ANOVA was used for the behavioral testing with $p < 0.05$ considered statistically significant. Pearson correlation was used to assess a potential relationship between levels of myo-inositol (Ins) and NOR behavioral outcome at 7 days following blast overpressure exposure, the correlation significance was assessed using SPSS™ statistical software and $p < 0.05$ considered statistically

significant. Unless indicated otherwise, data are presented as mean \pm standard error of the mean (SEM).

Statistics:

Effects of blast exposure were measured in separate experiments (i.e. 3, 24, 48 and 168 hours following blast overpressure exposure). In each experiment, separate sham-treated animals served as respective comparison groups for unknown influences (e.g. residual effects of isoflurane). Thus, for neurochemical experiments statistical differences between sham and blast-exposed rats were assessed with independent two-tailed Student's t-test with $p < 0.05$ considered significant. Immunohistochemistry studies were treated as two separate experiments to avoid the unknown influences and were assessed using independent two-tailed Student's t-test with $p < 0.05$ considered significant. A two-factorial repeated measured ANOVA was used for the behavioral testing with $p < 0.05$ considered statistically significant. Pearson correlation was used to assess a potential relationship between levels of *myo*-inositol (Ins) and NOR behavioral outcome at 7 days following blast overpressure exposure, the correlation significance was assessed using SPSS™ statistical software and $p < 0.05$ considered statistically significant. Unless indicated otherwise, data are presented as mean \pm standard error of the mean (SEM).

Results:

Object recognition behavior and working memory:

While no differences in NOR behaviors during T1 or T2 were observed at 72 hours following blast exposure compared sham treatment, a significant decrease ($F_{1,17} = 8.46$, $p < 0.01$) in time spent with the novel object between sham and blast-exposed rats during T2 was observed 168 hours (7 days) after exposure (Figure 5.2). Furthermore, the sham group, but not the blast-exposed group, showed a significant increase ($F_{1,17} = 9.12$, $p < 0.01$) in time spent with the novel object in T2 relative to T1 and the location where the novel object would be placed in T2, which is consistent with learned behavior in the controls and a deficit in blast exposed rats.

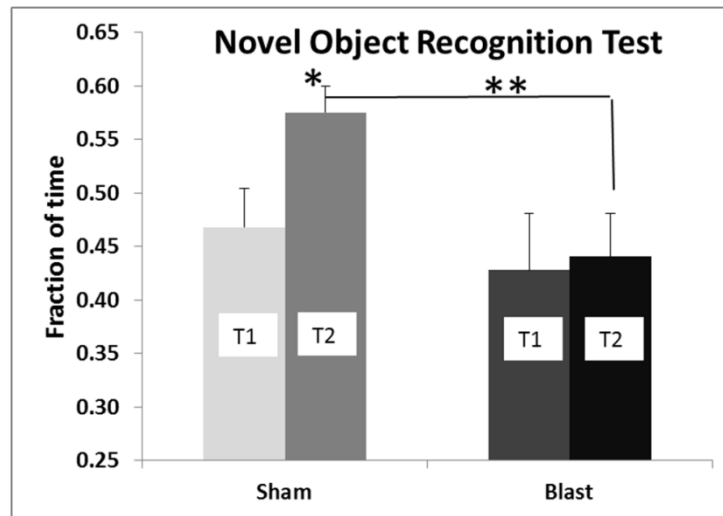


Figure 5.2: Sham rats learn the behavior and show good working memory (T1-T2 sham), while blast exposed rats do not show learning and are significantly different from sham rats in T2 from learning. T1 – Trial with familiar objects; T2 – Trial 2 with a novel object; * $p < 0.05$, ** $p < 0.002$.

Neurochemical assessment by $^1\text{H-MRS}$:

Following blast overpressure exposure, a significant decrease in glutathione (GSH) (1.08 ± 0.06 vs. 0.92 ± 0.03 nmol/mg) and *myo*-inositol (Ins) (5.65 ± 0.23 vs. 4.93 ± 0.18 nmol/mg) were observed at 3 hours. Decreased levels of betaine (BET) (5.03 ± 0.44 vs. 4.02 ± 0.13 nmol/mg) and increased levels of γ - amino butyric acid (GABA) (8.52 ± 0.31 vs. 9.62 ± 0.34 nmol/mg) were seen at 24 hours. Increased levels of glycerophosphocholine (GPC) (2.81 ± 0.12 vs. 3.22 ± 0.17 nmol/mg), phosphorylethanolamine (PEA) (9.93 ± 0.35 vs. 10.99 ± 0.39 nmol/mg), glutamate/creatine ratio (Glu/Cre) (1.97 ± 0.03 vs. 2.08 ± 0.02), and lactate/creatine (Lac/Cre) (1.68 ± 0.04 vs. 1.79 ± 0.03) ratio was found at 48 hours. Finally, increased levels of Ins (4.59 ± 0.25 vs. 5.30 ± 0.18 nmol/mg) were observed at 168 hours (7 days) (Figure 5.3).

No changes were found in Alanine, N-acetyl aspartate (NAA), N-acetyl aspartate glutamate, Succinate, Aspartate, Choline, Inositol, Taurine, Glycine, Phosphorylethanolamine at any time points.

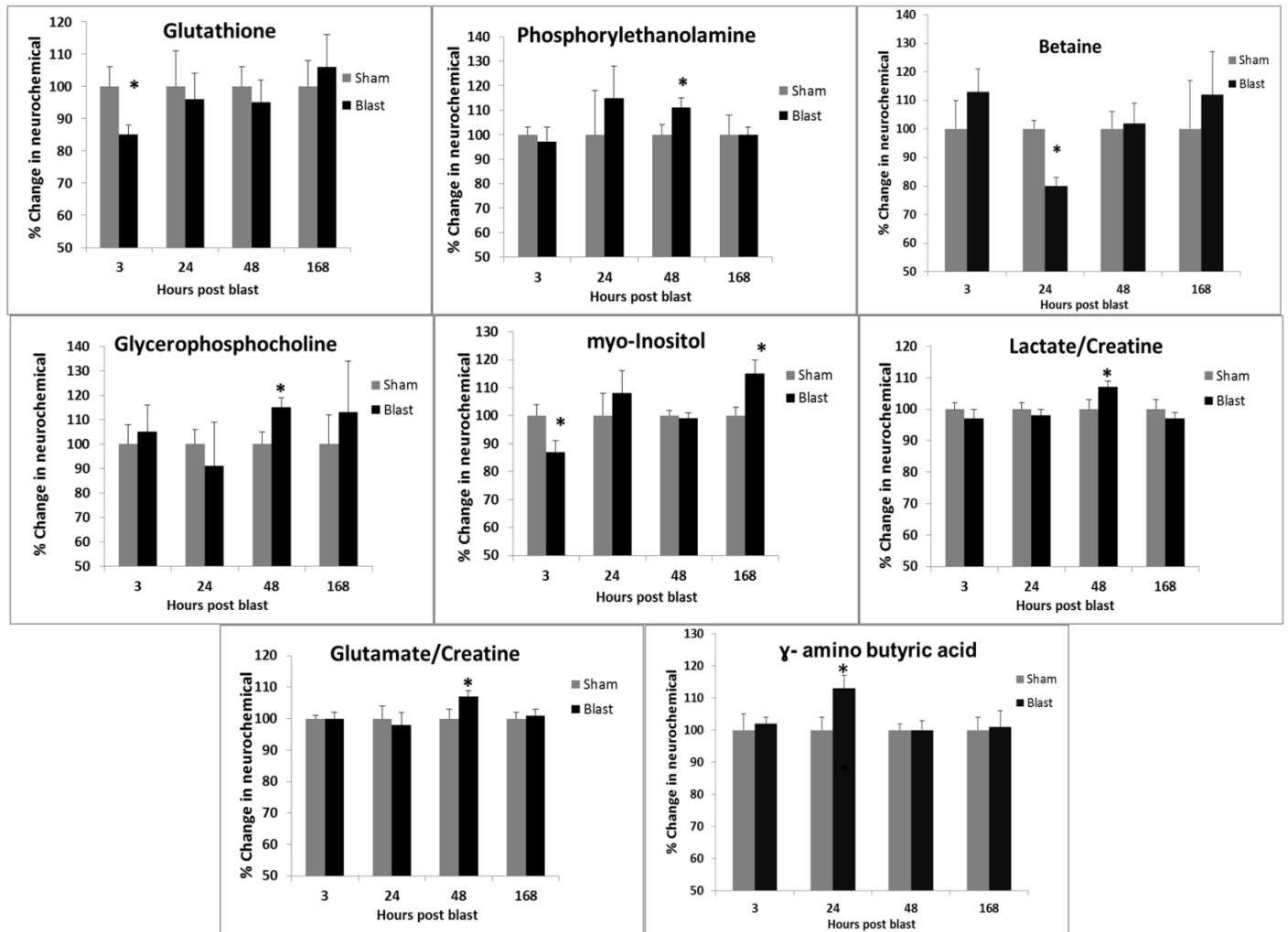


Figure 5.3: Temporal evaluation of the 1H-MRS neurochemical changes in the prefrontal cortex of rats following blast overpressure exposure, where blast group is compared to corresponding sham group, * $p < 0.05$.

NOR versus Ins Correlation:

A negative correlation between NOR behavior (time spent with the novel object in T2) and levels of Ins, measured at 7 days following blast exposure, ($R = -0.759$, * $p < 0.05$) was observed in sham group while the same correlation was not observed in blast group ($R = 0.202$) (Figure 5.4).

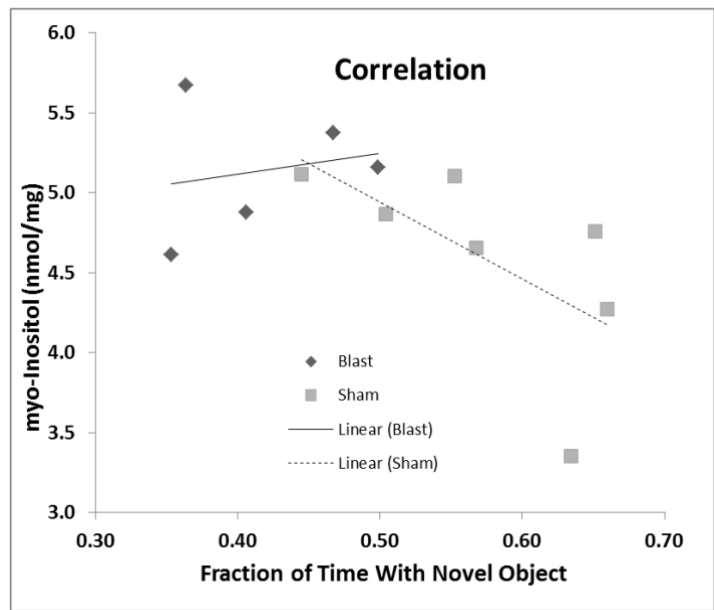


Figure 5.4: Myo-inositol (Ins) in the prefrontal cortex of sham animals had a significant negative correlation ($p < 0.05$) with working memory while this correlation was lost in overpressure exposed group of animals.

FJB and GFAP:

A significant increase in FJB+ staining was observed at 3, 48 and 168 hours following blast overpressure exposure compared to sham group, $*p < 0.05$ (Figure 5.5). No changes were observed in GFAP at 3 and 48 hours following blast overpressure in PFC between sham and the blast groups; however, a significant increase was observed at 168 hours following blast overpressure exposure compared to sham treatment, $*p < 0.01$ (Figure 5.6).

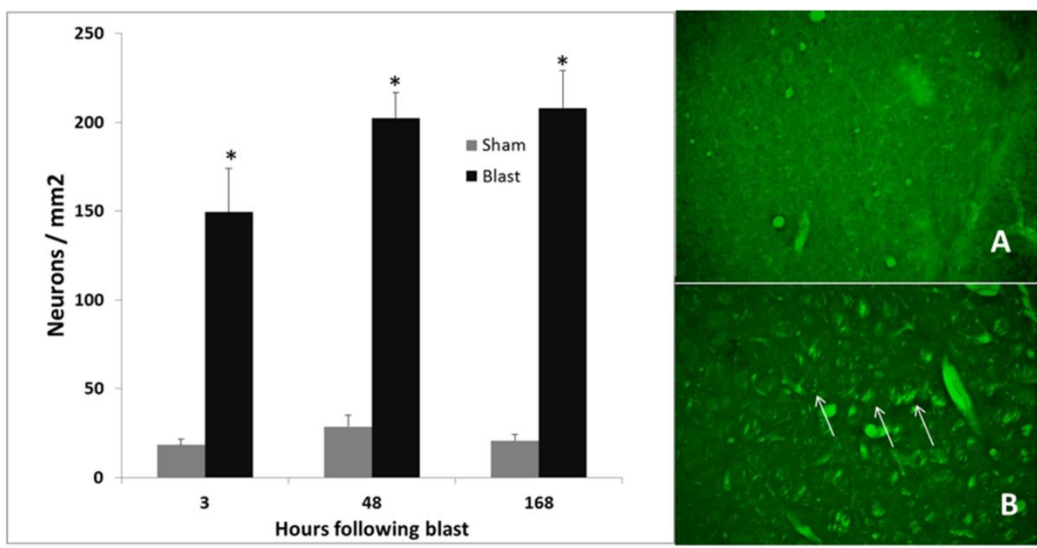


Figure 5.5: FluoroJade B positive (FJB+) stained neurons were significantly higher compared to shams at all time points. Representative histological images depict figures

sham (A) and blast (B) groups in prefrontal cortex, * $p < 0.05$; Arrows indicate FJB+ neurons.

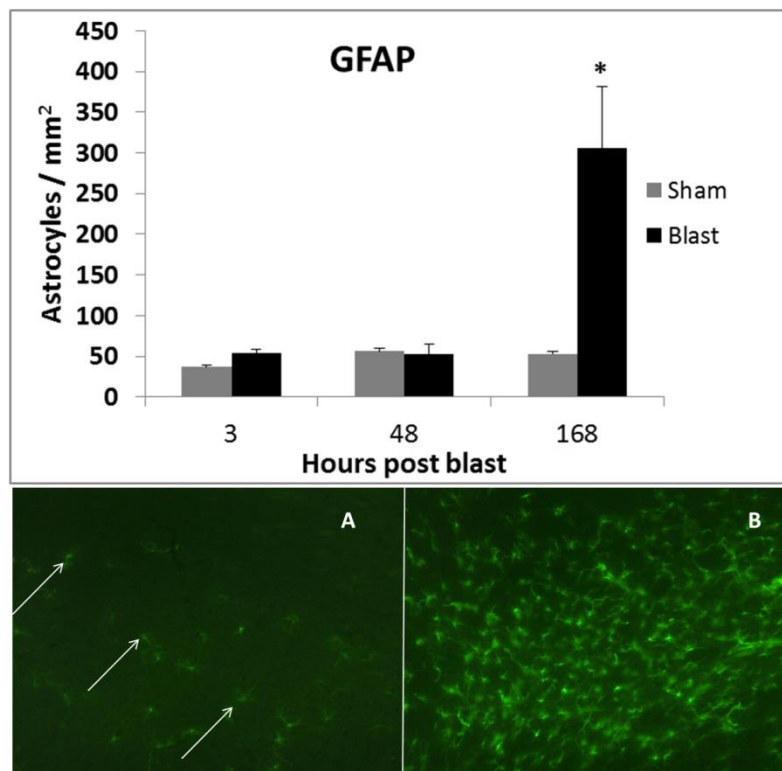


Figure 5.6: GFAP positive-stained astroglia were measured using immunohistochemistry at various time points. Significant levels of FJB+ neurons were found at 168, but not 3 or 48, hours following blast compared to sham animals, * $p < 0.01$. Representative figures sham (A) and blast (B) groups at 168 hours from prefrontal cortex; Arrows indicate GFAP positive astrocytes.

Discussion:

Injury to the PFC in the field of blast neurotrauma research has been understudied. Most of the studies primarily focused on examining the cognitive defects and injury are hippocampus after blast trauma. The PFC mediates and is involved in the processing of working memory and the transition of short term memories into long term memories via neurotransmission. This study demonstrates the significant injury that occurs to the PFC in a blast neurotrauma animal model that causes working memory impairment. These novel data provide fundamental knowledge on underlying mechanisms of blast neurotrauma that may be relevant to clinically reported memory issues.

Behavioral outcome:

Many clinical studies have reported deficits in attention and memory following BINT (Belanger et [1,33,34]. Although some studies describe cognitive deficits associated with BINT using animal models, none thus far have evaluated the short-term /working memory deficit following blast overpressure. Working memory is impaired at 168 hours (7 days) following blast overpressure in the exposed group compared to the sham group; however, we did not observe any behavioral deficits at 72 hours following blast exposure. This delayed onset of symptoms (i.e., compromised memory) following blast overpressure exposure is similar to clinical reports [2]. Although delayed onset of the symptoms are reported after blast, no specific brain region or neuropathological outcome in relation to cognition is not identified for the prognosis of injury. Here, to further understand molecular cascades and neurochemical changes associated with working memory impairment, assessment of the injured brains was done using ¹H-MRS and immunohistochemistry.

Neurochemical assessment using ¹H-MRS:

Early oxidative stress has been reported in association with cellular injury and death in animal models of traumatic brain injury and BINT [35-37]. Previous preclinical reports have reported acute oxidative stress in hippocampus, substantia nigra, and cortical regions of brain following blast overpressure exposure via down regulation in major anti-oxidants in brain such as GSH and superoxide dismutase (SOD) [27,35-38]. In this study, a decrease in the total concentration of GSH was observed at 3 hours in the PFC following blast overpressure exposure suggesting ongoing oxidative stress at an acute stage and likely reflects activation of the pentosephosphate pathway [39].

Oxidative stress may lead to a wide range of cellular damaging cascades eventually causing cell death. This process is primarily triggered by mitochondrial failure leading to compromised energy metabolism, inflammation due to cell membrane rupture, and irregular cellular homeostasis caused by the depletion of energy. In the current study, decreased levels of BET along with increased levels of GABA were found at 24 hours post blast which could reflect a compromise in energy metabolism since BET plays an important role in energy metabolism via methionine pathway [40-42]. GABA plays a critical role in energy metabolism during an energy crisis via the GABA shunting

pathway; both of these factors further supports the compromised metabolic activity following BINT [43,44].

Energy metabolism crisis was further supported by increased levels of Lac and Cre and the ratio of Lac/Cre because these metabolites are preferentially used under low oxygen conditions and during an energy crisis for the generation of ATP. In other words, Cre production of ATP and Lac, which is a catabolite of anaerobic metabolism, is generated during this compensatory energy process [45,46]. Along this same line, increased Glu/Cre at 48 hours post blast potentially indicates the activated compensatory energy mechanism against the ongoing mitochondrial energy crisis [47,48]. Gln and Glu can be converted to α -ketoglutarate and enter tricarboxylic acid (Kreb) cycle, which is upregulated under energy crisis [49]. The injury process demands high cellular energy for repair and counteracts the stress that could lead to neurodegeneration in surrounding tissues. Major metabolites like Glu, GABA, Cre, and Lac are regulated under cellular nutritional crisis and are metabolized through compensatory pathways such as GABA shunt and pentosephosphate pathway [27,41,50].

Our group has previously reported similar changes observed in GABA and Glu in the hippocampus that lead to activation of apoptosis pathway via caspase-3 signaling [27]. The GABA shunt has also been speculated to play a pivotal role in disorders such as epilepsy and Alzheimer's disease [51,52]. With the advancement of recent technology, Lac, Cre, GABA and Glu can be resolved in clinical NMR for diagnostic purpose [53]. These potential findings could be further evaluated with personnel exposed to blast overpressure at an acute phase. Energy metabolism compromise often combines with inflammatory cascades to activate cellular death cascades and this process has been observed in Alzheimer's disease and multiple sclerosis [54-57] .

Supporting evidence of inflammation was observed with elevated GPC levels at 48 hours following blast overpressure. GPC is a breakdown product of arachidonic acid via phospholipase A2 activity and acts as a marker for membrane breakdown and inflammation [27,41,58,59]. This process could be a result of cell membrane breakdown due to cell death. Inflammation and cellular death may be a response to clearing debris and restore homeostasis in the injured regions of brain [41,60,61]. In this study,

increased levels of Ins at 168 hours post blast suggests the process of astrogliosis. Ins is found mainly in astrocytes, regulates various hormonal and signaling pathways, and increased Ins at a sub-acute phase is a strong indicator of astrogliosis [62-66]. Various clinical reports of brain injury using NMR have shown increased levels of Ins following injury [67-69]. The process of cell death was further evaluated using the histological analysis for astrogliosis and neurodegeneration.

Astrogliosis and neurodegeneration:

Increased astrogliosis at 168 hours is an indicator of glial scarring possibly from the resultant neurodegeneration at 3, 48 and 168 hours post blast. Glial scarring results from the overexpression of astrocytes repair mechanism to prevent injury progression [70,71]. The process of glial scarring impairs neurotransmission by impeding axonal growth and sprouting, which could lead to chronic impairment in neuronal repair and function [72-74].

Correlation between behavior and myo-inositol:

In summary, early metabolic changes were consistent with a compromise in energy metabolism that resulted in sub-acute active neurodegeneration and glial scarring. Increased myo-inositol levels further supported the glial scarring and were associated with impaired working memory. Furthermore, these results from 1H-MRS could be directly translated into human studies to provide a valuable insight into diagnosis of BINT, and it is tempting to speculate that 1H-MRS Ins may be a potential biomarker for blast-induced memory impairment

Conclusion:

In summary, early metabolic changes were consistent with a compromise in energy metabolism that resulted in sub-acute active neurodegeneration and glial scarring. Increased *myo*-inositol levels further supported the glial scarring and were associated with impaired working memory. Furthermore, these results from ¹H-MRS could be directly translated into human studies to provide a valuable insight into diagnosis of BINT, and it is tempting to speculate that ¹H-MRS Ins may be a potential biomarker for blast-induced memory impairment.

Acknowledgements

We would like to thank Megan Roberts in assisting behavioral experiments, the WSU Bioengineering Center Staff for assisting with this project, especially Dr. Bin Wu and Mr. James Kopaz. This project was partially funded by the Department of Defense (Award no. W81XWH-08-2-0207).

Conflicts of interest

The authors declare that they have no conflict of interest.

References

1. Bogdanova Y, Verfaellie, M (2012) Cognitive Sequelae of Blast-Induced Traumatic Brain Injury: Recovery and Rehabilitation. *Neuropsychol Rev* 22(1): 4-20.
2. Kovesdi E, Kamnaksh A, Wingo D, Ahmed F, Grunberg NE, Long JB, Kasper CE, Agoston DV., (2012) Acute minocycline treatment mitigates the symptoms of mild blast-induced traumatic brain injury. *Front Neurol* 3:11.
3. Matthews SC, Strigo IA, Simmons AN, O'Connell RM, Reinhardt LE, Moseley SA, (2011) A multimodal imaging study in U.S. veterans of Operations Iraqi and Enduring Freedom with and without major depression after blast-related concussion. *Neuroimage* 54, Supplement 1(0): S69-S75.
4. Säljö A, Svensson B, Mayorga M, Hamberger A, Bolouri H, (2010) Low levels of blast raises intracranial pressure and impairs cognitive function in rats. *J Neurotrauma* 27(2):383-389.
5. Terrio H, Brenner LA, Ivins BJ, Cho JM, Helmick K, Schwab K, Scally K, Bretthauer R, Warden D, (2009) Traumatic Brain Injury Screening: Preliminary Findings in a US Army Brigade Combat Team. *J Head Trauma Rehabil* 24(1):14-23.
6. Vandevord PJ, Bolander R, Sajja VS, Hay K, Bir CA, (2012) Mild Neurotrauma Indicates a Range-Specific Pressure Response to Low Level Shock Wave Exposure. *Ann Biomed Eng* 40(1): 1-10.
7. McAllister TW, (2009) Psychopharmacological Issues in the Treatment of TBI and PTSD. *Clin Neuropsychol* 23(8): 1338-1367.
8. Okie S, (2005) Traumatic Brain Injury in the War Zone. *N Engl J Med* 352(20): 2043-2047.

9. Rosenfeld JV, Ford NL, (2010) Bomb blast, mild traumatic brain injury and psychiatric morbidity: A review. *Injury* 41(5): 437-443.
10. Vanderploeg RD, Belanger HG, Horner RD, Spehar AM, Powell-Cope G, Luther SL, Scott SG, (2012) Health Outcomes Associated With Military Deployment: Mild Traumatic Brain Injury, Blast, Trauma, and Combat Associations in the Florida National Guard. *Arch Phys Med Rehabil* 93(11): 1887-1895.
11. Cernak I, Merkle AC, Koliatsos VE, Bilik JM, Luong QT, Mahota TM, Xu L, Slack N, Windle D, Ahmed FA, (2011) The pathobiology of blast injuries and blast-induced neurotrauma as identified using a new experimental model of injury in mice. *Neurobiol Dis* 41(2): 538-551.
12. Elder GA, Mitsis EM, Ahlers ST, Cristian A, (2010) Blast-induced Mild Traumatic Brain Injury. *Psychiatr Clin North Am* 33(4): 757-781.
13. Hayes, JP, Morey RA, Tupler LA, (2011) A case of frontal neuropsychological and neuroimaging signs following multiple primary-blast exposure. *Neurocase* 18(3): 258-269.
14. Koliatsos VE, Cernak I, Xu L, Song Y, Savonenko A, Crain BJ, Eberhart CG, Frangakis CE, Melnikova T, Kim H, Lee D, (2011) A Mouse Model of Blast Injury to Brain: Initial Pathological, Neuropathological, and Behavioral Characterization. *J Neuropathol Exp Neurol* 70(5): 399-416.
15. Säljö A, Arrhén F, Bolouri H, Mayorga M, Hamberger A, (2008) Neuropathology and pressure in the pig brain resulting from low-impulse noise exposure. *J Neurotrauma* 25(12):1397-406.

16. Brown JW, (2011) Medial prefrontal cortex activity correlates with time-on-task: What does this tell us about theories of cognitive control? *Neuroimage* 57(2): 314-315.
17. Goldstein LE, Rasmusson AM, Bunney BS, Roth RH, (1996) Role of the Amygdala in the Coordination of Behavioral, Neuroendocrine, and Prefrontal Cortical Monoamine Responses to Psychological Stress in the Rat. *J Neurosci* 16(15): 4787-4798.
18. Groenewegen HJ, Wright CI, Uylings HBM, (1997) The anatomical relationships of the prefrontal cortex with limbic structures and the basal ganglia. *J Psychopharmacol* 11(2): 99-106.
19. Koenigs, M, (2012) The role of prefrontal cortex in psychopathy. *Rev Neurosci* 23(3):253-62
20. Rushworth MF, Noonan MP, Boorman ED, Walton ME, Behrens TE, (2011) Frontal Cortex and Reward-Guided Learning and Decision-Making. *Neuron* 70(6): 1054-1069.
21. Stuss DT, (2011) Functions of the Frontal Lobes: Relation to Executive Functions. *J Int Neuropsychol Soc* 17(05): 759-765.
22. Thierry AM, Gioanni Y, Dégénétais E, Glowinski J, (2000) Hippocampo-prefrontal cortex pathway: Anatomical and electrophysiological characteristics. *Hippocampus* 10(4): 411-419.
23. Vertes RP, (2006) Interactions among the medial prefrontal cortex, hippocampus and midline thalamus in emotional and cognitive processing in the rat. *Neuroscience* 142(1): 1-20.
24. Mao JC, Pace E, Pierozynski P, Kou Z, Shen Y, VandeVord P, Haacke EM, Zhang X, Zhang J, (2012) Blast-Induced Tinnitus and Hearing Loss in Rats: Behavioral and Imaging Assays. *J Neurotrauma* 29(2): 430-44

25. Ennaceur A, Delacour J, (1988) A new one-trial test for neurobiological studies of memory in rats. 1: Behavioral data. *Behav Brain Res* 31(1):47-59.
26. Antunes M, Biala G, (2012) The novel object recognition memory: neurobiology, test procedure, and its modifications. *Cogn Process* 13(2):93-110
27. Sajja VS, Galloway MP, Ghoddoussi F, Thiruthalinathan D, Kepsel A, Hay K, Bir CA, Vandevord PJ, (2012) Blast-induced neurotrauma leads to neurochemical changes and neuronal degeneration in the rat hippocampus. *NMR Biomed* 25(12): 1331-1339.
28. Paxinos G, and Watson C, *The rat brain in stereotaxic coordinates*, 2nd edition. San Diego; Academic Press. 1986.
29. Cheng LL, Ma MJ, Becerra L, Ptak T, Tracey I, Lackner A, González RG, (1997) Quantitative neuropathology by high resolution magic angle spinning proton magnetic resonance spectroscopy. *Proc Natl Acad Sci USA* 94(12): 6408-6413.
30. Provencher S, (1993) Estimation of metabolite concentrations from localized proton {NMR} spectra. *Magn Reson Med* 30: 672-679.
31. Provencher SW, (2001) Automatic quantitation of localized in vivo ¹H spectra with LCModel. *NMR Biomed* 14(4): 260-264.
32. Schmued LC, Hopkins KJ, (2000) Fluoro-Jade B: a high affinity fluorescent marker for the localization of neuronal degeneration. *Brain Res* 874(2): 123-130.
33. Belanger HG, Kretzmer T, Yoash-Gantz R, Pickett T, Tupler LA, (2009) Cognitive sequelae of blast-related versus other mechanisms of brain trauma. *J Int Neuropsychol Soc* 15(01): 1-8.

34. Bhattacharjee Y, (2008) Shell Shock Revisited: Solving the Puzzle of Blast Trauma. *Science*, 319(5862): 406-408.
35. Cernak I, Wang Z, Jiang J, Bian X, Savic J, (2001) Ultrastructural and Functional Characteristics of Blast Injury-Induced Neurotrauma. *J Trauma Acute Care Surg* 50(4): 695-706.
36. DeWitt SD, Prough DS, (2009) Blast-Induced Brain Injury and Posttraumatic Hypotension and Hypoxemia. *J Neurotrauma* 26(6): 877-887.
37. Readnower RD, Chavko M, Adeeb S, Conroy MD, Pauly JR, McCarron RM, Sullivan PG, (2010) Increase in blood–brain barrier permeability, oxidative stress, and activated microglia in a rat model of blast-induced traumatic brain injury. *J Neurosci Res* 88(16): 3530-3539.
38. Abdul-Muneer PM, Schuetz H, Wang F, Skotak M, Jones J, Gorantla S, Zimmerman MC, Chandra N, Haorah J, (2013) Induction of Oxidative and Nitrosative damage leads to Cerebrovascular Inflammation in Animal Model of Mild Traumatic Brain Injury Induced by Primary Blast. *Free Radic Biol Med*. n/a
39. Pocernich CB, Butterfield DA, (2012) Elevation of glutathione as a therapeutic strategy in Alzheimer disease. *Biochim Biophys Acta* 1822(5): 625-630.
40. Li Z, Vance DE, (2008) Thematic Review Series: Glycerolipids. Phosphatidylcholine and choline homeostasis. *J Lipid Res* 49(6): 1187-1194.
41. Moore GJ, Galloway MP, (2002) Magnetic resonance spectroscopy: neurochemistry and treatment effects in affective disorders. *Psychopharmacol Bull* 36(2): 5-23.

42. Passe TJ, Charles HC, Rajagopalan P, Krishnan KR, (1995) Nuclear magnetic resonance spectroscopy: A review of neuropsychiatric applications. *Prog Neuropsychopharmacol Biol Psychiatry* 19(4): 541-563.
43. Kasser TR, Harris RB, Martin RJ, (1985) Level of satiety: GABA and pentose shunt activities in three brain sites associated with feeding. *Am J Physiol Regul Integr Comp Physiol* 248(4): R453-R458.
44. Schousboe A, Sonnewald U, Waagepetersen HS, (2003) Differential roles of alanine in GABAergic and glutamatergic neurons. *Neurochem Int* 43(5): 311-315.
45. Holtzman D, Meyers R, O'Gorman E, Khait I, Wallimann T, Allred E, Jensen F., (1997) In vivo brain phosphocreatine and ATP regulation in mice fed a creatine analog. *Am J Physiol* 272:C1567-77.
46. Kekelidze T, Khait I, Togliatti A, Benzecry JM, Wieringa B, Holtzman D, (2001) Altered brain phosphocreatine and ATP regulation when mitochondrial creatine kinase is absent. *J Neurosci Res* 66(5):866-72.
47. Di Costanzo A, Trojsi F, Tosetti M, Schirmer T, Lechner SM, Popolizio T, Scarabino T, (2007) Proton MR spectroscopy of the brain at 3 T: an update. *Eur Radiol* 17(7): 1651-1662.
48. Nucci-da-Silva MP, Amaro E, (2009) A systematic review of magnetic resonance imaging and spectroscopy in brain injury after drowning. *Brain Inj* 23(9): 707-714.
49. Patel AB, de Graaf RA, Mason GF, Rothman DL, Shulman RG, Behar KL (2005) The contribution of GABA to glutamate/glutamine cycling and energy metabolism in the rat cortex in vivo. *Proc Natl Acad Sci USA* 102:5588–5593
50. Bolaños JP, Almeida A, Moncada S, (2010) Glycolysis: a bioenergetic or a survival

pathway? Trends Biochem Sci 35(3): 145-149.

51. An SJ, Park SK, Hwang IK, Choi SY, Kim SK, Kwon OS, Jung SJ, Baek NI, Lee HY, Won MH, Kang TC, (2003) Gastrodin decreases immunoreactivities of γ -aminobutyric acid shunt enzymes in the hippocampus of seizure-sensitive gerbils. J Neurosci Res 71(4): 534-543.

52. Mamelak M, (2012) Sporadic Alzheimer's Disease: The Starving Brain. J Alzheimers Dis 31(3): 459-474.

53. Yang M, Wang S, Hao F, Li Y, Tang H, Shi X, (2012) NMR analysis of the rat neurochemical changes induced by middle cerebral artery occlusion. Talanta 88(0): 136-144.

54. Bosco D, Fava A, Plastino M, Montalcini T, Pujia A, (2011) Possible implications of insulin resistance and glucose metabolism in Alzheimer's disease pathogenesis. J Cell Mol Med 15(9): 1807-1821.

55. Lassmann H, van Horssen J, (2011) The molecular basis of neurodegeneration in multiple sclerosis. FEBS Letters 585(23): 3715-3723.

56. Paling D, Golay X, Wheeler-Kingshott C, Kapoor R, Miller D, (2011) Energy failure in multiple sclerosis and its investigation using MR techniques. J Neurol 258(12): 2113-2127.

57. Wilcox CS, (2010) Effects of tempol and redox-cycling nitroxides in models of oxidative stress. Pharmacol Ther 126(2): 119-145.

58. Andrade CS, Otaduy MC, Valente KD, Maia DF, Park EJ, Valério RM, Tsunemi MH, Leite CC, (2011) Phosphorus magnetic resonance spectroscopy in malformations of cortical

development. *Epilepsia* 52(12): 2276-2284.

59. Forster DM, James MF, Williams SR, (2012) Effects of Alzheimer's disease transgenes on neurochemical expression in the mouse brain determined by ¹H MRS in vitro. *NMR Biomed* 25(1): 52-58.

60. Agoston DV, Gyorgy A, Eidelman O, Pollard HB, (2009) Proteomic biomarkers for blast neurotrauma: targeting cerebral edema, inflammation, and neuronal death cascades. *J Neurotrauma*. 26, 901-11.

61. Jenkins BG, Kraft E, (1999) Magnetic resonance spectroscopy in toxic encephalopathy and neurodegeneration. *Curr Opin Neurol* 12(6): 753-760.

62. Fan YQ, Lee J, Oh S, Liu HJ, Li C, Luan YS, Yang JM, Zhou HM, Lü ZR, Wang YL, (2012) Effects of osmolytes on human brain-type creatine kinase folding in dilute solutions and crowding systems. *Int J Biol Macromol* 51(5): 845-858.

63. Yong Suk Hur, Ki Deok Kim, Sun Ha Paek, Seung Hyun Yoo, (2010) Evidence for the existence of secretory granule (dense-core vesicle)-based inositol 1,4,5-trisphosphate-dependent Ca²⁺ signaling system in astrocytes. *PLoS ONE*, 5(8): e11973.

64. Kelm MK, Weinberg RJ, Criswell HE, Breese GR, (2010) The PLC/IP3R/PKC pathway is required for ethanol-enhanced GABA release. *Neuropharmacology* 58(7): 1179-1186.

65. Nelson TJ, Sun MK, Hongpaisan J, Alkon DL, (2008) Insulin, PKC signaling pathways and synaptic remodeling during memory storage and neuronal repair. *Eur J Pharmacol* 585(1): 76-87.

66. Song D, Du T, Li B, Cai L, Gu L, Li H, Chen Y, Hertz L, Peng L, (2008) Astrocytic alkalization by therapeutically relevant lithium concentrations: implications for myo – inositol depletion. *Psychopharmacol* 200(2): 187-195.
67. Babikian T, Freier MC, Ashwal S, Riggs ML, Burley T, Holshouser BA, (2006) MR spectroscopy: Predicting long-term neuropsychological outcome following pediatric TBI. *J Magn Reson Imaging* 24(4): 801-811.
68. Wilson M, Cummins CL, Macpherson L, Sun Y, Natarajan K, Grundy RG, Arvanitis TN, Kauppinen RA, Peet AC, (2012) Magnetic resonance spectroscopy metabolite profiles predict survival in paediatric brain tumours. *Eur J Cancer* 49(2): 457-64
69. Yoon SJ, Lee JH, Kim ST, Chun MH, (2005) Evaluation of traumatic brain injured patients in correlation with functional status by localized ¹H-MR spectroscopy. *Clin Rehab* 19(2): 209-215.
70. Sofroniew M, Vinters H, (2010) Astrocytes: biology and pathology. *Acta Neuropathol* 119(1): 7-35.
71. Suzuki T, Sakata H, Kato C, Connor JA, Morita M, (2012) Astrocyte activation and wound healing in intact-skull mouse after focal brain injury. *Eur J Neurosci* 36(12): 3653-3664.
72. Ebrahimi F, Koch M, Pieroh P, Ghadban C, Hobusch C, Bechmann I, Dehghani F, (2012) Time dependent neuroprotection of mycophenolate mofetil: effects on temporal dynamics in glial proliferation, apoptosis, and scar formation. *J Neuroinflammation* 9(1): 89.
73. Sofroniew MV, Molecular dissection of reactive astrogliosis and glial scar formation. *Trends Neurosci*, 2009. 32(12): 638-647.

74. Tuinstra HM, Ducommun MM, Briley WE, Shea LD, (2013) Gene delivery to overcome astrocyte inhibition of axonal growth: An in vitro Model of the glial scar. *Biotechnol Bioeng* 110(3): 947-

Chapter 6

Summary

Numerous pathological outcomes have been identified in relation to BINT.

Neurochemical alterations/imbalance, oxidative stress, mitochondrial dysfunction and BBB disruption have been identified to be important pathological events that are involved at an acute stage following BOP. However, the time course for the progression of pathological sequelae leading to cognitive deficits is unknown. In this study, neurochemical alterations, working memory, anxiety and histopathological assays of cell death (cleaved caspase-3), neurodegeneration (fluorograde B), glial activation (Iba1 and GFAP), mature neuronal population (NeuN), oxidative stress (superoxide dismutase 1, SOD1) were evaluated in medial prefrontal cortex (PFC), hippocampus (HIP), amygdala (AMY) and nucleus accumbens (NAC) of animals exposed to blast.

Neurochemical and histopathological outcome following BOP exposure

Acute changes (3 hours – 48 hours) in neurochemistry were observed to be primarily associated with oxidative stress (reduced levels of glutathione or SOD1) in HIP, PFC, AMY and NAC regions. Previous studies have shown elevated levels of reactive oxidative stress using oxidative stress markers, reduced SOD1 levels at an acute stage following BOP exposure [162-168]. However, the basis for the enriched oxidative stress environment is unknown. In the current study, decreased levels of SOD1 were found in the PFC and NAC regions. Neurochemical imbalance and/or mitochondrial stress in combination with oxidative stress followed by elevated inflammation is hypothesized to be the basis for the associated cell death.

Oxidative stress is known to initiate cell injury pathways eventually causing cell death. This process is primarily triggered by mitochondrial failure leading to compromised energy metabolism, inflammation due to cell membrane rupture, and irregular cellular homeostasis caused by the depletion of energy [169 – 172]. Oxidative stress acts directly on mitochondrial processes binding to NAD/NADPH decreasing the production of ATP required for cellular homeostasis. In addition, reactive oxygen species (hydrogen peroxide and superoxide anions) inhibit the process of phosphorylation primarily in

mitochondria which are required for function of secondary messenger systems.

Mitochondrial failure leads to disrupted energy homeostasis and triggers the apoptotic cascades, leading to programmed cell death. In the current study, decreased levels of BET along with compromised levels of GABA were found acutely (3-48 hours) post blast which could reflect a compromise in energy metabolism since BET plays an important role in energy metabolism via the methionine pathway and it likely reflects activation of the pentose phosphate pathway [173-176]. GABA can act as an inhibitory neurotransmitter in the brain and plays a critical role in energy metabolism during an energy crisis via the GABA shunting pathway. Thus decreased levels of GABA further supports the compromised metabolic activity acutely following BOP exposure in the PFC region.

The observed increased levels of Lac and Cre and the ratio of Lac/Cre further supports an energy metabolism crisis as these metabolites are preferentially used under low oxygen environments and conditions of cellular stress for the generation of ATP. ATP and Lac production using Cre, which is a catabolite of anaerobic metabolism, is generated during compensatory energy processes [177,179].

Moreover, increased Glu/Cre post blast potentially indicates the activated compensatory energy mechanism against the ongoing mitochondrial energy crisis. Gln and Glu can be converted to α -ketoglutarate and enter the tricarboxylic acid (Kreb) cycle, which is up regulated under energy crisis. The cellular injury repair process involves clearing the dysfunctional mitochondria, internal cellular organelles and reintegration of cellular membrane, which demands high cellular energy despite the cellular stress due to mitochondrial failure. Mitochondrial failure due to oxidative stress in neurons which have high energy demands primarily to carry out its functions such integration of action potentials and neurotransmission in addition to mitochondrial repair. In order to counteract the stress that could lead to neurodegeneration, neurons use alternative energy supportive cascades, involves major metabolites such as Glu, GABA, Cre, and Lac. These metabolites are upregulated under cellular metabolic crisis and are metabolized through compensatory pathways such as GABA shunt and pentose phosphate pathway with astrocyte support [175, 176,181].

The GABA shunt has been speculated to play a pivotal role in several neurological disorders such as epilepsy and Alzheimer's disease (Figure 6.1). With the advancement of recent technology, Lac, Cre, GABA and Glu can be resolved in clinical NMR for diagnostic purpose.

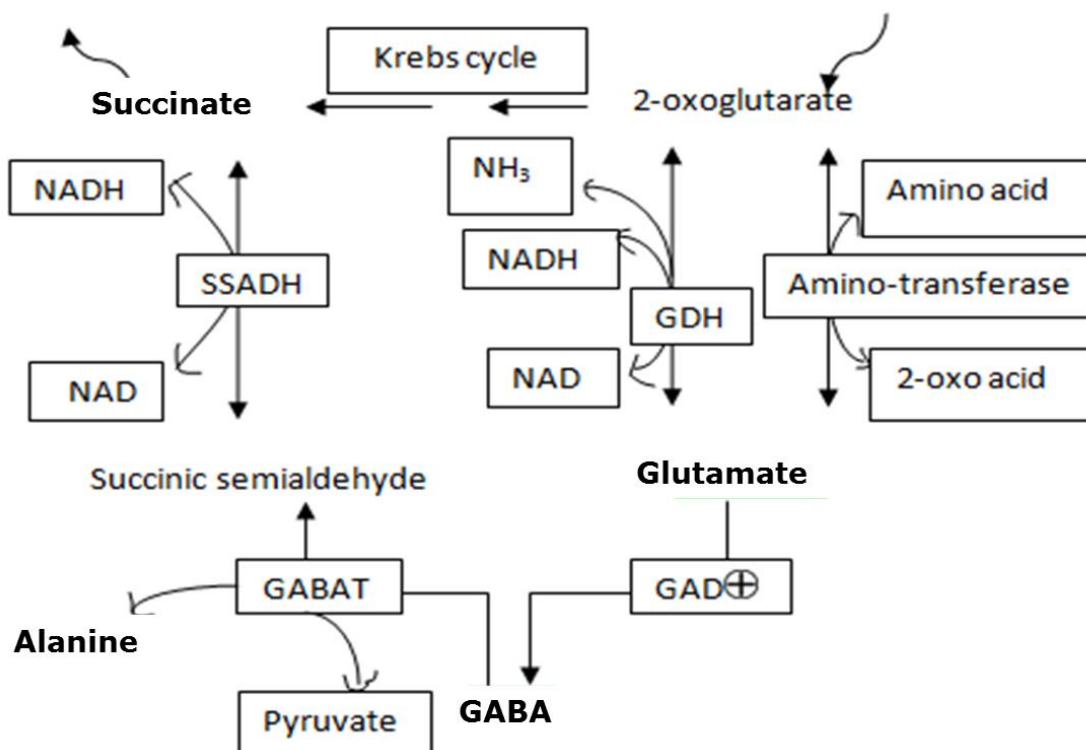


Figure 6.1: GABA shunt plays an important role in supporting Krebs's cycle to regulate cellular energy metabolism and homeostasis

Changes in these metabolites can be studied and evaluated using clinically NMR to identify individuals with metabolic disorders in brain when exposed to blast. It is common to observe both energy metabolism compromise and the activation of inflammation cascades which subsequently trigger cellular death pathways. The combined activation of the pathways has been reported to occur in Alzheimer's disease and multiple sclerosis [182-184]. The combination of metabolic distress and inflammation could reflect neurodegeneration and programmed cell death in the cognitive regions of brain. In this study, an increase of apoptotic markers at an acute stage was identified.

Supporting evidence of acute inflammation was observed with elevated GPC levels in addition to decreased PEA levels at 48 hours following blast overpressure. GPC is a

breakdown product of arachidonic acid via phospholipase A2 activity and acts as a marker for membrane breakdown and inflammation [185 -187]. This process could be a result of cell membrane breakdown due to cell death. In this study, a rise in the apoptosis marker Casp-3 was found at acute/sub-acute stage after BOP exposure in HIPP, NAC and AMY (3 hours – 7 days), not chronic stage (1-3 months) but at all time points in PFC after BOP exposure (3 hours – 3 months) (Figure 6.2; Table 6.1).

Time point →	One month (Mean ± SEM) Sham vs Blast (*p < 0.05)	Three months (Mean ± SEM) Sham vs blast (*p < 0.05)
Type of stain	Region of brain (integrated density)	Region of brain (integrated density)
GFAP	HIPP: 4752 ± 854 vs 14954 ± 4098* AMY: 2982 ± 1173 vs 10143 ± 1170* PFC: 458 ± 113 vs 1103 ± 258* NAC: 249 ± 57 vs 251 ± 124	HIPP: 4241 ± 206 vs 6074 ± 766* AMY: 1711 ± 749 vs 4557 ± 1008* PFC: 2467 ± 158 vs 4256 ± 214* NAC: 435 ± 67 vs 426 ± 51
FJB	HIPP: 5264 ± 947 vs 5786 ± 824 AMY: 3573 ± 884 vs 11862 ± 1252* PFC: 432 ± 258 vs 1944 ± 412* NAC: 432 ± 147 vs 447 ± 151	HIPP: 7249 ± 3532 vs 23376 ± 5565* AMY: 7405 ± 1489 vs 32407 ± 2371* PFC: 1668 ± 658 vs 8594 ± 1205* NAC: 697 ± 147 vs 1296 ± 251*
NeuN	HIPP: 1431 ± 113 vs 1415 ± 307 AMY: 389 ± 61 vs 218 ± 46* PFC: 1882 ± 230 vs 944 ± 226* NAC: 1116 ± 207 vs 535 ± 74*	HIPP: 2022 ± 305 vs 1230 ± 192* AMY: 328 ± 53 vs 147 ± 30* PFC: 1561 ± 195 vs 545 ± 37* NAC: 605 ± 76 vs 308 ± 61*
SOD1	HIPP: 2614 ± 1562 vs 2557 ± 1193 AMY: 1071 ± 267 vs 1080 ± 144 PFC: 383 ± 93 vs 136 ± 50* NAC: 159 ± 27 vs 50 ± 13*	HIPP: 1932 ± 185 vs 1812 ± 90 AMY: 4908 ± 333 vs 4719 ± 165 PFC: 770 ± 110 vs 393 ± 90* NAC: 128 ± 40 vs 29 ± 12*
Iba1	HIPP: 7818 ± 444 vs 11775 ± 2019* AMY: 4170 ± 256 vs 6864 ± 939* PFC: 2532 ± 128 vs 3291 ± 245* NAC: 1123 ± 97 vs 1605 ± 101*	HIPP: 1647 ± 699 vs 5668 ± 1581* AMY: 1225 ± 321 vs 3056 ± 531* PFC: 948 ± 117 vs 1365 ± 102* NAC: 1812 ± 258 vs 3044 ± 154*
Caspase-3	HIPP: 1564 ± 523 vs 1678 ± 626 AMY: 1541 ± 153 vs 1419 ± 196 PFC: 576 ± 58 vs 894 ± 205* NAC: 175 ± 47 vs 178 ± 51	HIPP: 4623 ± 190 vs 4645 ± 159 AMY: 6960 ± 316 vs 7133 ± 369 PFC: 1982 ± 131 vs 2854 ± 163* NAC: 375 ± 67 vs 406 ± 36

Table 6.1: Raw data of various stains at 1 month and 3 months post blast in hippocampus (HIPP), medial prefrontal cortex (PFC), amygdala (AMY) and nucleus accumbens (NAC), *p < 0.05 when compared to respective sham group

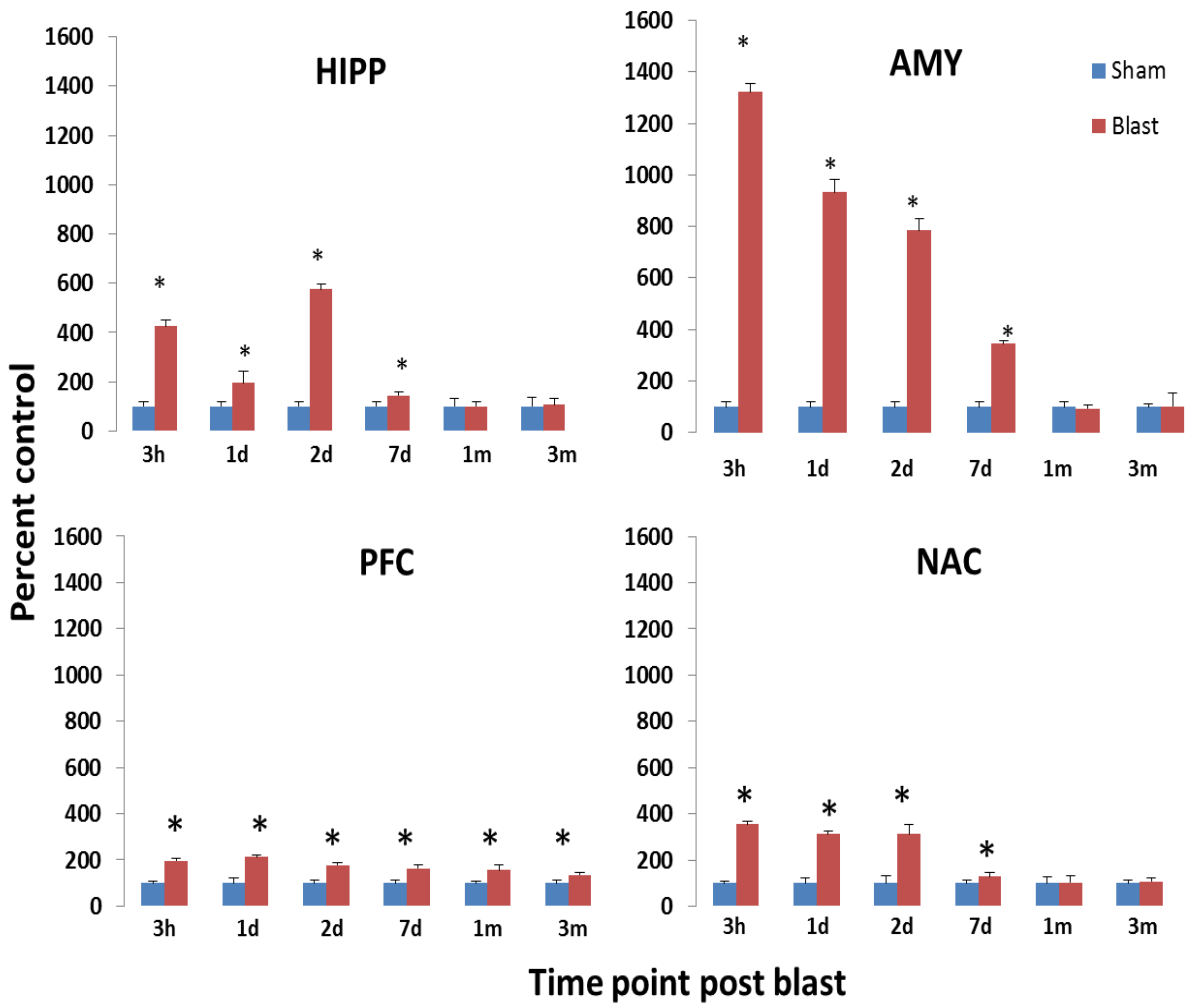


Figure 6.2: Temporal evaluation of the programmed cell death marker, cleaved caspase-3 in hippocampus (HIPP), amygdala (AMY), medial prefrontal cortex (PFC) and nucleus accumbens (NAC) ; 3h – 3 hours, 1d – 1 day, 2d – 2 day, 7d – 7 days, 1m – 1 month, 3m – 3 months; *p < 0.05 when compared to respective sham group

Compensatory mechanisms are available to help repair damaged cells *via* activation of astrocytes which provide additional support for energy to combat programmed cell death as seen in HIPP, NAC and AMY. These regions have balanced Casp 3 levels by the 1 month time point. Astrocytes utilize the in GABA shunt pathway to provide the required energy metabolites (Glu, Ala). Furthermore, they help reduce inflammation by releasing anti-inflammatory cytokines such IL-4, IL-6, IL-10, and helps with up regulation of neurotropic factors like blood derived growth factor (BDNF) and glial cell line derived neurotropic factor. However, in the blast groups, a delayed activation of astrocytes was observed in the PFC, possibly due to delayed signaling of cytokines to up regulate astrocytes.

It is possible impairment of PFC region as a resultant of impaired HIPP, AMY and NAC. PFC has direct innervations from HIPP and AMY, impairment in HIPP and AMY could cause impairment in PFC region. Degenerating axons from neuronal death in HIPP and AMY may lead to release of inflammatory cytokines like MCP-1, TNF- α and IFN-gamma in PFC. The role of delayed activation astrocytes in PFC could be a reason for prolonged apoptosis (which was observed up to 3 months following blast) could be resultant of inflammation from cell debris from death (Figure 6.3). A varied response was observed in the activation GFAP and cleaved caspase-3 in the NAC, PFC, HIPP and NAC. AMY could be more vulnerable due to activation of fear conditioning pathways and elevated stress could result in increased cellular death.

In addition, continual inflammation and cell death may be a response to clearing debris and restore homeostasis in the injured regions of brain. Increased in Ins was found in PFC at 168 hours following BOP exposure. Found mainly in astrocytes, Ins regulates various secondary messenger signaling pathways (inositol tri-phosphate – Diacylglycerol), and increased Ins at a sub-acute phase is an indicator of astrogliosis [188,189]. Using NMR, various clinical reports of brain injury have shown increased levels of Ins following injury, possibly to support the injury repair process *via* astrogliosis and up regulation of anti-inflammatory cascades [190-192].

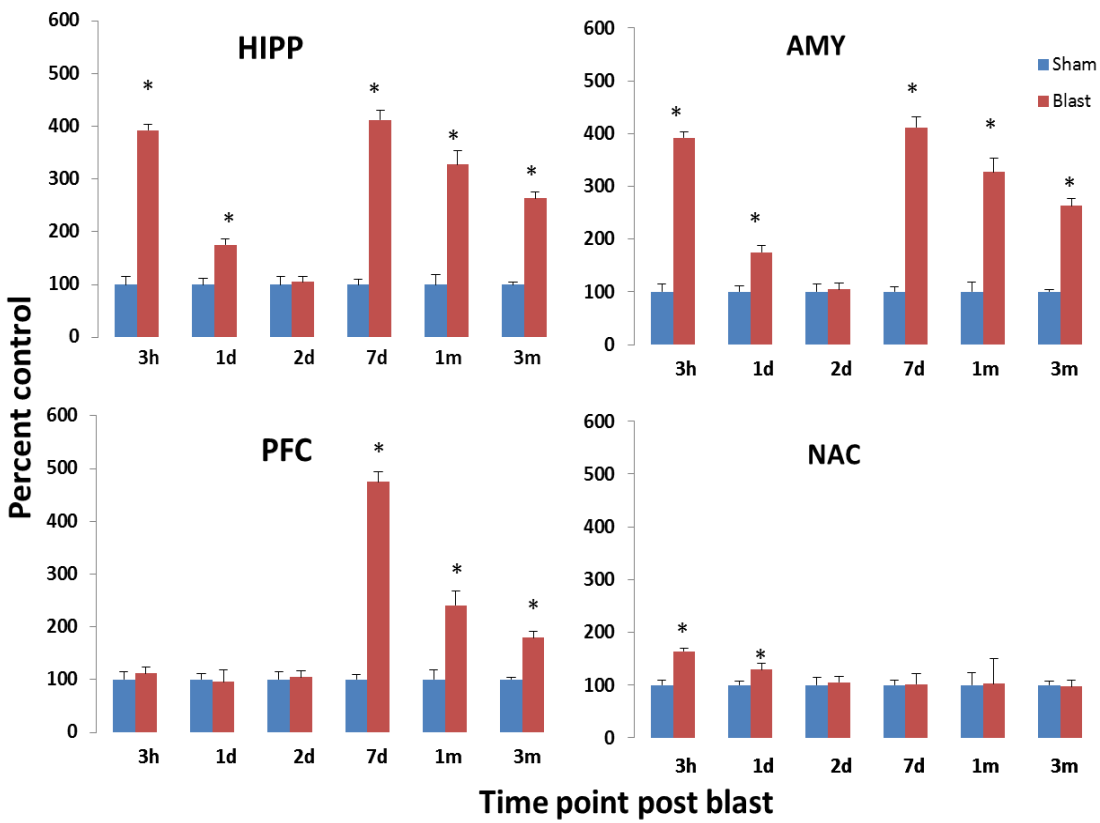


Figure 6.3: Temporal evaluation of GFAP, an astrogliosis marker, in hippocampus (HIPP), amygdala (AMY), medial prefrontal cortex (PFC) and nucleus accumbens (NAC) ; 3h – 3 hours, 1d – 1 day, 2d – 2 day, 7d – 7 days, 1m – 1 month, 3m – 3 months; *p < 0.05 when compared to respective sham group

An increase in microglia, evaluated using Iba1 staining, was seen at the chronic stage which could suggest the microglia are clearing the debris of the degenerated neurons as well as retracting astrocytes (Figure 6.4).

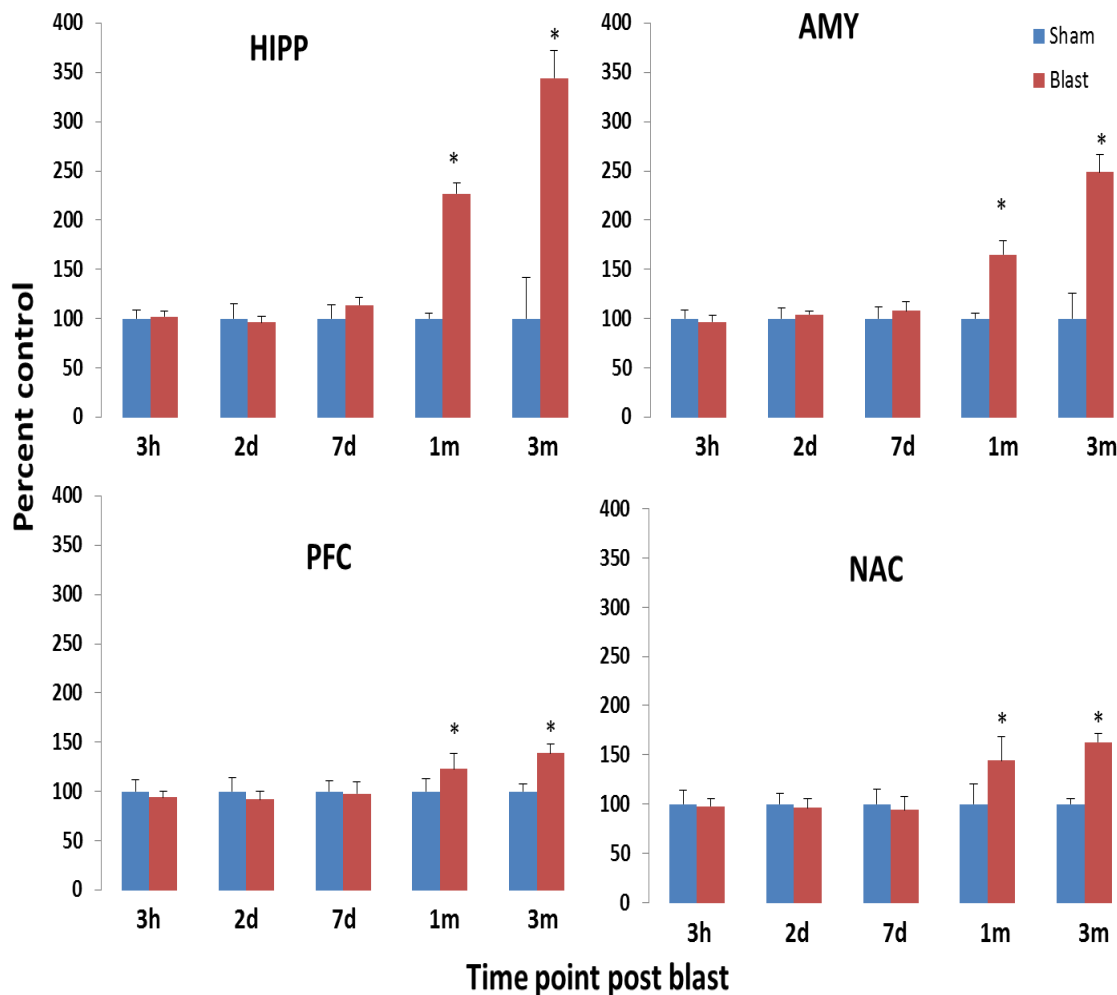


Figure 6.4: Chronic elevated microglia levels (measured using Iba1) were found in hippocampus (HIPP), amygdala (AMY), medial prefrontal cortex (PFC) and nucleus accumbens (NAC) following BOP. No changes were observed at an acute and sub-acute stage (3 hours – 7 days) following BOP; * $p < 0.05$ when compared to respective sham group

Evidence of neuronal loss was supported by increased neurodegeneration (Figure 6.5) and loss of neurons (Figures 6.6) which was found at acute and chronic stages. The data suggested that neuronal loss could lead to marked increase in astrogliosis in HIPP, AMY, NAC and PFC. All regions evaluated were found to have an acute loss of neurons which was sustained throughout the 3 month evaluation period.

All though continual FJB positive cells are observed, it is understood the degenerating neurons can turn over to functional neurons with neuroprotective cascades *via* anti-inflammatory cascades and support from astrocytes [191]. In addition, previous studies have shown at chronic stage, FJB can stain reactive astrocytes [191]. In addition to

AMY, HIPP is vulnerable in various neurodegenerative disorders, due to extensive neurogenesis in the region. However, the extent of the cellular death in each region is different; the amount of neuronal population that was decreased was similar in AMY, HIPP, NAC and PFC.

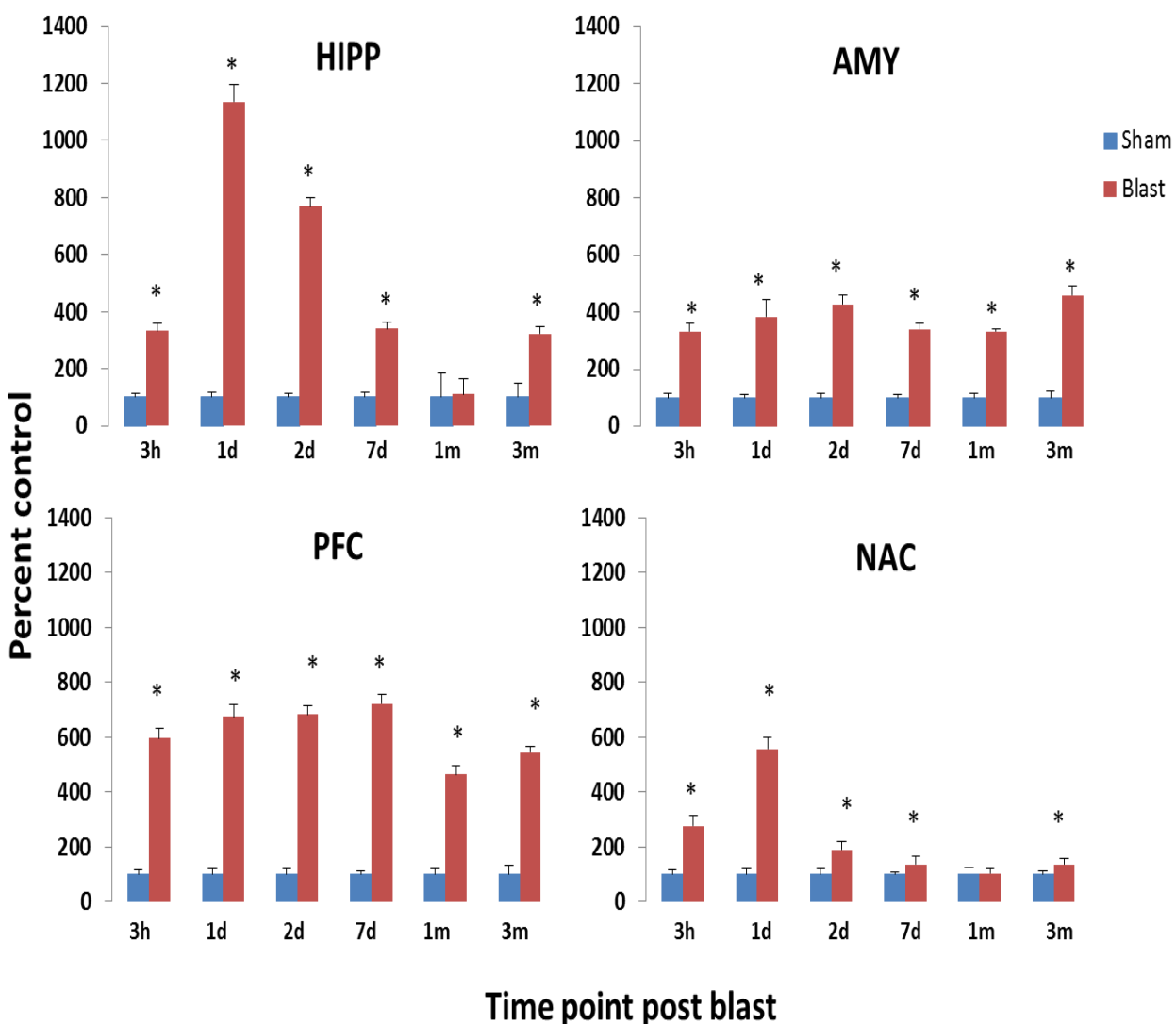


Figure 6.5: Temporal evaluation of neurodegeneration using fluorojade B, in hippocampus (HIPP), amygdala (AMY), medial prefrontal cortex (PFC) and nucleus accumbens (NAC) ; 3h – 3 hours, 1d – 1 day, 2d – 2 day, 7d – 7 days, 1m – 1 month, 3m – 3 months; *p < 0.05 when compared to respective sham group

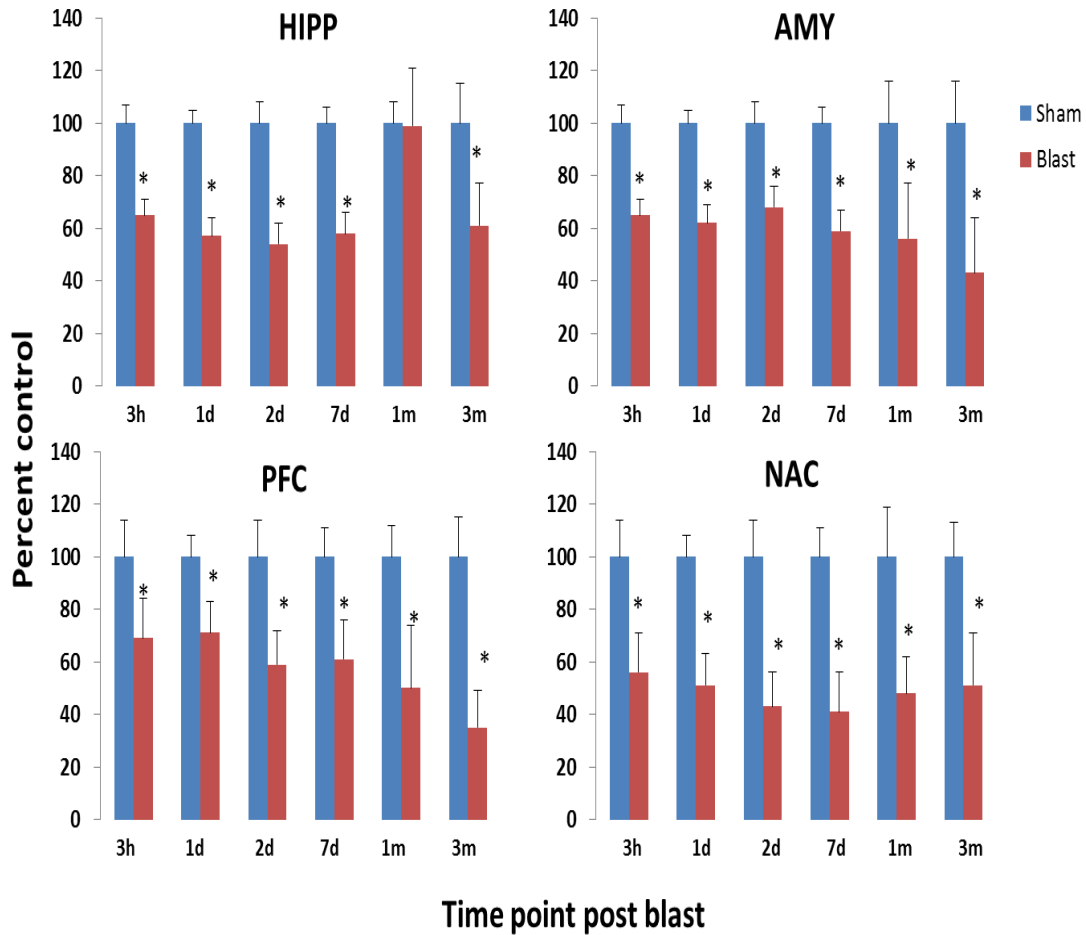


Figure 6.6: Temporal evaluation of mature neurons measured by NeuN staining, in hippocampus (HIPP), amygdala (AMY), medial prefrontal cortex (PFC) and nucleus accumbens (NAC) ; 3h – 3 hours, 1d – 1 day, 2d – 2 day, 7d – 7 days, 1m – 1 month, 3m – 3 months; *p < 0.05 when compared to respective sham group

Decreased levels of SOD1 were observed at a sub-acute and chronic stage following BOP exposure in PFC and NAC but not in HIPP and AMY (Figure 6.7). Substantial loss of cells in the regions of PFC and NAC at the chronic stage could reflect the decreased

SOD1 levels (loss of neurons and astrocyte levels are reduced to comparative sham).

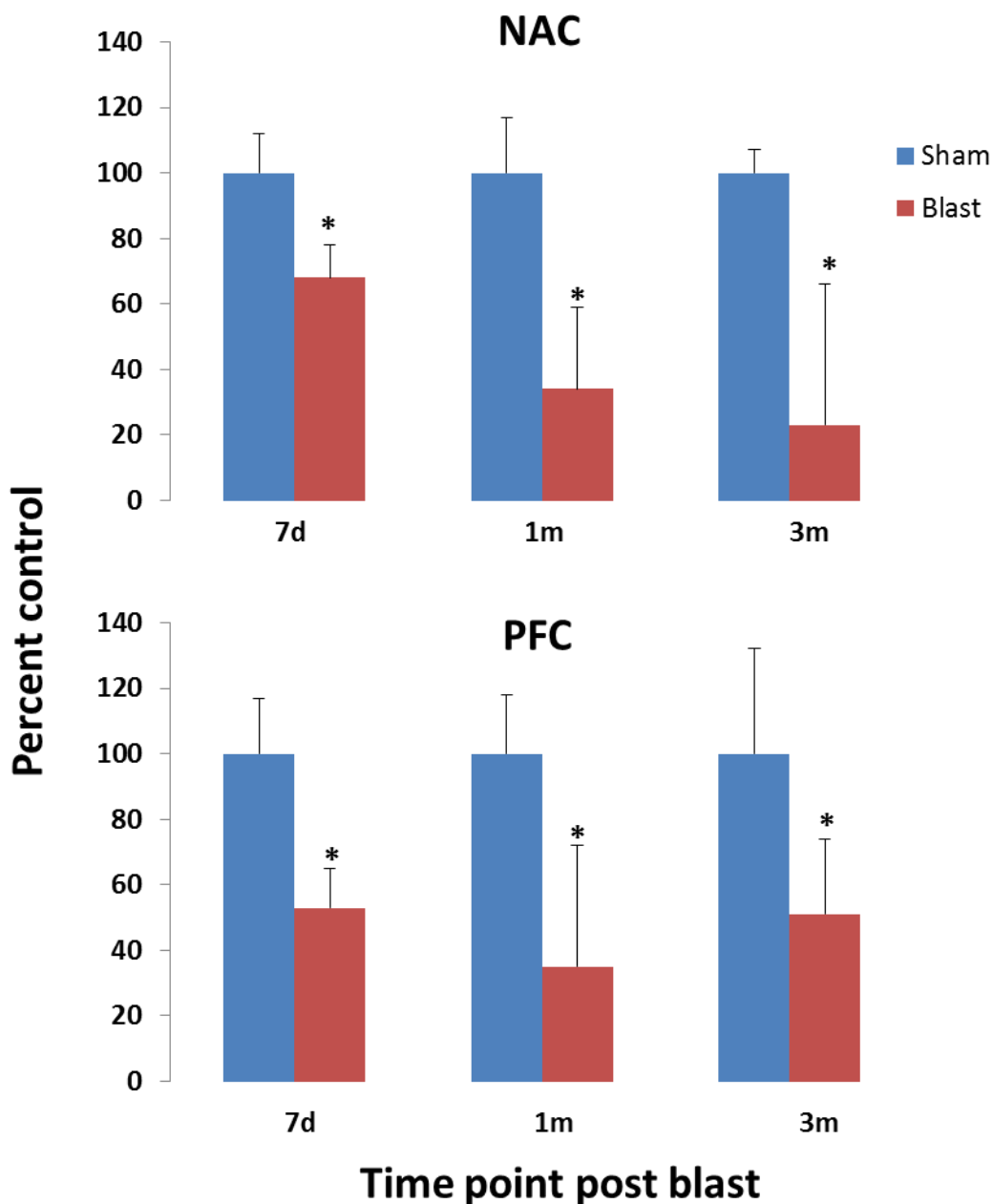


Figure 6.7: Decreased SOD1 levels in medial prefrontal cortex (PFC) and nucleus accumbens (NAC), but no changes were observed at all-time points in hippocampus (HIPP), amygdala (AMY) following BOP. In addition, no changes were observed at an acute and sub-acute stage (3 hours – 48 hours) following BOP in all the regions

This supports the idea that other cellular populations such as could be affected with BOP exposure and has to be evaluated in further studies. In this study, the primary cognitive regions of brain (HIPP, PFC, AMY and NAC) were observed to have a substantial loss of neurons and activated astrogliosis process. A decrease in neurons may cause functional deficits. Behavioral deficits are reported due to the pathological sequelae with neurochemical changes, apoptosis and astrogliosis [191-200]. As such,

behavioral and cognitive assessments were conducted in order to determine an association between the neuropathology and functional deficits [200,202].

Behavioral outcomes (working memory and anxiety) following BOP exposure

Several psychiatric and psychological disorders present themselves following brain injuries (TBI, stroke). Memory deficits and anxiety are documented to be occurred following blast exposure. As such, these behavioral outcomes were assessed.

Elevated anxiety-like behavior was observed in blast groups measured from 2 days to 3 months when animals were tested by the light and dark task (Figure 6.8). This data is consistent with increased cell death and neurodegeneration in the amygdala and nucleus accumbens at an early stage. Clinical reports suggested that increased stress, anxiety and memory impairment are linked (25,56).

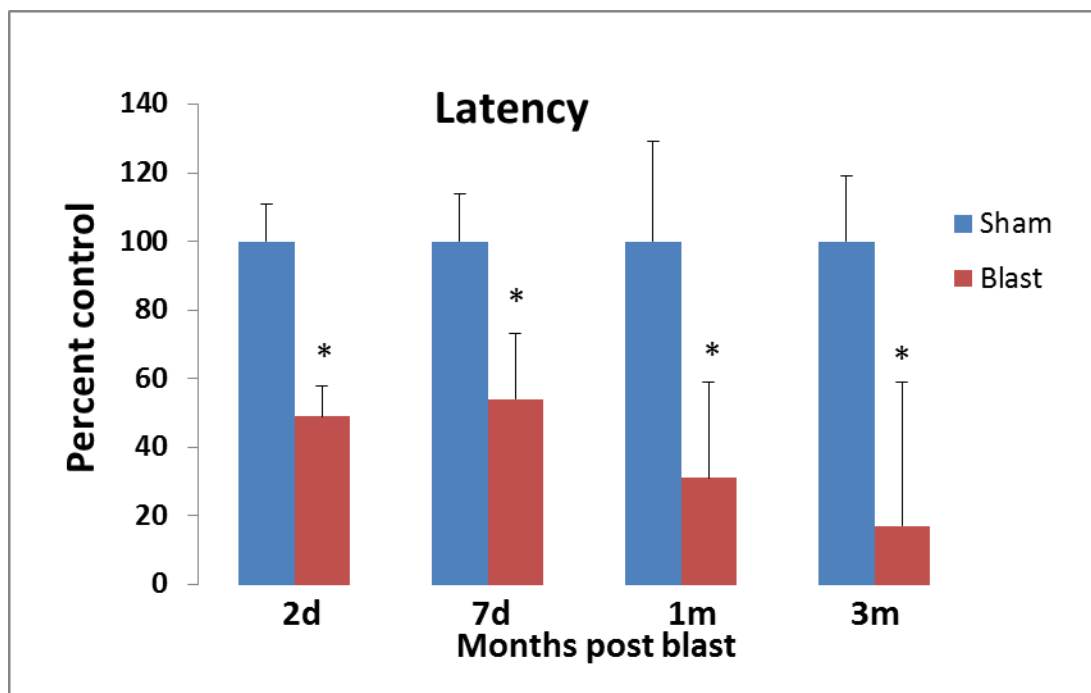


Figure 6.8: Anxiety-like behavior was observed from 3 days – 3 months following blast overpressure exposure. 2d – 2 days, 7d – 7 days, 1m – 1 month, 3m – 3 months.

However, in the current study, anxiety was found during the acute stages while impaired memory was delayed. Increased anxiety can result in substantial stress biologically at cellular levels. This is consistent loss of intracellular oxidative stress and astrogliosis in NAC. In addition, increased reactive astrocytes were correlated with elevated anxiety after BOP exposure in the amygdalar region of brain at a chronic stage (3 months).

Decreased performance in NOR task (Figure 6:9) or impaired memory correlated with increased microglial levels in hippocampal region (Figure 6.10). Data showed that microglial and astrocyte activation played an important role in tardive cognitive deficits. A review on TBI has suggested astrogliosis could be involved in long-lasting cognitive deficits due to the change of neuronal networking from activated astroglia and microglia [202].

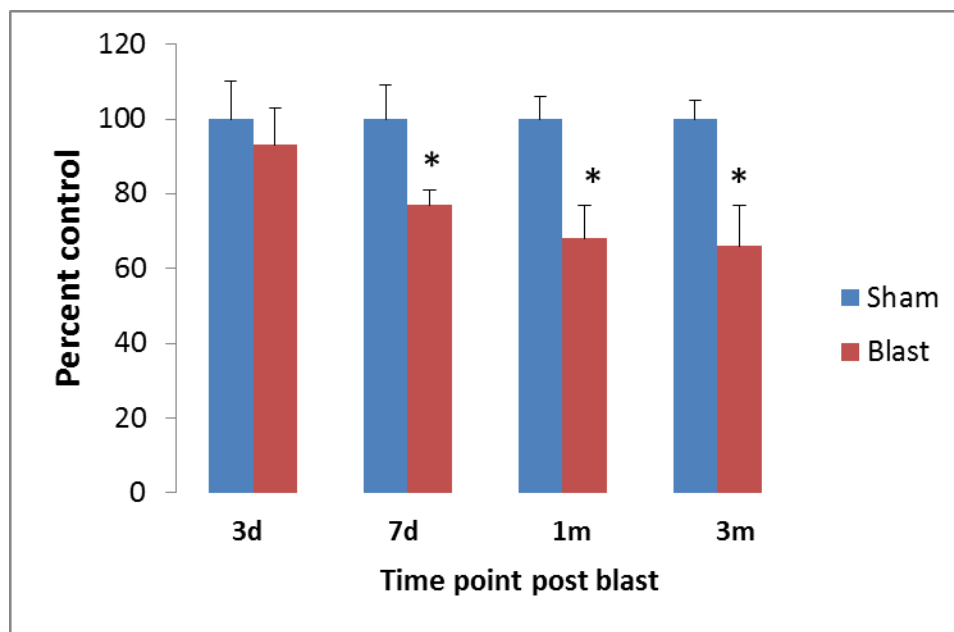


Figure 6.9: Impaired working memory was observed from 7 days – 3 months following blast overpressure exposure. 3d – 3 day, 7d – 7 days, 1m – 1 month, 3m – 3 months.

A key finding of the current studies was that *myo*-inositol levels in the PFC were correlated with negative performance in the NOR task at a sub-acute stage. Thus, increased levels of *myo*-inositol marked impaired memory. Since *myo*-inositol is primarily present in astrocytes, increased levels would indicate astrogliosis (Figure 6.11). Although a detailed assessment (working vs long term memory) on memory is lacking, clinical studies have reported memory issues following BINT [200-203]. Similar to clinical reports, animals exhibited anxiety-like behavior at an acute phase after BOP exposure, while working memory impairment was observed starting at a sub-acute phase (7 days) following BOP exposure.

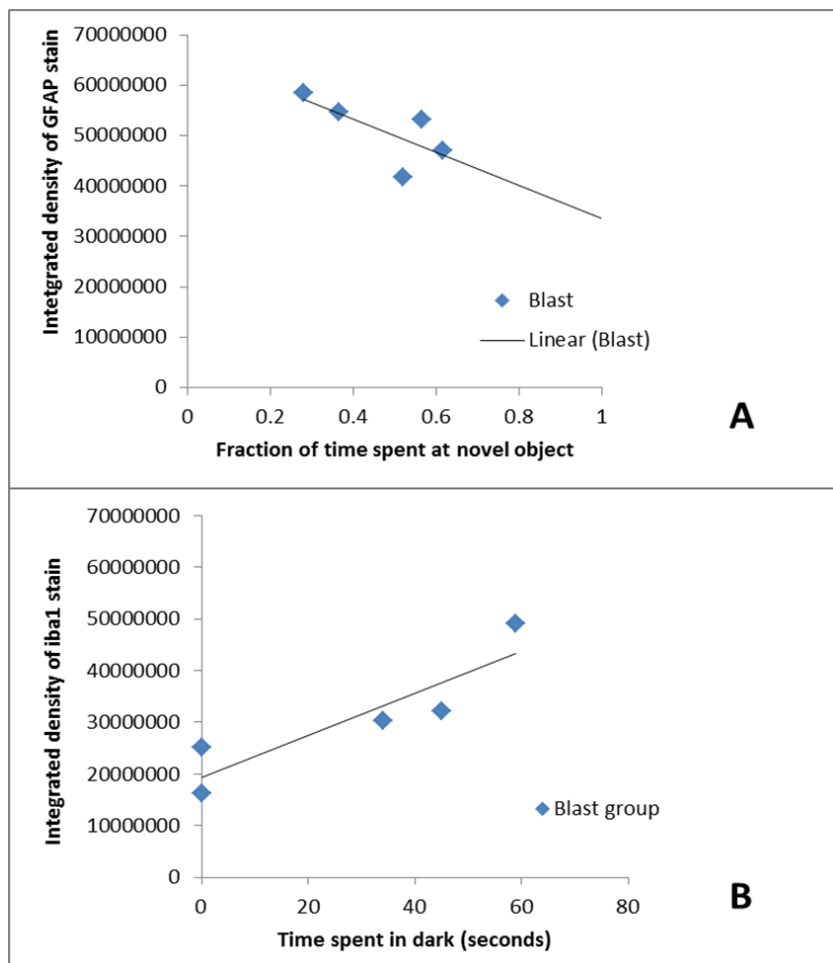


Figure 6.10: (A) Positive correlation between impaired memory and astrocyte activation in hippocampus at 3 months could be involved tardive working memory issues; (B) Time spent in dark (indicator of anxiety) was correlated elevated microglial levels in blast group showed microglial activation in amygdular region of brain at 3 months following BOP exposure.

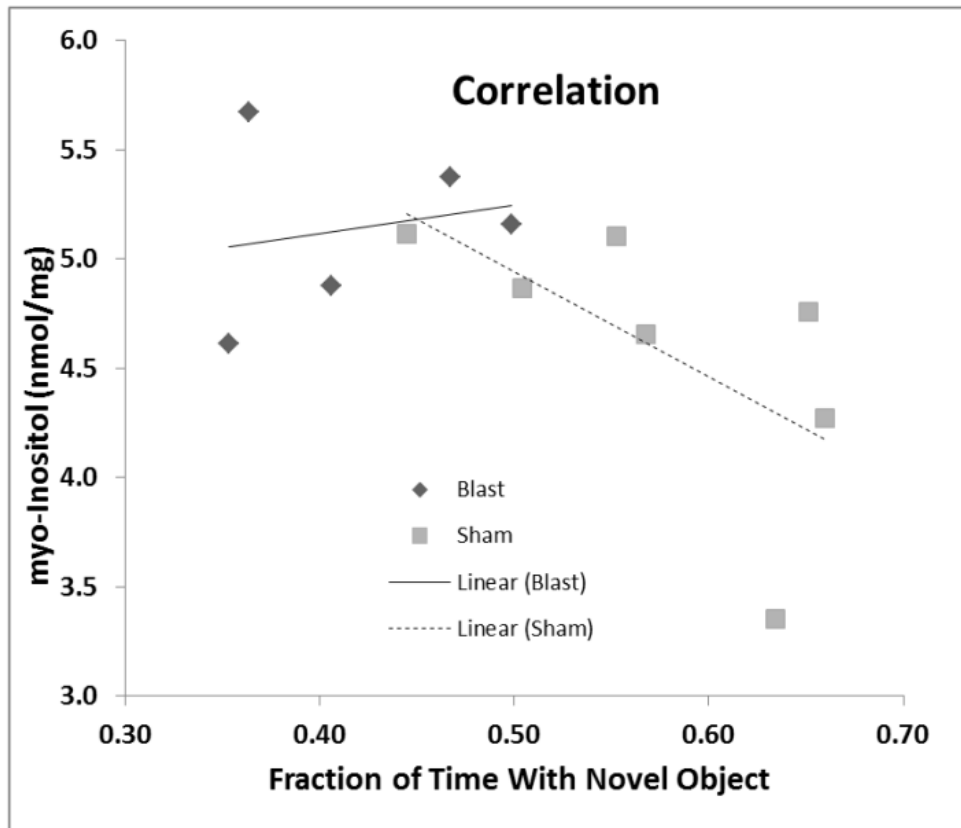


Figure 6.11: Myo-inositol levels in the prefrontal cortex of sham animals had a significant negative correlation ($p < 0.05$) with working memory while this correlation was lost in blast exposed animals at 7 days post blast.

Conclusion

In summary, early mitochondrial impairment in addition to oxidative stress is identified at an acute stage. Although NAA levels may reflect acute changes in mitochondrial integrity, levels were unchanged under the present conditions in HIPP, AMY, NAC and PFC. Neither NAA nor creatine levels were altered at this early stage (24-48 hours) after BINT in HIPP; however, the GSH/NAA ratio was decreased significantly, consistent with the relationship of mitochondrial damage in HIPP. In addition to its role in mitochondrial acetate homeostasis, the high concentration of NAA and its localization to neuronal mitochondria make it a surrogate marker of neuronal density in clinical MRS. The absence of an effect on NAA at these early time points suggests that NAA is not a suitable marker of early hippocampal disruption from BINT. Alternatively, the large NAA reserve (~5–10 mM) may buffer against significant alterations at this early stage of insult.

BINT decreased levels of GSH, a major anti-oxidant in neurons, which is consistent with a cellular response to increased reactive oxygen species and/or a compromised ability to reduce oxidized GSH by GSH:NADPH reductase. Decreased GSH and a compromised tricarboxylic acid cycle would also be expected to increase the pentose phosphate pathway in an attempt to maintain NADPH for GSH reductase. In accordance with HIPP data, mitochondrial damage was consistent in NAC, AMY and PFC with the activation of GABA shunting pathway. Elevated *myo*-inositol levels in PFC further supported the glial scarring and were associated with impaired working memory at a sub-acute stage (7 days) following BOP exposure. Early metabolic changes and oxidative stress were consistent with a compromise in energy metabolism that resulted in sub-acute active neurodegeneration and glial scarring. GABA shunting pathway was activated and data suggested that phospholipase A2 activated arachadonic pathway is involved in cellular death cascades.

Although the neurochemistry and neuropathology following blast appears to be somewhat diffuse, there were differences among the specific regions evaluated. It is important to understand the relationship HIPP, AMY, PFC and NAC as it is associated with cognition, reward, motivation, and addiction. Afferents to the NAC arrive from the PFC, a key decision-making region, and the amygdala, which is the region for controlling fear responses as well as disordered fear integration (anxiety). Hippocampal projections to AMY and PFC play an important role in decision making and fear induced stress. Memory deficits and anxiety are seen commonly associated with BINT which could be a result from the early changes in metabolites, neurodegeneration and astrogliosis. This environment creates cellular stress which could translate into impaired signaling networks these regions. Since these four regions work closely together, injury to any of these four cognitive regions can significantly affect behavioral outcomes and thought processes.

It is key to note the temporal development of the behavioral outcomes. Anxiety-like behavior was observed at an acute stage (3 days post blast), while working memory impairment was observed at the sub-acute stage (7 days post blast). This study identified the early metabolic changes and the development of anxiety at an acute stage (up to 72 hours); however, the development of working memory impairment is likely

related to the substantial loss of neurons and elevated astrocytes in PFC at 7days impairing the signaling cascades with other cognitive regions.

Chronic working memory issues and anxiety-associated behavior can be further be related to chronic activation of astrocytes in HIPPP and microglia in AMY respectively. Furthermore, these results from ¹H-MRS can directly translate into human studies to provide valuable insight into diagnosis of BINT. It is tempting to speculate that levels of Ins in the brain measured using NMR may be a potential biomarker for blast-induced memory impairment. In addition, with the advancement of technology, clinical MRS (or NMR) could resolve peaks of Glu, GABA, Lac, Cre, Ins, cholines and NAA. NMR can be used as a critical diagnostic tool and measure of treatment effectiveness in BINT to understand the changes in the essential cognitive regions like HIPPP, PFC, AMY and NAC. However, the use of NMR for neuroscience is in a nascent stage as a diagnostic tool. Understanding the metabolic profiles clinically would provide an insight into the potential changes which can not only be related to animal studies that identify key metabolic changes but also for the identification of key biomarkers.

Limitations

Each of the study aims presented with experimental limitations. The limitations taken in whole or in part may have affected the results observed in this work. Specific limitations are discussed below.

1. Animal studies present several challenging limitations. First, in order to understand the fundamental injuries that occur from primary blast, the blast animal model was simplified. It was decided that each animal would be subjected to single whole body BOP exposure (17 psi or 117KPa) in frontal orientation. In addition, chest protection (typically used in battlefield by military personnel) was not used. Secondly, all animals were anesthetized with isoflurane during the short blast exposure. Isoflurane is neuroprotective [204] and could acutely modify the neurochemical levels.
2. It has been reported that levels of glutamate and glutamine are altered as isoflurane facilitates GABA receptor-mediated inhibition [204]. As such, the effect of blast exposure in non-anesthetized animal would be predicted

to be more severe than the present observations. In addition, in order to limit the number of animals utilized within the study, it was decided that neuropathology would be restricted to the four analyzed brain regions (HIPPO, PFC, AMY, NAC). As such, neuropathology in other regions of the brain would provide a more complete account of the injury from blast.

3. MRS data was evaluated *ex vivo* in different regions of brain, although *ex vivo* data provided valuable information with well resolved spectra on individual regions, the spectra could be different for the peaks such as lactate which increases due to metabolic regulation by euthanasia.
4. Clinical reports suggest mental stress prior to blast exposure, typically experienced by soldiers could enhance the injury. While animal transport and handling may provide acute stress, the animals unlikely undergo the chronic stress seen by our soldiers. Stress can effect the activity of regions like AMY and NAC leading to abnormal neuronal signaling and neurochemical imbalance. Stress in addition can elevate the neuronal activity initiating fear conditioning pathways
5. The current study is limited to working memory, which can affect additional high order cognitive issues such as long-term memory. Effect of blast on potential role in dementia/Alzheimer's disease has to be evaluated. Long term memory deficits could lead to demential and eventually into Alzheimer's.

Despite these limitations, this study provided valuable insight on fundamental changes that occurs as a result of BOP exposure. Novel results concerning the metabolic profiles, cell death patterns and the temporal development of behavioral deficits offer a strong baseline for studies with different parameters (head orientation and protective gear) in the future, as well as understand the effectiveness of drug treatments for BINT

Future Directions

Based on the results of these studies, there are several possible directions for future investigations

1. The enzymatic cascades of phospholipase A2 should be evaluated using assays to confirm the enzymatic activity of phospholipase A2. It has been demonstrated that aggregation of amyloid-beta plaques in Alzheimer's disease is mediated *via* phospholipase-A2 enzyme cascade [205]. Inhibiting phospholipase-A2 reduces the production of inflammatory products like GPC and interleukins, which increases inflammation and subsequent cell death. Phospholipase-A2 inhibitors could be as potential candidate for treatment studies in relation to BINT.
2. Mitochondrial failure was demonstrated throughout the study in relation to the Krebs cycle. Enzymes within the Krebs cycle should be assayed in order to understand the critical role of energy crisis associated with mitochondrial failure. These studies can be used to decipher the specific molecular cascades that are affected by BOP exposure.
3. Since the current project was limited to study working memory deficits, long term memory deficits should also be considered. Clinical reports have linked long term memory deficits to BINT [7,9,10] . The role of these deficits further progressing to dementia/Alzheimer's disease symptoms should be evaluated. Standard behavioral batteries to score the advancement of the clinical symptoms like alzheimer's has to be incorporated into follow up studies performed at psychiatric and neurological centers.
4. Several recent reports voiced concern that Veterans with BINT will have advanced neurodegeneration which may lead into Alzheimer's disease [28,206]. As such, chronic assays on tau and alpha-synuclein proteins could give an insight on pathophysiological prognosis of BINT into Alzheimer's disease and depression/mood-disorders. It has been noted that increased of tau, alpha-synuclein, and amyloid-beta aggregates in relation to Alzheimer's disease.
5. It is critical to understand the effects of BOP exposure without anesthesia in order to most accurately evaluate and determine the extent of injury. In addition, pre-stress conditioning of animals should be considered in future

- studies in order to understand the role that stress may play in BINT. During these studies, it would be critical to evaluate the role of dopamine, serotonin and norepinephrine as these neurochemicals play an essential role in regulating mental stress.
6. Head orientation (side-on position), chest protection and multiple exposures to blast overpressure needs to be evaluated. It will be to critical understand the prognosis of injury in the most realistic environment that our military personnel are exposed to. It would be critical to collaborate with military population in order to mist accurately model the combat environment. .
 7. Inflammatory cascades of BINT are still under studied. Current data provides evidence of the potential role inflammation in relation to astrogliosis *via* activation of pro-inflammatory factors. However, details to interpret which inflammatory markers are key need to be further evaluated.
 8. Correlation between behavioral deficits and changes in cerebrospinal fluid and serum biomarkers could be advantageous to the medical community. Biomarkers are valuable in developing diagnostic techniques for the personnel affected with BINT as well as measuring recovery and treatment effectiveness.
 9. Scaling of the rodent studies using high order animal model such as porcine and monkeys could help to understand the changes in brain metabolites and evaluating specific pathways of injury cascades like mitochondrial failure and drug studies using non-invasive magnetic resonance spectroscopy to directly translate the changes clinically.
 10. Recent studies have shown dentate gyrus (DG) region of hippocampus is affected during BINT [24,192]. Since neuronal stem cells promote regeneration following injury, it is critical to understand changes in the DG stem cell population and their differentiation and regulation patterns.

References

1. Born, C., Blast trauma: The fourth weapon of mass destruction. *Scandinavian Journal of Surgery*, 2005. 94:279–285.
2. Sah, P., et al., The amygdaloid complex: anatomy and physiology. *physiological reviews*, 2003. 83(3):803-834.
3. Mahan, A.L. and K.J., Ressler, Fear conditioning, synaptic plasticity and the amygdala: implications for posttraumatic stress disorder. *Trends in Neurosciences*, 2012. 35(1):24-35.
4. Sowards, T.V., Neural structures and mechanisms involved in scene recognition: A review and interpretation. *Neuropsychologia*, 2011. 49(3):277-298.
5. Cernak, I., et al., The pathobiology of blast injuries and blast-induced neurotrauma as identified using a new experimental model of injury in mice. *Neurobiology of Disease*, 2011. 41(2):538-551.
6. Bazarian, J.J., et al., Long-term neurologic outcomes after traumatic brain injury. *The Journal of Head Trauma Rehabilitation*, 2009. 24(6):439-451.
7. Bruce, C. and D., Bass, Traumatic brain Injury among Veterans returning from Afghanistan and Iraq. *Psychiatric Times*, 2011. 28(7):1-5.
8. Cernak, I. and L.J., Noble-Haeusslein, Traumatic brain injury: an overview of pathobiology with emphasis on military populations. *Journal of Cerebral Blood Flow Metabolism*, 2009. 30(2): 255-266.
9. Elder, G.A., et al., Blast-induced mild traumatic brain injury. *The Psychiatric clinics of North America*, 2010. 33(4): 757-781.
10. Hoge, C.W., et al., Mild traumatic brain injury in U.S. soldiers returning from Iraq. *New England Journal of Medicine*, 2008. 358(5):453-463.
11. Nampiaparampil, D.E., Prevalence of chronic pain after traumatic brain injury. *JAMA: The Journal of the American Medical Association*, 2008. 300(6): 711-719.
12. Warden, D., Military TBI during the Iraq and Afghanistan wars. *Journal of rehabilitation research & development*, 2006. 21(5): 398-402.

13. Elder, G.A. and A. Cristian., Blast-related mild traumatic brain injury: mechanisms of injury and impact on clinical care. *Mount Sinai Journal of Medicine: A Journal of Translational and Personalized Medicine*, 2009. 76(2):111-118.
14. Hicks, R.R., et al., Neurological Effects of Blast Injury. *The Journal of Trauma*, 2010. 68(5): p. 1257-1263.
15. Rosenfeld, J.V. and N.L. Ford, Bomb blast, mild traumatic brain injury and psychiatric morbidity: A review. *Injury*, 2010. 41(5):437-443.
16. Ruff, R.L., Ruff, S.S., and X.F. Wang., Improving sleep: initial headache treatment in OIF/OEF veterans with blast-induced mild traumatic brain injury. *Journal of rehabilitation research & development*, 2009. 46(9):1074-1081.
17. Hayes, J.P., R.A. Morey, and L.A. Tupler, A case of frontal neuropsychological and neuroimaging signs following multiple primary-blast exposure. *Neurocase*, 2011:1-12.
18. Helfer, T.M., et al., Noise-induced hearing injury and comorbidities among postdeployment U.S. army soldiers: April 2003-June 2009. *American Journal of Audiology*, 2011. 20(1):33-41.
19. Kocsis, J.D. and Tessler, A., Pathology of blast-related brain injury. *Journal of rehabilitation research & development*, 2009. 46(6): 667-672.
20. Mao, J., et al., Blast-induced tinnitus and hearing loss in rats: Behavioral and imaging Assays. *Journal of Neurotrauma*, 2012. 29(2):430-444.
21. Heltemes, K.J., et al., Alcohol abuse disorders among U.S. service members with mild traumatic brain injury. *Military Medicine*, 2011. 176(2): 147-150.
22. Quinlan, J.D., Care of the returning veteran. *American Family Physician*, 2010. 82: 42-49.
23. Terrio, H., et al., Traumatic brain injury screening: Preliminary findings in a US army brigade combat team. *The Journal of Head Trauma Rehabilitation*, 2009. 24(1): 14-23.
24. VandeVord, P., et al., Mild neurotrauma indicates a range-specific pressure response to low level shock wave exposure. *Annals of Biomedical Engineering*. 40(1):227-236.

25. Vasterling, J.J., M. Verfaellie, and K.D. Sullivan., Mild traumatic brain injury and posttraumatic stress disorder in returning veterans: Perspectives from cognitive neuroscience. *Clinical Psychology Review*, 2009. 29(8): 674-684.
26. Belanger, H.G., et al., Cognitive sequelae of blast-related versus other mechanisms of brain trauma. *Journal of the International Neuropsychological Society*, 2009. 15(01):1-8.
27. Bellamy, R.F., et al., *Textbook of military medicine, conventional warfare: Ballistic, blast, and burn Injuries*”, series on combat casualty care. Office of the Surgeon General, Dept. of the Army, Walter Reed Army Medical Center, Washington, DC, 1988.
28. Bhattacharjee, Y., Shell shock revisited: Solving the puzzle of blast trauma. *Science*, 2008. 319(5):406-408.
29. Clemedson, C.J. and A. Jönsson., Transmission of elastic disturbances caused by air shock waves in a living body. *Journal of Applied Physiology*, 1961. 16(3):426-430.
30. Courtney, A.C. and M.W. Courtney., A thoracic mechanism of mild traumatic brain injury due to blast pressure waves. *Medical Hypotheses*, 2009. 72(1):76-83.
31. Mac Donald, C.L., et al., Detection of blast-related traumatic brain injury in U.S. military personnel. *New England Journal of Medicine*, 2011. 364(22):2091-2100.
32. Clemedson, C.J., Blast Injury. *Physiological Reviews*, 1956. 36(3):336-354.
33. DeWitt, D.S. and D. S. Prough., Blast-induced brain injury and posttraumatic hypotension and hypoxemia. *Journal of Neurotrauma*, 2009. 26(6):877-887.
34. Dobscha, S.K., et al., Systematic review of the literature on pain in patients with polytrauma Including traumatic brain injury. *Pain Medicine*, 2009. 10(7):1200-1217.
35. DR, Richmond., et.al., *The biological effects of repeated blast exposure. Report.* Lovelace Biomedical and Environmental Research Institute, Inc. Albuquerque, NM, 1981.

36. French, L.M., Military traumatic brain injury: an examination of important differences. *Annals of the New York Academy of Sciences*, 2010. 1208(1): 38-45.
37. Fritz, H.G., et al., A pig model with secondary increase of intracranial pressure after severe traumatic brain injury and temporary blood loss. *Journal of Neurotrauma*, 2005. 22(7): 807-821.
38. Säljö, A., et al., Neuropathology and pressure in the pig brain resulting from low-impulse noise exposure. *Journal of Neurotrauma*, 2008. 25(12): 1397-406.
39. O'Connor, C., et al., Effects of daily versus weekly testing and pre-training on the assessment of neurologic impairment following diffuse traumatic brain injury in rats. *Journal of Neurotrauma*, 2003. 20(10): 985-993.
40. Ciraulo, D.L. and E.R. Frykberg, The surgeon and acts of civilian terrorism: blast injuries. *Journal of the American College of Surgeons*, 2006. 203(6): 942-950.
41. Cynthia, A., et al., Comparison of concussive symptoms, cognitive performance, and psychological symptoms between acute blast-versus nonblast-induced mild traumatic brain injury. 2010. 17:36-45.
42. Hicks, M.H.R., et al., Casualties in civilians and coalition soldiers from suicide bombings in Iraq, 2003–10: a descriptive study. *The Lancet*, 2011. 378(9): 906-914.
43. MacManus, D., et al., Violent behaviour in UK military personnel returning home after deployment. *Psychological Medicine*, 2012. 42(8):1663-1673
44. Matthews, S.C., et al., A multimodal imaging study in U.S. veterans of Operations Iraqi and Enduring Freedom with and without major depression after blast-related concussion. *NeuroImage*, 2011. 54, Supplement 1(0):S69-S75.
45. Cawley, P.J. and N.A. Mokadam, Delayed complications from exposure to improvised explosive devices. *Annals of Internal Medicine*, 2010. 153(4): 278-279.

46. Leonardi, A.D., et al., Intracranial pressure increases during exposure to a shock wave. *Journal of Neurotrauma*, 2011. 28(1):85-94
47. Yeo, R.A., et al., Magnetic resonance spectroscopy detects brain injury and predicts cognitive functioning in children with brain injuries. *Journal of Neurotrauma*, 2006. 23(10):1427-1435.
48. Young, M., Mechanics of blast injury. *War Medicine*, 1945. 8:73.
49. Riggio, S., Traumatic brain injury and its neurobehavioral sequelae. *Neurologic clinics*, 2011. 29(1): 35-47.
50. Sponheim, S.R., et al., Evidence of disrupted functional connectivity in the brain after combat-related blast injury. *NeuroImage*, 2011. 54, Supplement 1(0): S21-S29.
51. Svetlov, S.I., et al., Morphologic and biochemical characterization of brain injury in a model of controlled blast overpressure exposure. *The Journal of Trauma*, 2010. 69(4): 795-804.
52. Taber, K.H., D.L. Warden, and R.A. Hurley, Blast-related traumatic brain injury: What is known? *J Neuropsychiatry Clinical Neuroscience*, 2006. 18(2): 141-145.
53. Tavazzi, B., et al., Temporal window of metabolic brain vulnerability to concussions: Oxidative and nitrosative stresses—Part II. *Neurosurgery*, 2007. 61(2): 390-396.
54. Thompson, J.M., K.C. Scott, and L. Dubinsky, Battlefield brain. *Canadian Family Physician*, 2008. 54(11): 1549-1551.
55. Warden, D.L., et al., Case report of a soldier with primary blast brain injury. *NeuroImage*, 2009. 47, Supplement 2(0): T152-T153.
56. Belujon, P. and A.A. Grace, Hippocampus, amygdala, and stress: interacting systems that affect susceptibility to addiction. *Annals of the New York Academy of Sciences*, 2011. 1216(1): 114-121.
57. van Erp, A.M.M. and K.A. Miczek, Aggressive behavior, increased accumbal dopamine, and decreased cortical serotonin in rats. *The Journal of Neuroscience*, 2000. 20(24):9320-9325.

58. Bolander, R., et al., Skull flexure as a contributing factor in the mechanism of injury in the rat when exposed to a shock wave. *Annals of Biomedical Engineering*, 2011. 39(10): 2550-2559.
59. Säljö, A., et al., Low levels of blast raises intracranial pressure and impairs cognitive function in rats. *Journal of Neurotrauma*, 2009. 26(8):1345-1352.
60. Romba, J.J and p. Martin., The propagation of air shock waves on a biophysical model. Technical Memorandum 17-61. Aberdeen Proving Ground, MD. U.S. Army Ordnance, Human Engineering Laboratories, 1961.
61. Leonardi, A.D., et al., Head orientation affects the intracranial pressure response resulting from shock wave loading in the rat. *Journal of Biomechanics*, 2012. 45(15):2595-2602.
62. Jacques Goeller, A.W., Derrick Treichler, Joseph O'Bruba, and Greg Weiss, Investigation of cavitation as a possible damage mechanism in blast-induced traumatic brain injury. *Journal of Neurotrauma*, 2012. 29(10):1970-1984.
63. Propper, B.W., et al., Wartime thoracic injury: Perspectives in modern warfare. *Annals Thoracic Surgery*, 2010. 89(4):1032-1036.
64. Wood, G.W., et al., Attenuation of blast pressure behind ballistic protective vests. *Injury Prevention*, 2012.
65. Aarabi, B. and J.M. Simard, Traumatic brain injury. *Current Opinion in Critical Care*, 2009. 15(6):548-553.
66. Maller, J.J., et al., Traumatic brain injury, major depression, and diffusion tensor imaging: Making connections. *Brain Research Reviews*, 2010. 64(1):213-240.
67. Pandey, D.K., et al., Depression-like and anxiety-like behavioral aftermaths of impact accelerated traumatic brain injury in rats: A model of comorbid depression and anxiety? *Behavioural Brain Research*, 2009. 205(2): 436-442.
68. Moore, G.J. and M. Galloway., Magnetic resonance spectroscopy: neurochemistry and treatment effects in affective disorders. *Psychopharmacology bulletin*, 2002. 36(2): 5-23.

69. Edden, R.A.E., M.G. Pomper, and P.B. Barker, In vivo differentiation of N-acetyl aspartyl glutamate from N-acetyl aspartate at 3 Tesla. *Magnetic Resonance in Medicine*, 2007. 57(6): 977-982.
70. Jessen, F., et al., N-Acetylaspartylglutamate (NAAG) and N-Acetylaspartate (NAA) in patients with Schizophrenia. *Schizophrenia Bulletin*, 2013. 39(1):197-205.
71. Readnower, R.D., et al., Increase in blood–brain barrier permeability, oxidative stress, and activated microglia in a rat model of blast-induced traumatic brain injury. *Journal of Neuroscience Research*, 2010. 88(16): 3530-3539.
72. Mariusz, Z. and K. Ghodrat, Biomechanical perspective on blast injury, in *Concussive Brain Trauma*. 2011, CRC Press. 733-752.
73. Cernak, I., et al., Ultrastructural and functional characteristics of blast injury-induced neurotrauma. *The Journal of Trauma and Acute Care Surgery*, 2001. 50(4): 695-706.
74. Kovesdi, E., et. al., Acute minocycline treatment mitigates the symptoms of mild blast-induced traumatic brain injury. *Frontiers in Neurology*, 2012, 3:11.
75. Kocsis, J. D. and A., Tessler, Pathology of blast-related brain injury. *Journal of Rehabilitation Research and Development*. 2009, 46: 667-672.
76. Kovesdi, E., et al., The effect of enriched environment on the outcome of traumatic brain injury; a behavioral, proteomics, and histological study. *Frontiers in Neuroscience*, 2011. 5:42..
77. Kwon, S. K., et al., 2011. Stress and traumatic brain injury: a behavioral, proteomics, and histological study. *Frontiers in Neurology*. 2, 12.
78. Lee, W. H., et al., Irradiation induces regionally specific alterations in pro-inflammatory environments in rat brain. *International Journal of Radiation Biology*, 2010. 86, 132-144.
79. Lee, Y. W., et al., Redox-regulated mechanisms of IL-4-induced MCP-1 expression in human vascular endothelial cells. *American Journal of Physiology and Heart Circulation*,. 2003. 284: H185-H192.

80. R, B. Bolander, A multi-species analysis of biomechanical responses of the head to a shock wave. PhD Thesis, Wayne State University, Detroit, MI, 2011.
81. Markesbery, W.R., Neuropathologic alterations in mild cognitive impairment: A Review. *Journal of Alzheimer's Disease*, 2010. 19(1):221-228.
82. Miller, D.B. and J.P. O'Callaghan, Aging, stress and the hippocampus. *Ageing Research Reviews*, 2005. 4(2): 123-140.
83. Barbas, H., Connections underlying the synthesis of cognition, memory, and emotion in primate prefrontal cortices. *Brain Research Bulletin*, 2000. 52(5): 319-330.
84. Townsend, J. and L.L. Altshuler, Emotion processing and regulation in bipolar disorder: a review. *Bipolar Disorders*, 2012. 14(4):326-339.
85. Koob, G.F., Brain stress systems in the amygdala and addiction. *Brain Research*, 2009. 1293(0): 61-75.
86. Belin, D., et al., Parallel and interactive learning processes within the basal ganglia: Relevance for the understanding of addiction. *Behavioural Brain Research*, 2009. 199(1): 89-102.
87. Carlezon Jr, W.A. and M.J. Thomas, Biological substrates of reward and aversion: A nucleus accumbens activity hypothesis. *Neuropharmacology*, 2009. 56, Supplement 1(0): 122-132.
88. Salamone, J., et al., Effort-related functions of nucleus accumbens dopamine and associated forebrain circuits. *Psychopharmacology*, 2007. 191(3): 461-482.
89. Vertes, R.P., Interactions among the medial prefrontal cortex, hippocampus and midline thalamus in emotional and cognitive processing in the rat. *Neuroscience*, 2006. 142(1): 1-20.
90. Akai, F. and T. Yanagihara, Identity of the dorsal hippocampal region most vulnerable to cerebral ischemia. *Brain Research*, 1993. 603(1): 87-95.
91. Yassa, M.A. and C.E.L. Stark, Pattern separation in the hippocampus. *Trends in Neurosciences*, 2011. 34(10): 515-525.

92. Wang, Z., et al., MAGnetic resonance imaging of hippocampal subfields in posttraumatic stress disorder. *Archives of General Psychiatry*, 2010. 67(3): 296-303.
93. Amaral, D.L.P., et.al., "Hippocampal neuroanatomy". *The Hippocampus Book*. 2006, Chapter 3.
94. Andersen, P.S.A., Raastad M The hippocampal lamella hypothesis revisited. *Brain Research*, 2000. 886 (1): 165–171.
95. Heath, R.G. and J.W. Harper, Ascending projections of the cerebellar fastigial nucleus to the hippocampus, amygdala, and other temporal lobe sites: Evoked potential and histological studies in monkeys and cats. *Experimental Neurology*, 1974. 45(2): 268-287.
96. Schmidt, B., D.F. Marrone, and E.J. Markus, Disambiguating the similar: The dentate gyrus and pattern separation. *Behavioural Brain Research*, 2012. 226(1):56-65.
97. Sauvage, M.M., ROC in animals: Uncovering the neural substrates of recollection and familiarity in episodic recognition memory. *Consciousness and Cognition*, 2010. 19(3): 816-828.
98. Derdikman, D. and E.I. Moser, A manifold of spatial maps in the brain. *Trends in cognitive sciences*, 2010. 14(12): 561-569.
99. Rolls, E.T., A computational theory of episodic memory formation in the hippocampus. *Behavioural Brain Research*, 2010. 215(2): 180-196.
100. Hasselmo, M.E., et al., Cellular dynamical mechanisms for encoding the time and place of events along spatiotemporal trajectories in episodic memory. *Behavioural Brain Research*, 2010. 215(2): 261-274.
101. Ahmed, O.J. and M.R. Mehta, The hippocampal rate code: anatomy, physiology and theory. *Trends in Neurosciences*, 2009. 32(6): 329-338.
102. Orsmond, G.I. and L.K. Miller, Cognitive, musical and environmental correlates of early music instruction. *Psychology of Music*, 1999. 27(1):18-37.
103. Todd, M. and C. Barrow, Teaching memory-impaired people to touch type: The acquisition of a useful complex perceptual-motor skill. *Neuropsychological Rehabilitation*, 2008. 18(4):486-506.

104. Jeffery, K.J., Self-localization and the entorhinal–hippocampal system. *Current Opinion in Neurobiology*, 2007. 17(6): 684-691.
105. Moser, E.I., E. Kropff, and M.-B. Moser, Place Cells, Grid Cells, and the Brain's Spatial Representation System. *Annual Review of Neuroscience*, 2008. 31(1): 69-89.
106. Teipel, S., et al., Novel MRI techniques in the assessment of dementia. *European Journal of Nuclear Medicine and Molecular Imaging*, 2008. 35(0): 58-69.
107. deToledo-Morrell, L., T.R. Stoub, and C. Wang, Hippocampal atrophy and disconnection in incipient and mild Alzheimer's disease, *Progress in Brain Research*, E.S. Helen, Editor. 2007, Elsevier. 741-823.
108. Witter, M.P., The perforant path: projections from the entorhinal cortex to the dentate gyrus, *Progress in Brain Research*, E.S. Helen, Editor. 2007, Elsevier. 43-61.
109. Ionov, I.D., Specific mechanism for blood inflow stimulation in brain area prone to alzheimer's disease lesions. *International Journal of Neuroscience*, 2007. 117(10):1425-1442.
110. Furtak, S.C., et al., Functional neuroanatomy of the parahippocampal region in the rat: The perirhinal and postrhinal cortices. *Hippocampus*, 2007. 17(9):709-722.
111. Thierry, A.-M., et al., Hippocampo-prefrontal cortex pathway: Anatomical and electrophysiological characteristics. *Hippocampus*, 2000. 10(4): 411-419.
112. Groenewegen, H.J., C.I. Wright, and H.B.M. Uylings, The anatomical relationships of the prefrontal cortex with limbic structures and the basal ganglia. *Journal of Psychopharmacology*, 1997. 11(2):99-106.
113. Stuss, D.T., Functions of the frontal lobes: Relation to executive functions. *Journal of the International Neuropsychological Society*, 2011. 17(05): 759-765.
114. Rushworth, M., et al., Frontal cortex and reward-guided learning and decision-making. *Neuron*, 2011. 70(6):1054-1069.

115. Brown, J.W., Medial prefrontal cortex activity correlates with time-on-task: What does this tell us about theories of cognitive control? *NeuroImage*, 2011. 57(2): 314-315.
116. Carrion, V.G. and H. Kletter, Posttraumatic stress disorder: shifting toward a developmental framework. *Child and Adolescent Psychiatric Clinics of North America*, 2012. 21(3): 573-591.
117. Hughes, K.C. and L.M. Shin, Functional neuroimaging studies of post-traumatic stress disorder. *Expert Review of Neurotherapeutics*, 2011. 11(2): 275-285.
118. Skelton, K., et al., PTSD and gene variants: New pathways and new thinking. *Neuropharmacology*, 2012. 62(2): 628-637.
119. Poletti, M. and U. Bonuccelli, Orbital and ventromedial prefrontal cortex functioning in Parkinson's disease: Neuropsychological evidence. *Brain and Cognition*, 2012. 79(1): 23-33.
120. Roy, M., D. Shohamy, and T.D. Wager, Ventromedial prefrontal-subcortical systems and the generation of affective meaning. *Trends in cognitive sciences*, 2012. 16(3): 147-156.
121. Colgin, L.L., Oscillations and hippocampal–prefrontal synchrony. *Current Opinion in Neurobiology*, 2011. 21(3): 467-474.
122. Koenigs, M., The role of prefrontal cortex in psychopathy, 2012. p. 253.
123. O'Doherty, J.P., Contributions of the ventromedial prefrontal cortex to goal-directed action selection. *Annals of the New York Academy of Sciences*, 2011. 1239(1): 118-129.
124. Murphy, C.M., et al., Anatomy and aging of the amygdala and hippocampus in autism spectrum disorder: an in vivo magnetic resonance imaging study of Asperger syndrome. *Autism Research*, 2012. 5(1): 3-12.
125. Amaral, D.G., et al., The amygdala: is it an essential component of the neural network for social cognition? *Neuropsychologia*, 2003. 41(4):517-522.
126. Bannerman, D.M., et al., Regional dissociations within the hippocampus—memory and anxiety. *Neuroscience & Biobehavioral Reviews*, 2004. 28(3): 273-283.

127. Davis, M., D.L. Walker, and K.M. Myers, Role of the amygdala in fear extinction measured with potentiated startle. *Annals of the New York Academy of Sciences*, 2003. 985(1): 218-232.
128. Johansen, J.P., et al., Molecular mechanisms of fear learning and memory. *Cell*, 2011. 147(3): 509-524.
129. Liu, R.S.N., et al., A longitudinal study of brain morphometrics using quantitative magnetic resonance imaging and difference image analysis. *NeuroImage*, 2003. 20(1): 22-33.
130. Silberman, Y., et al., Neurobiological mechanisms contributing to alcohol–stress–anxiety interactions. *Alcohol*, 2009. 43(7): 509-519.
131. Aroniadou-Anderjaska, V., F. Qashu, and M.F.M. Braga, Mechanisms regulating GABAergic inhibitory transmission in the basolateral amygdala: implications for epilepsy and anxiety disorders. *Amino Acids*, 2007. 32(3): 305-315.
132. Cahill, L. and J.L. McGaugh, Mechanisms of emotional arousal and lasting declarative memory. *Trends in Neurosciences*, 1998. 21(7): 294-299.
133. Goldstein, L.E., et al., Role of the amygdala in the coordination of behavioral, neuroendocrine, and prefrontal cortical monoamine responses to psychological stress in the rat. *The Journal of Neuroscience*, 1996. 16(15): 4787-4798.
134. Mohapel, P., et al., Differential sensitivity of various temporal lobe structures in the rat to kindling and status epilepticus induction. *Epilepsy Research*, 1996. 23(3): 179-187.
135. Pitkänen, A., et al., Amygdala damage in experimental and human temporal lobe epilepsy. *Epilepsy Research*, 1998. 32(1–2): 233-253.
136. Wilde, E.A., et al., Hippocampus, amygdala, and basal ganglia morphometrics in children after moderate-to-severe traumatic brain injury. *Developmental Medicine & Child Neurology*, 2007. 49(4):294-299.
137. Basar, K., et al., Nucleus accumbens and impulsivity. *Progress in Neurobiology*, 2010. 92(4):533-557.

138. Russo, S.J., et al., The addicted synapse: mechanisms of synaptic and structural plasticity in nucleus accumbens. *Trends in Neurosciences*, 2010. 33(6): 267-276.
139. Yin, H.H., S.B. Ostlund, and B.W. Balleine, Reward-guided learning beyond dopamine in the nucleus accumbens: the integrative functions of cortico-basal ganglia networks. *European Journal of Neuroscience*, 2008. 28(8): 1437-1448.
140. Mikell, C.B., et al., The hippocampus and nucleus accumbens as potential therapeutic targets for neurosurgical intervention in Schizophrenia. *Stereotactic and Functional Neurosurgery*, 2009. 87(4): 256-265.
141. Ma, Y.-Y., C. Cepeda, and C.-L. Cui, Chapter 6 - The role of striatal nmda receptors in drug addiction, in *International Review of Neurobiology*, L. Xiao-Hong, Editor. 2009, Academic Press. 131-146.
142. Oever, M.C., S. Spijker, and A.B. Smit, The synaptic pathology of drug addiction synaptic plasticity, M.R. Kreutz and C. Sala, Editors. 2012, Springer Vienna. 469-491.
143. Northoff, G., Psychopathology and pathophysiology of the self in depression — Neuropsychiatric hypothesis. *Journal of Affective Disorders*, 2007. 104(1–3): 1-14.
144. Koob, G.F., Neurobiology of addiction: Toward the development of new therapies. *Annals of the New York Academy of Sciences*, 2000. 909(1): 170-185.
145. Leshner, A.I. and G.F. Koob, Drugs of abuse and the brain. *Proceedings of the Association of American Physicians*, 1999. 111(2):99-108.
146. Self, D.W. and E.J. Nestler, Relapse to drug-seeking: neural and molecular mechanisms. *Drug and Alcohol Dependence*, 1998. 51(1): 49-60.
147. Lüscher, C. and R.C. Malenka, Drug-evoked synaptic plasticity in addiction: From molecular changes to circuit remodeling. *Neuron*, 2011. 69(4): 650-663.
148. Myhrer, T., Identification of neuronal target areas for nerve agents and specification of receptors for pharmacological treatment. *NeuroToxicology*, 2010. 31(6):629-638.

149. Papp, E., et al., Glutamatergic input from specific sources influences the nucleus accumbens-ventral pallidum information flow. *Brain Structure and Function*, 2012. 217(1): 37-48.
150. Bang, S.J. and K.G. Commons, Forebrain GABAergic projections from the dorsal raphe nucleus identified using GAD67-GFP knock-in mice. *The Journal of Comparative Neurology*, 2012: 520(18):4157-4167.
151. Sharp, B.M., et al., Gene expression in accumbens GABA neurons from inbred rats with different drug-taking behavior. *Genes, Brain and Behavior*, 2011. 10(7): 778-788.
152. Bjork, J.M. and S.J. Grant, Does traumatic brain injury increase risk for substance abuse? *Journal of Neurotrauma*, 2009. 26(7):1077-1082.
153. Spelman, J., et al., Post deployment care for returning combat veterans. *Journal of General Internal Medicine*, 2012. 27(9): 1200-1209.
154. Maguen, S., et al., The impact of head injury mechanism on mental health symptoms in veterans: Do number and type of exposures matter? *Journal of Traumatic Stress*, 2012. 25(1): 3-9.
155. Ghoddoussi, F., et al., Methionine sulfoximine, an inhibitor of glutamine synthetase, lowers brain glutamine and glutamate in a mouse model of ALS. *Journal of the Neurological Sciences*, 2010. 290(1):41-47.
156. Schmued, L.C. and K.J. Hopkins, Fluoro-Jade B: a high affinity fluorescent marker for the localization of neuronal degeneration. *Brain Research*, 2000. 874(2): 123-130.
157. Peruga, I., et al., Inflammation modulates anxiety in an animal model of multiple sclerosis. *Behavioural Brain Research*, 2011. 220(1): 20-29.
158. Ennaceur, A., One-trial object recognition in rats and mice: Methodological and theoretical issues. *Behavioural Brain Research*, 2010. 215(2): 244-254.
159. Peruga, I., et al., Inflammation modulates anxiety in an animal model of multiple sclerosis. *Behavioural Brain Research*, 2011. 220(1): 20-29.
160. Belanger, H.G., et. al., Cognitive sequelae of blast-related versus other mechanisms of brain trauma. *Journal of International Neuropsychological Society*, 2009. 15:1-8.

161. Bhattacharjee, Y., Shell shock revisited: Solving the puzzle of blast trauma. *Science*, 2008.319:406-08.
162. Cernak, I., et.al., Ultrastructural and functional characteristics of blast injury-induced neurotrauma. *Journal of Trauma Acute Care Surgery*, 2001. 50, 695-706.
163. DeWitt, S.D., and D.S. Prough, Blast-induced brain injury and posttraumatic hypotension and hypoxemia. *Journal of Neurotrauma*. 2009. 26:877-887.
164. Readnower, R.D., et. al., Increase in blood–brain barrier permeability, oxidative stress, and activated microglia in a rat model of blast-induced traumatic brain injury. *Journal of Neuroscience Research* 2010. 88(16): 3530-539.
165. Abdul-Muneer, P.M., et.al., Induction of oxidative and nitrosative damage leads to cerebrovascular inflammation in animal model of mild traumatic brain injury induced by primary blast. *Free Radical Biology in Medicine*. 2013. 60:282-291
166. Pocernich, C.B. and D.A. Butterfield, Elevation of glutathione as a therapeutic strategy in Alzheimer disease. *Biochemistry Biophysics Acta*, 2012.1822(5): 625-630.
167. Li, Z., and D.E., Vance, Thematic review series: Glycerolipids, phosphatidylcholine and choline homeostasis. *J Lipid Research*. 2008.49(6):1187-1194.
168. Moore, G.J., and M.P., Galloway, Magnetic resonance spectroscopy: neurochemistry and treatment effects in affective disorders. *Psychopharmacology Bulletin*, 2002. 36(2), 5-23.
169. Passe, T.J., et.al., Nuclear magnetic resonance spectroscopy: A review of neuropsychiatric applications. *Prognosis in Neuropsychopharmacology and Biological Psychiatry*, 1995. 19(4):541-563.
170. Kasser, TR., Harris, RB., and R.J., Martin, Level of satiety: GABA and pentose shunt activities in three brain sites associated with feeding. *American Journal of Physiology*, 1985. 248(4):R453-R458.

171. Schousboe, A., Sonnewald, U., and H.S., Waagepetersen, Differential roles of alanine in GABAergic and glutamatergic neurons. *Neurochemistry International*, 2003.43(5):311-315.
172. Holtzman, D., et.al., In vivo brain phosphocreatine and ATP regulation in mice fed a creatine analog. *American Journal of Physiology*, 1997. 272:C1567-577.
173. Kekelidze, T., et.al., Altered brain phosphocreatine and ATP regulation when mitochondrial creatine kinase is absent. *Journal of Neuroscience Research*. 2001. 66(5):866-872.
174. Di Costanzo, A., et.al., Proton MR spectroscopy of the brain at 3 T: an update. *European journal of Radiology*, 2007.17(7),1651-662.
175. Nucci-da-Silva, M.P., and E., Amaro, A systematic review of magnetic resonance imaging and spectroscopy in brain injury after drowning. *Brain Injury*, 2009. 23(9):707-714.
176. Patel, AB., et.al., The contribution of GABA to glutamate/glutamine cycling and energy metabolism in the rat cortex in vivo. *Proceedings of National Academy of Sciences USA*, 2005. 102: 5588–593.
177. Bolaños, J.P., Almeida, A., and S., Moncada, Glycolysis: a bioenergetic or a survival pathway? *Trends in Biochemical Sciences*, 2010. 35(3):145-149.
178. An, S.J., et.al., Gastrodin decreases immunoreactivities of γ -aminobutyric acid shunt enzymes in the hippocampus of seizure-sensitive gerbils. *Journal of Neuroscience Research*. 2003. 71(4):534-43.
179. Mamelak, M., Sporadic Alzheimer's Disease: The Starving Brain. *Journal of Alzheimers Disease*, 2012. 31(3), 459-74.
180. Yang, M., et.al., NMR analysis of the rat neurochemical changes induced by middle cerebral artery occlusion. *Talanta*, 2012. 88:136-144.
181. Bosco, D., et.al., Possible implications of insulin resistance and glucose metabolism in Alzheimer's disease pathogenesis. *Journal of Cellular and Molecular Medicine*. 2011. 15:1807-821.
182. Lassmann, H., and J., van Horssen, The molecular basis of neurodegeneration in multiple sclerosis. *FEBS Letters*. 2011. 585:3715-3723.

183. Paling, D., et.al., Energy failure in multiple sclerosis and its investigation using MR techniques. *Journal of Neurology*, 2011. 258:2113-2127.
184. Wilcox, CS., Effects of tempol and redox-cycling nitroxides in models of oxidative stress. *Pharmacological Therapy*. 2010. 126:119-1145.
185. Andrade, C.S., et.al., Phosphorus magnetic resonance spectroscopy in malformations of cortical development. *Epilepsia*, 2011. 52:2276-2284.
186. Forster, D.M., James, M.F., and S.R., Williams, Effects of Alzheimer's disease transgenes on neurochemical expression in the mouse brain determined by ¹H MRS in vitro. *NMR in Biomedicine*. 2012. 25:52-58.
187. Agoston, D.V., et.al., Proteomic biomarkers for blast neurotrauma: targeting cerebral edema, inflammation, and neuronal death cascades. *Journal of Neurotrauma*, 2009. 26:901-911.
188. Jenkins, B.G., and E., Kraft, Magnetic resonance spectroscopy in toxic encephalopathy and neurodegeneration. *Current Opinion in Neurology*, 1999. 12:753-60.
189. Fan, Y.Q., et.al., Effects of osmolytes on human brain-type creatine kinase folding in dilute solutions and crowding systems. *International Journal of Biological Macromolecules*, 2012. 51:845-858.
190. Hur, YS., et.al., Evidence for the existence of secretory granule (dense-core vesicle)-based inositol 1,4,5-trisphosphate-dependent Ca²⁺ signaling system in astrocytes. *PLoS ONE*, 2010. 5: e11973.
191. Ye, X., et al., Fluoro-Jade and silver methods: application to the neuropathology of scrapie, a transmissible spongiform encephalopathy. *Brain Res Brain Res Protoc*. 2001, 8(2):104-112.
192. Kelm, MK., et.al., The PLC/IP3R/PKC pathway is required for ethanol-enhanced GABA release. *Neuropharmacology*, 2010. 58:1179-1186.
193. Nelson, TJ., et.al., Insulin, PKC signaling pathways and synaptic remodeling during memory storage and neuronal repair. *European Journal of Pharmacology*, 2008. 585:76-87.

194. Song, D., et.al., Astrocytic alkalization by therapeutically relevant lithium concentrations: implications for myo -inositol depletion. *Psychopharmacology*, 2008. 200:187-195.
195. Babikian, T., et.al., MR spectroscopy: Predicting long-term neuropsychological outcome following pediatric TBI. *Journal of Magnetic Resonance Imaging*, 2006. 24:801-811.
196. Wilson, M., et.al., Magnetic resonance spectroscopy metabolite profiles predict survival in paediatric brain tumours. *European Journal of Cancer*. 2012. 49:457-464
197. Yoon, S.J., et.al., Evaluation of traumatic brain injured patients in correlation with functional status by localized 1H-MR spectroscopy. 2005. *Clinical Rehabilitation*, 19:209-215.
198. Sofroniew, M. and H., Vinters., Astrocytes: biology and pathology. *Acta Neuropathologica*, 2010. 119:7-35.
199. Suzuki, T., et.al., Astrocyte activation and wound healing in intact-skull mouse after focal brain injury. *European Journal of Neuroscience*, 2012. 36:3653-664.
200. Ebrahimi, F., et.al., Time dependent neuroprotection of mycophenolate mofetil: effects on temporal dynamics in glial proliferation, apoptosis, and scar formation. *J Neuroinflammation*, 2012. 9:89.
201. Sofroniew, M.V., Molecular dissection of reactive astrogliosis and glial scar formation. *Trends in Neurosciences*, 2009. 32:638-647.
202. Tuinstra, H.M., et.al., Gene delivery to overcome astrocyte inhibition of axonal growth: An in vitro Model of the glial scar. *Biotechnology in Bioengineering*, 2013. 110:947-957.
203. Svetlov, S.I., et.al., Neuro-glial and systemic mechanisms of pathological responses in rat models of primary blast overpressure compared to "composite" blast. *Frontiers in Neurology*, 2012. 3:15.
204. Jia, F., et.al., Isoflurane is a potent modulator of extrasynaptic GABA(A) receptors in the thalamus. *Journal of Pharmacology Experimental Therapy*, 2008. 324(3):1127-1135.

205. Sanchez-Mejia, R.O., and L., Mucke, Phospholipase A2 and arachidonic acid in Alzheimer's disease. *Biochemical Biophysics Acta*, 2010. 1801(8):784-790.
206. Kochanek, P.M. , et.al., Screening of Biochemical and Molecular Mechanisms of Secondary Injury and Repair in the Brain after Experimental Blast-Induced Traumatic Brain Injury in Rats. *Journal of Neurotrauma*, 2013. 30(11):920-37.